







Université du Québec  
à Rimouski

**Optimisation des Paramètres du Soudage au Laser pour les  
Alliages d'Aluminium 6061 et 5052/5086 : Une Approche  
Statistique et Expérimentale**

Mémoire présenté  
dans le cadre du programme de maîtrise en ingénierie  
en vue de l'obtention du grade de maître ès sciences appliquées (M. Sc. A.)

PAR  
© ABDESSAMAD LAKHAL

Novembre 2023



**Composition du jury :**

**Xiangbing Kong, président du jury, Université du Québec à Rimouski**

**Noureddine Barka, directeur de recherche, Université du Québec à Rimouski**

**Hendra Hermawan, examinateur externe, Université Laval**

Dépôt initial le 21 Août 2023

Dépôt final le 27 Novembre 2023



UNIVERSITÉ DU QUÉBEC À RIMOUSKI  
Service de la bibliothèque

Avertissement

La diffusion de ce mémoire ou de cette thèse se fait dans le respect des droits de son auteur, qui a signé le formulaire « *Autorisation de reproduire et de diffuser un rapport, un mémoire ou une thèse* ». En signant ce formulaire, l'auteur concède à l'Université du Québec à Rimouski une licence non exclusive d'utilisation et de publication de la totalité ou d'une partie importante de son travail de recherche pour des fins pédagogiques et non commerciales. Plus précisément, l'auteur autorise l'Université du Québec à Rimouski à reproduire, diffuser, prêter, distribuer ou vendre des copies de son travail de recherche à des fins non commerciales sur quelque support que ce soit, y compris Internet. Cette licence et cette autorisation n'entraînent pas une renonciation de la part de l'auteur à ses droits moraux ni à ses droits de propriété intellectuelle. Sauf entente contraire, l'auteur conserve la liberté de diffuser et de commercialiser ou non ce travail dont il possède un exemplaire.



À ma mère, à ma famille et à celle que j'ai choisie, mes amis, votre soutien indéfectible a été ma force tout au long de ce parcours. Ce travail est le fruit de votre amour et de votre encouragement. Merci infiniment.



## **REMERCIEMENTS**

Il m'est impossible d'entamer cette aventure sans mentionner la personne qui a été le pilier central de mon parcours de recherche, le professeur Noureddine Barka. Sa profonde expertise et sa guidance éclairée ont été le phare dans la mer tumultueuse de cette expérience. Le professeur Barka a été bien plus qu'un directeur de recherche; il a été un mentor, un guide et un support constant. Son dévouement envers l'excellence et sa quête incessante de connaissances ont été une source d'inspiration tout au long de ce voyage. Sa capacité à voir au-delà des évidences et à orienter mes pensées vers des perspectives nouvelles et stimulantes a grandement enrichi ce travail.

Chaque discussion avec lui a été une occasion d'apprentissage et de découverte, et chaque commentaire et critique qu'il a apporté a contribué à aiguiser ma pensée et à affiner mes arguments. Il a su allier rigueur et flexibilité, me poussant toujours à donner le meilleur de moi-même sans me restreindre pour suivre mes intuitions et développer mes propres idées. Pour tout cela et bien plus encore, je lui suis profondément reconnaissant.

Le professeur Barka, votre guidance et votre soutien ont été inestimables. Ce mémoire est autant le fruit de votre enseignement que de mes efforts. Merci du fond du cœur.

Mes collègues, Asim et Pedram, méritent une mention spéciale pour leur esprit de collaboration, leur soutien inconditionnel et leur camaraderie indéfectible. Vous avez ajouté une dimension d'enthousiasme et de solidarité à mon parcours de recherche.

Je tiens à exprimer ma gratitude à l'Université du Québec à Rimouski et au département d'ingénierie pour leur soutien inébranlable et les opportunités uniques qu'ils m'ont offertes.

Une mention spéciale à tous les auxiliaires et techniciens, votre travail souvent invisible est la colonne vertébrale de nos réalisations.

À ma famille, votre amour inébranlable, vos encouragements constants et votre foi en moi ont été la fondation sur laquelle j'ai bâti mon travail. Un hommage particulier à ma mère, qui a sacrifié ses rêves pour que je puisse réaliser les miens.

Mes amis, mes compagnons de voyage, vous avez été ma deuxième famille, celle que j'ai choisie. Merci d'avoir été le rayon de soleil lors des jours sombres et de m'avoir apporté des moments de joie et de répit. Un salut spécial à « FAFA », « SANGOS » et « THE 3 MUSKETEERS », votre amitié et votre soutien ont ajouté des couleurs à mon voyage universitaire.

En conclusion, chaque mot dans ce mémoire porte l'empreinte de chacun de vous, et pour cela, je vous suis éternellement reconnaissant.

## RÉSUMÉ

Ce mémoire se concentre sur l'optimisation du soudage au laser, en particulier pour les alliages d'aluminium, qui sont essentiels afin d'optimiser l'utilisation de l'énergie et de minimiser les émissions dans l'industrie automobile. Les méthodes d'assemblage diverses sont explorées, avec un accent particulier sur le soudage au laser, y compris des techniques spécifiques comme le soudage au laser hybride et le soudage au laser avec gaz de protection. L'importance de la surveillance et de l'intelligence artificielle pour l'optimisation des processus est également soulignée, y compris l'utilisation de capteurs et d'apprentissage en profondeur pour l'inspection de la qualité en temps réel.

Des expériences détaillées ont été menées pour optimiser les paramètres du soudage laser pour deux combinaisons d'alliages d'aluminium, à savoir 6061 T6 et 5052 H32, ainsi que 6061 T6 et 5086 H32. L'analyse de la variance (ANOVA) est employée pour analyser l'influence de la distance focale, la puissance et la vitesse du laser sur la résistance mécanique des soudures. Les expériences relèvent que la distance focale était le facteur le plus déterminant pour les deux combinaisons d'alliages, tandis que la vitesse vient après la puissance dans la liste des facteurs qui ont grande influence.

En utilisant la régression linéaire multiple et la méthode de la surface de réponse, des modèles prédictifs ont été élaborés pour prédire la charge de cisaillement par longueur de soudure. Les résultats de ce mémoire fournissent des informations précieuses pour Optimiser la fiabilité et la performance des procédés de soudage au laser des alliages d'aluminium.

Mots clés : Soudage au laser, Alliages d'aluminium, Optimisation des paramètres, Intelligence artificielle, Inspection de la qualité en temps réel, ANOVA, Régression linéaire multiple, Méthode de la surface de réponse.



## **ABSTRACT**

This thesis presents an in-depth study of laser welding, emphasizing its growing importance in various industries due to its inherent benefits and complexity. The study particularly focuses on the application of this technology for welding aluminum alloys, an essential practice in the automotive industry to enhance fuel efficiency and reduce emissions.

A thorough examination of various joining methods and specific laser welding techniques, such as hybrid laser welding and laser welding with backing gas, is presented. The study underscores the necessity of real-time quality inspection, highlighting the role of sensor technologies and artificial intelligence. By employing multi-sensor monitoring and deep learning, this research explores the exciting future of an intelligent quality assessment system in welding monitoring.

Two key experiments are presented where laser welding parameters - focal position, speed, and laser power - are thoroughly investigated for their effects on the mechanical integrity of laser-welded connections in two different combinations of aluminum alloys: AA 6061 with AA 5052, and AA 6061 with AA 5086 H32. Analysis of variance (ANOVA), multiple linear regression, and response surface methodology are utilized to quantitatively evaluate the influence of each parameter. The focal position was found to be the most influential, indicating its profound impact on the weld's mechanical strength. This thesis serves as an insightful resource for researchers and industries aiming to optimize their laser welding processes, enhance product quality, and achieve sustainable manufacturing practices. The findings enhance our understanding of the laser welding process and provide practical guidelines for industrial applications demanding high-quality aluminum laser welds.

**Keywords:** Laser Welding, Real-Time Quality Monitoring, Artificial Intelligence, Aluminum Alloys, Sustainable Industrial Applications, Green Manufacturing, Multi-Sensor Monitoring Technology, Deep Learning, Joining Methods, Hybrid Laser Welding, Welding Sensors, ANOVA, Response Surface Methodology.

## TABLE DES MATIÈRES

REMERCIEMENTS.....	ix
RÉSUMÉ .....	xi
abstract .....	xiii
TABLE DES MATIÈRES .....	xv
LISTE DES TABLEAUX .....	xix
LISTE DES FIGURES .....	xxi
INTRODUCTION GÉNÉRALE .....	1
1. CONTEXTE ET GÉNÉRALITÉS .....	1
2. FONDAMENTAUX DE LA SOUDURE AU LASER .....	7
3. PROBLÉMATIQUES.....	8
4. OBJECTIFS .....	9
5. MÉTHODOLOGIE .....	11
6. ORGANISATION DU MÉMOIRE.....	13
CHAPITRE 1 Exploration des procédés de soudage au laser : Revue des techniques d'optimisation, surveillance de la qualité en temps réel et rôle de l'IA dans les applications industrielles durables .....	15
1.1 RÉSUMÉ EN FRANÇAIS DU PREMIER ARTICLE.....	15
1.2 CONTRIBUTION .....	16
1.3 TITRE DU PREMIER ARTICLE .....	16
1.4 ABSTRACT .....	16
1.5 INTRODUCTION .....	17
1.6 JOINING METHODS:.....	22

1.6.1	Adhesive bonding .....	22
1.6.2	Overlamination .....	24
1.6.3	mechanical joining .....	26
1.6.4	Welding.....	27
1.7	REVIEW OF LASER WELDING TECHNIQUES .....	33
1.7.1	Hybrid laser welding.....	33
1.7.2	Laser welding with backing gas.....	34
1.7.3	Laser welding trajectory .....	34
1.7.4	Laser fusion repair .....	35
1.8	MONITORING PROCESSES AND AI.....	35
1.8.1	Monitoring processes .....	35
1.8.2	Fundamental sensors utilized in monitoring .....	39
1.8.3	Monitoring methods.....	43
1.9	DATA FUSION METHODS .....	46
1.9.1	Optimization of the Process Parameters .....	47
1.9.2	Predicting Seam Characteristics .....	48
1.9.3	Tracking of the weld seam.....	48
1.9.4	Defects classification .....	49
1.9.5	Simulation validation.....	49
1.9.6	Command and control in processes .....	50
1.10	CONCLUSIONS .....	51
CHAPITRE 2 Optimisation des propriétés mécaniques dans le soudage laser d'aluminium hétérogène : Une étude sur les alliages 6061 T6 et 5052 H32 .....		54
2.1	RÉSUMÉ EN FRANÇAIS DU DEUXIÈME ARTICLE .....	54
2.2	CONTRIBUTION.....	54
2.3	TITRE DU PREMIER ARTICLE .....	55
2.4	ABSTRACT.....	55
2.5	INTRODUCTION.....	55
2.6	EXPERIMENTAL PROCEDURE.....	58
2.6.1	The materials.....	58
2.6.2	Design of Experiments.....	59
2.6.3	Welding and test plates .....	60

2.7	CHARACTERIZATION OF WELD .....	61
2.8	MECHANICAL PROPERTIES OF WELD.....	63
2.8.1	Micro hardness .....	63
2.8.2	Tensile strength test.....	66
2.9	RESULT AND DISCUSSION .....	68
2.9.1	Analysis of Variance (ANOVA) .....	68
2.9.2	The ANOVA analysis: .....	71
2.9.3	Response surface method: .....	73
2.10	CONCLUSION.....	76
	<b>CHAPITRE 3 Optimisation des paramètres de soudage au laser pour l'amélioration des propriétés mécaniques des alliages d'aluminium dissemblables 6061 T6 et 5086 H32.....</b>	<b>77</b>
3.1	RÉSUMÉ EN FRANÇAIS DU DEUXIÈME ARTICLE.....	77
3.2	CONTRIBUTION .....	77
3.3	TITRE DU PREMIER ARTICLE .....	78
3.4	ABSTRACT .....	78
3.5	INTRODUCTION .....	79
3.6	EXPERIMENTAL SET-UP .....	83
3.7	CHARACTERIZATION OF WELD .....	86
3.8	MECHANICAL PROPERTIES OF WELD.....	88
3.8.1	Hardness profile.....	88
3.8.2	Tensile strength test:.....	90
3.9	RESULTS AND ANALYSIS .....	93
3.9.1	Analysis of Variance .....	93
3.9.2	The ANOVA analysis: .....	95
3.9.3	Response surface method: .....	97
3.10	CONCLUSION.....	101
	<b>CONCLUSION GÉNÉRALE.....</b>	<b>105</b>
	<b>RÉFÉRENCES BIBLIOGRAPHIQUES.....</b>	<b>113</b>



## **LISTE DES TABLEAUX**

Table 1: propriétés mécaniques de l'aluminium. ....	4
Table 2: Monitoring objectives, monitoring signal and monitoring technology in different monitoring stages.....	38
Table 3 : Nominal chemical composition of 6061 T6 and 5052 H32 Al alloys used in this investigation. ....	59
Table 4: Tensile properties of 6061 T6 and 5052 H32 Al Alloys used in this investigation. ....	59
Table 5: Factors and Levels for Experiment.....	60
Tableau 6: Factors and Levels for Experiment.....	60
Table 7: The maximum shear load per weld length.....	66
Table 8: ANOVA table for the maximum shear load per weld length. ....	70
Table 9: ANOVA of multiple linear regression model.....	72
Table 10: Nominal chemical composition of 6061 T6 and 5086 H32 Al alloys used in this investigation. ....	83
Table 11: Tensile properties of 6061 T6 and 5086 H32 Al Alloys used in this investigation. ....	83
Table 12: Factors and Levels for Experiment.....	84
Table 13: Experimental Design. ....	85
Table 14: The maximum shear load per weld length.....	91
Table 15: ANOVA table for the maximum shear load per weld length. ....	94
Tableau 16: ANOVA of multiple linear regression model.....	97



## LISTE DES FIGURES

Figure 1: Système de soudage GMAW robotisé ; (a) Système de soudage. (b) Capteur de vision [17].....	6
Figure 2: Schéma de soudage par résistance par points (a); électrode composite intégrée (b) et (c) [16]. .....	6
Figure 3: Le processus de soudage par friction-malaxage [18].....	6
Figure 4: Diagramme schématique des expériences de micro-soudage par point laser (LSMW) [19].....	7
Figure 5: Strong demand for lightweight automobile materials. (a) Goals for fuel efficiency in various countries (passenger vehicles); (b) The number of light vehicles manufactured for the largest vehicle market [6]. .....	19
Figure 6: Vehicle composed of a variety of lightweight material, Material distribution according to the Mach-II body-in-white. [4].....	20
Figure 7: (a) Compared to traditional methods of forming, incremental forming is more cost-effective and can be done at low volumes. (b) Balance between part complexity and the number of parts made for each forming process [13] .....	21
Figure 8: Comparison of Stiffness (Left) and Stress Distribution (Right) in Adhesively Bonded Joints Versus Riveted Joints [54]. .....	24
Figure 9: Variety of Common Materials and Cross-Sections Employed Overlaminated in Joints [46].....	25
Figure 10: categories of joining: temporary joining and permanent joining [27]. .....	26
Figure 11: Conventional friction welding, also known as rotational welding [30] .....	28
Figure 12: (a) schematic illustration of friction stir welding, (b) schematic illustration of friction stir processing [173], [174]. .....	29
Figure 13: Diagrammatic Representation of an Ultrasonic Welding System [35]. .....	31
Figure 14: Process monitoring and feedback control experimental setup using a single-mode CW fiber laser [70].....	36

Figure 15: The diagram illustrating laser welding and the explanation of the distinct monitoring phases [110]. .....	37
Figure 16: The categorization of sensors and methodologies [110]. .....	39
Figure 17: NIR camera-based online diagnostics. (a) Black body emission spectra based on Planck's law for different temperatures compared to Si and InGaAs detector sensitivity. (b) Comparison of images of the welding zone and its surrounding captured with a Si camera (left) or an InGaAs camera (right) [36], [121]......	40
Figure 18: The spectral range for monitoring and the schematic diagram of this monitoring method [125]......	41
Figure 19: An alternative visual monitoring system. (a) A coaxial surveillance system that also has an auxiliary light source. (b) A system including two high-speed cameras for measuring melt velocities. (c) Observational system works on both the top and bottom [132], [137], [138]. .....	42
Figure 20: The figure depicts a schematic image illustrating the measurement of molten pool depth using an ultrasonic phased array system [143]......	43
Figure 21: (a) illustrates the schematic diagram of the ICI (Internal Control Instrumentation) system, (b) displays the measured depths obtained using the ICI system, represented by green dots [161]. .....	45
Figure 22: The sensing system comprised six distinct sensors, as shown in the setup [166].....	46
Figure 23: Different monitoring objectives are accomplished through the utilization of various AI-based technologies for data processing and analysis [110]......	47
Figure 24: Welding experiment and numerical simulation results compared: (a) and (e) case I: partial penetration, (b) and (f) case II: full penetration, (c) case III: full penetration [209]......	50
Figure 25: Automatic Fiber Laser System, six-axis-robotic system FANUC M-710ic with IPG Photonics YLS-3000 (Ytterbium Fiber Lasers). .....	61
Figure 26: x5 magnification microscope observation of the welded portion of each specimen .....	62
Figure 27: a x100 magnification microscope observation the microstructure of the welded portion for test 3, the picture shows the BM and Fusion area.....	63
Figure 28: Hardness measurement path [238].....	64

Figure 29: Hardness profile (a) Focal position +3mm, (b) Focal position +5mm, (c) Focal position +7mm.....	65
Figure 30: Shear load to welding length ratio (kN/m). Displacement (mm) curves for all the tested specimens .....	67
Figure 31: the maximum and the average shear load per weld length for each specimen.....	68
Figure 32: Depiction of keyhole dynamics in response to disruptions and laser beam engagement with the melted surface at both (a) positive and (b) negative defocusing locations [41]. .....	69
Figure 33: Parameters effect graph.....	71
Figure 34: Experimental data vs Predicted value.....	73
Figure 35: Response Surface for shear the load per weld length with Focal Position fixed at 3 mm.....	74
Figure 36: Response Surface for the shear the load per weld length with Speed fixed at 4 m/min.....	74
Figure 37: Response Surface for the shear the load per weld length with Power fixed at 2.9 kW. ....	75
Figure 38: Automatic Fiber Laser System, six-axis-robotic system FANUC M-710ic with IPG Photonics YLS-3000 (Ytterbium Fiber Lasers).....	84
Figure 39: x5 magnification microscope observation of the welded portion of each specimen.....	87
Figure 40: a x100 magnification microscope observation the microstructure of the welded portion for test 3, the picture shows the BM and Fusion part.....	88
Figure 41: Hardness measurement path.....	89
Figure 42: Hardness profile (a) Focal position +3mm, (b) Focal position +5mm, (c) Focal position +7mm.....	90
Figure 43: Shear load to welding length ratio (kN/m). Displacement (mm) curves for all the tested specimens.....	92
Figure 44: the maximum and the average shear load per weld length for each specimen.....	92

Figure 45: Depiction of keyhole dynamics in response to disruptions and laser beam engagement with the melted surface at both (a) positive and (b) negative defocusing locations [282].....	93
Figure 46: Parameters effect graph. ....	95
Figure 47: Experimental data vs Predicted value.....	97
Figure 48: Response Surface for shear the load per weld length with Focal Position fixed at 3 mm. ....	98
Figure 49: Response Surface for the shear the load per weld length with Speed fixed at 4 m/min. ....	99
Figure 50: Response Surface for the shear the load per weld length with Power fixed at 2.9 kW.....	100





## **INTRODUCTION GÉNÉRALE**

### **1. CONTEXTE ET GÉNÉRALITÉS**

La question du changement climatique a pris une importance cruciale au cours des dernières décennies, émergeant comme l'un des défis les plus urgents à relever par l'humanité. Les problèmes liés aux émissions de gaz à effet de serre, à l'élévation de la température dans le monde entier ne sont plus simplement des sujets de recherche scientifique, mais des préoccupations qui touchent chaque aspect de notre vie quotidienne et de notre économie [1].

Le changement climatique actuel est principalement dû à l'augmentation de la concentration des gaz à effet de serre dans l'atmosphère, une situation largement attribuable à l'activité humaine. Ces gaz, avec le dioxyde de carbone en tête de liste, emprisonnent la chaleur solaire dans notre atmosphère, conduisant à une hausse des températures mondiales, un phénomène appelé réchauffement climatique. Les répercussions de cette hausse des températures sur notre planète sont considérables, allant de la disparition des calottes glaciaires polaires à la montée du niveau des mers et l'éradication de diverses espèces [1].

En outre, l'exploitation croissante des ressources naturelles pose un autre défi majeur. Les ressources naturelles, telles que les métaux, sont essentielles à la production dans de nombreux secteurs industriels. Cependant, leur utilisation non durable met en péril leur disponibilité pour les générations futures et contribue à l'augmentation des coûts de production [2].

En tant que premier consommateur de ressources naturelles et l'un des plus grands émetteurs de gaz à effet de serre, l'industrie est confrontée à ces problèmes. En fait, la transformation de l'industrie a joué un rôle clé dans la transition vers une économie verte et durable et pourrait être un point de basculement pour relever ces différents défis. [1], [2].

Parmi les plus grands enjeux auxquels l'industrie fait face actuellement, la réduction des déchets provenant de processus de fabrication inappropriés et le conformisme à des normes environnementales de plus en plus strictes. L'exploitation des matériaux qui contribuent à réduire l'effet environnemental suscite l'intérêt des industriels dans des secteurs de production différents [3], [4].

La faible densité de l'aluminium en fait donc l'un des choix parfaits pour fournir des produits plus légers, en particulier dans le secteur du transport. Cette décision entraîne des conséquences sur le coût des produits et l'efficacité énergétique, entraînant une réduction des émissions des gaz à effet de serre [1]. Il est également estimé que l'incorporation de matériaux de faible masse dans la fabrication de pièces et des composants automobiles permettra de se conformer aux normes de plus en plus exigeantes en ce qui concerne la préservation de l'air et l'amélioration de l'efficience [5]. Un autre aspect intéressant de l'utilité de l'aluminium est sa capacité de recyclage, qui est l'un des bénéfices essentiels du matériau. Certains matériaux coulés ont été spécialement développés pour être fabriqués depuis des ferrailles refondues. [4].

Plus de 500 variantes distinctes d'alliages d'aluminium existent, et par souci de simplicité, ces derniers sont classifiés en différentes catégories, connues sous le nom de séries d'alliages. La classification de ces alliages s'effectue grâce à l'utilisation du Système International de Désignation des Alliages, une structure de catégorisation, largement adoptée par de nombreux pays, qui repose sur la composition chimique des alliages d'aluminium. Ce système est largement plébiscité par le secteur aérospatial pour catégoriser les matériaux employés dans la construction aéronautique. Chaque alliage d'aluminium est attribué à l'une des huit séries selon les composants principaux de l'alliage. C'est la composition chimique prédominante de l'alliage qui détermine la série à laquelle il appartient [6]. Ci-dessous la liste des principales séries d'alliages de corroyage d'aluminium et de leurs principaux éléments constitutifs :

- Série 1XXX : les alliages de cette série sont composés principalement d'aluminium à hauteur de 99 % (minimum).

- Série 2XXX : Les alliages de cette série contiennent principalement du cuivre.
- Série 3XXX : Les alliages de cette série sont composés principalement de manganèse.
- Série 4XXX : Les alliages de cette série contiennent principalement du silicium.
- Série 5XXX : Les alliages de cette série sont composés principalement de magnésium.
- Série 6XXX : Les alliages de cette série contiennent principalement du magnésium et du silicium.
- Série 7XXX : Les alliages de cette série sont composés principalement de zinc.
- Série 8XXX : Les alliages de cette série contiennent d'autres éléments en plus de l'aluminium.

L'aluminium se distingue par une multitude de propriétés qui le rendent particulièrement attrayant pour des applications d'ingénierie. Parmi ces caractéristiques, on peut citer un rapport résistance/poids remarquable, une facilité de traitement, une haute malléabilité, une conductivité thermique exceptionnelle, une résistance à la corrosion supérieure, et une excellente finition naturelle. Ces alliages d'aluminium offrent une durabilité considérable et une haute capacité de résister à la corrosion, ce qui est parfaitement important pour des utilisations dans des conditions marines, de plus la protection de surface ne serait plus nécessaire, tout en minimisant les coûts de maintenance. Ils sont également capables de maintenir leurs propriétés intrinsèques face à des variations de température importantes, renforçant ainsi leur durabilité. La table 1 illustre les valeurs correspondant aux propriétés mécaniques et physiques de l'aluminium [6]–[8].

Cette étude se concentre sur les alliages d'aluminium appartenant aux familles 5000 et 6000. Ces alliages présentent des caractéristiques mécaniques avantageuses, une capacité à résister à la traction modérée, une excellente résistance à la corrosion, ainsi que de bonnes performances d'usinage. De plus, leur utilisation est répandue dans l'industrie automobile et aérospatiale. Ils ont également prouvé leur efficacité dans des applications navales et sous-marines [9], [10].

Table 1: Propriétés mécaniques de l'aluminium

Propriétés	Valeurs	Unités
Résistance à la traction	10–90 (70–620)	ksi (MPa)
Limite d'élasticité	3–84.1 (20–580)	ksi (MPa)
Allongement	<1–30	%
Dureté	30–150	HB
Conductivité électrique	18–60	%IACS
Limite de fatigue	8–21 (55–145)	ksi (MPa)
Résistance au cisaillement	6–46 (42–325)	ksi (MPa)
Module d'élasticité	9.5–11.2 (65–80)	$10^6$ psi
Gravité spécifique	2.57–2.95	-

L'exploitation performante de l'aluminium requiert l'évolution et l'amélioration des approches spécifiques de conversion et de jonction. Les processus de rassemblement comprennent diverses techniques, notamment le soudage, la liaison adhésive et les fixations mécaniques. Les deux dernières techniques, de part leur faible consommation énergétique, présentent des solutions offrant d'excellentes performances mécaniques. Toutefois, elles sont contraintes par la nécessité d'accéder à deux faces de l'assemblage pour leur mise en œuvre [11].

Les assemblages adhésifs ont une faiblesse intrinsèque à la traction par épłuchage, ce qui doit être pris en compte dans la conception des véhicules. Les adhésifs haute performance couramment utilisés contiennent des formules faisant appel à l'époxy ou de solvant, ce qui engendre d'importantes considérations écologiques, principalement en terme de résistance aux chocs [12].

Le soudage est parmi les techniques couramment plébiscitées du fait des multiples bénéfices qu'il présente. Parmi ces avantages figurent son coût relativement bas, sa rapidité et sa facilité d'emploi, son potentiel d'automatisation, ainsi que sa capacité à être employé pour la production à grande échelle. Toutefois, ces bénéfices sont tempérés par les défis

associés à l'oxydation de surface lors du soudage de l'aluminium et par les coûts généralement élevés associés à l'investissement initial et à l'exploitation [11].

L'expérience extensive dans le secteur de la soudure industrielle constitue assurément une promesse de l'évolution continue des différentes techniques disponibles. De plus, avec le développement technologique, même les techniques onéreuses, telles que les lasers, deviennent de plus en plus utilisables dans le domaine automobile, répondant ainsi aux besoins spécifiques de ce secteur [11], [13].

Parmi les technologies dans le domaine de soudage les plus couramment utilisées et décrites par les chercheurs, on retrouve le soudage à l'arc dans la figure 1, le soudage par résistance décrit dans la figure 2, le soudage par friction-malaxage dans la figure 3 et le soudage laser présenté dans la figure 4. L'un des défis rencontrés lors de l'utilisation de la méthode de soudure par résistance appliquée à l'aluminium réside dans la désagrégation de sa couche d'oxyde en surface. La température de fusion de l'oxyde étant bien supérieure, un système de chauffage à l'aide d'une résistance plus intense est nécessaire pour effectuer la désintégration et ainsi autoriser la création de la jonction soudée [14].

Quant à l'assemblage par fusion de l'aluminium en utilisant l'arc électrique, il est compliqué en raison de la présence d'une couche d'oxyde à température de fusion élevée qui persiste même une fois que le métal a fondu. La littérature rapporte également d'autres limitations comme la propension à la formation de fissures dans les soudures, la déformation significative provoquée par l'apport de chaleur, ainsi que la nécessité des traitements thermiques post-soudage [15].

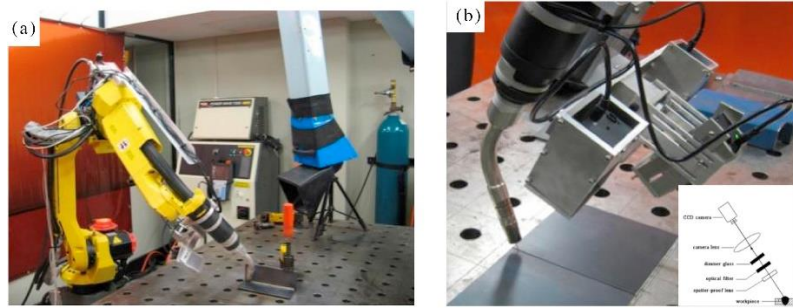


Figure 1: Système de soudage GMAW robotisé ; (a) Système de soudage. (b) Capteur de vision [17]

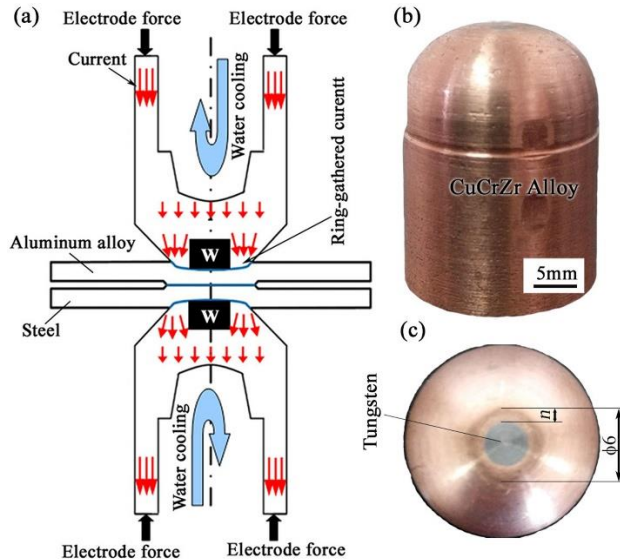


Figure 2: Schéma de soudage par résistance par points (a); électrode composite intégrée (b) et (c) [16]

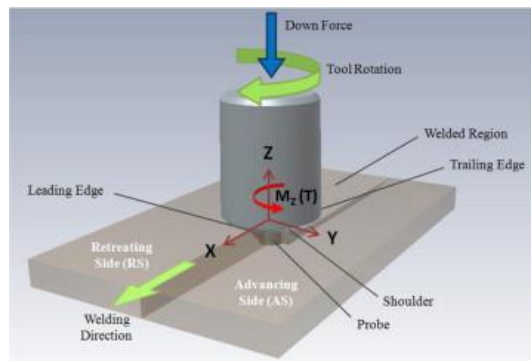


Figure 3: Le processus de soudage par friction-malaxage [18]

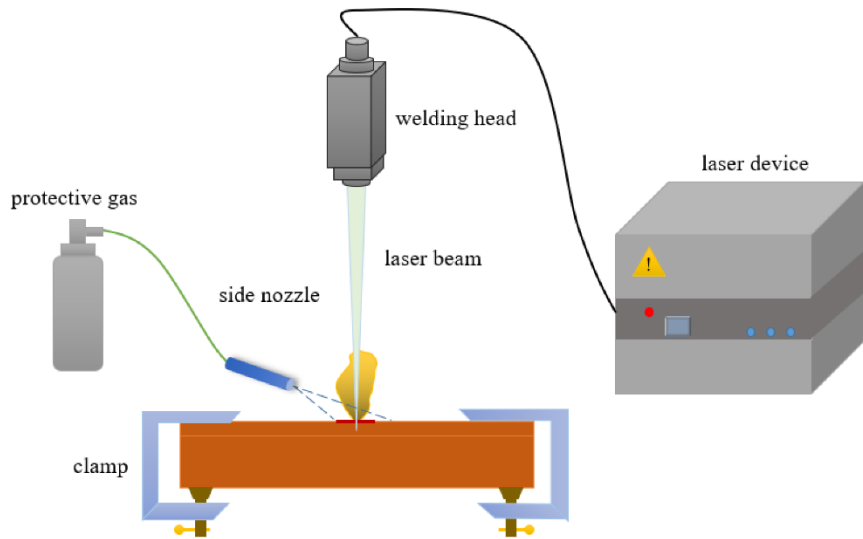


Figure 4: Diagramme schématique des expériences de micro-soudage par point laser (LSMW) [19]

## 2. FONDAMENTAUX DE LA SOUDURE AU LASER

La production de rayonnement laser est gouvernée par les principes de la physique quantique, qui confinent les particules atomiques et les composés moléculaires à des niveaux d'état énergétique discrets spécifiques à leur nature. Pour un atome individuel, le niveau d'énergie le plus faible est atteint lorsque tous ses électrons occupent les orbites les plus proches du noyau, une condition dénommée "état fondamental". Quand un ou plusieurs électrons présents dans un atome absorbent de l'énergie, ils ont la capacité de migrer vers des trajectoires orbitales plus éloignées, dans ce cas l'atome est considéré comme "excité". Habituellement, ces niveaux d'excitation ne conservent pas leur stabilité ; quand les électrons reviennent d'un état énergétique supérieur vers un état énergétique inférieur, ils libèrent l'énergie excédentaire sous forme de rayonnement lumineux.

Albert Einstein a compris que cette libération d'énergie peut se produire de deux façons. Généralement, des quantités discrètes de lumière, appelées photons, sont émises de manière spontanée, sans aucune influence extérieure. Cependant, un photon de passage peut induire

l'excitation d'un atome ou d'une molécule à émettre de la radiation lumineuse, dans le cas où l'énergie du photon coïncide précisément avec l'énergie qu'un électron libérerait spontanément en retournant à un état de moindre énergie. Le mécanisme dominant dépend du ratio entre les états d'énergies faibles et élevées. Habituellement, les états de niveau d'énergie inférieur prévalent.

Cette action implique qu'un photon émis de manière spontanée a une probabilité accrue d'être absorbé, provoquant ainsi le déplacement d'un électron d'un état d'énergie réduite à un état d'élevée en énergie plutôt que de déclencher un état d'énergie élevée à descendre à un état d'énergie réduite en rayonnant un deuxième photon. Pourvu que les niveaux d'énergie réduits soient plus fréquents, la décharge stimulée sera marginalisée [20].

La technique du soudage laser a suscité un intérêt considérable en raison de sa capacité à offrir des vitesses de traitement et de production élevées, en plus de divers autres avantages. Parmi ceux-ci, on compte l'induction minimale de déformation thermique, résultante d'une contribution calorifique totale moins intense. Cette particularité découle de l'utilisation d'un faisceau fortement concentré et à haute densité énergétique qui permet de chauffer rapidement une zone de taille très réduite, produisant ainsi une soudure mince et une région altérée par l'effet thermique étroit. Les joints soudés obtenus sont habituellement de grande qualité et leur formation est simplifiée, ce qui les rend aptes à la production de pièces personnalisées. Les équipements de soudage se prêtent bien à être automatisés, du fait de leur programmabilité et de leur polyvalence en ce qui concerne les matériaux susceptibles d'être traités, y compris l'aluminium, et aux diverses configurations de liaisons envisageables [21]–[23]. Néanmoins, le soudage laser est perçu comme une méthode coûteuse à mettre en place. Pour l'aluminium, elle est limitée à des niveaux d'épaisseur allant de 2 à 6 mm, du fait de la contrainte dimensionnelle, l'apport thermique inégal a tendance à provoquer une pénétration inégale et une fluctuation du bain de fusion, occasionnant des imperfections qui nécessitent une surveillance en vue de garantir une qualité optimale et pour bénéficier pleinement des vitesses élevées et des avantages offerts par cette technique de soudage [15], [23]–[25].

### 3. PROBLÉMATIQUES

Comprendre pleinement l'impact des phénomènes liés au soudage laser, aussi bien du point de vue mécanique, thermique que métallurgique, sur la qualité finale des produits représente un enjeu crucial. La mise en place de stratégies visant à minimiser les effets indésirables du processus de soudage est également d'une importance capitale pour préserver les caractéristiques mécaniques des composants assemblés. Il est à noter que les anomalies ou défaillances présentes dans les soudures ont le potentiel de générer des risques de rupture, soulevant ainsi des problèmes de sécurité importants [31]. Au sein du domaine du soudage laser, ces défaillances sont souvent regroupées en trois catégories principales : les défauts de forme, les anomalies internes et les lacunes en termes de qualité [30][32].

Dans cette optique, la validation de la conformité des pièces fabriquées se révèle être une étape cruciale au sein des procédés de production. C'est pourquoi le développement de méthodes et de solutions pour évaluer et surveiller la qualité du soudage en utilisant des technologies de surveillance qui suscite un intérêt croissant au sein de l'industrie [33], [34]. Afin de garantir un résultat final de qualité optimale, la surveillance continue du processus, l'ajustement des paramètres de soudage, ainsi que la capacité à anticiper les irrégularités, s'avèrent des éléments indispensables.

#### **4. OBJECTIFS**

Le principal but de ce mémoire réside dans la conduite de plusieurs investigations approches scientifiques et méthodiques sur l'emploi du soudage laser pour différents alliages d'aluminium, plus précisément l'AA 6061 combiné à l'AA 5052 et l'AA 6061 associé à l'AA 5086. L'intention est de développer une compréhension approfondie des diverses implications des interactions entre le laser et le matériau. Cette connaissance pourrait ensuite être directement appliquée pour résoudre les problèmes rencontrés par l'utilisation de la technologie de soudage au laser dans le processus de fabrication en série, et pour concevoir des schémas prévisionnels des propriétés mécaniques et de la qualité structurelle microscopique des tôles d'aluminium assemblées. Ces modèles dépendraient des paramètres du processus et permettraient d'éviter le processus long et coûteux de la méthode

d'expérimentations et d'itérations. Dans le cadre de ce projet de recherche, un laser à fibre à onde continue est employé pour souder les divers alliages d'aluminium dans des configurations de joint de recouvrement. Les différentes phases de ce mémoire offrent une opportunité pour analyser et quantifier l'influence des paramètres du processus sur la qualité de la soudure, ainsi que leur contribution à la variation de ces diverses caractéristiques. Cette analyse est réalisée en utilisant des méthodes statistiques appropriées. En se fondant sur ces phases, plusieurs alternatives pour les modèles prédictifs sont envisagées, puis évaluées en fonction de critères spécifiques. L'objectif est d'avoir le modèle prédictif le plus exact et le plus résilient.

Ce mémoire a comme premier objectif l'exploration littéraire des diverses techniques d'assemblage mécanique, en mettant l'accent particulièrement sur les méthodes utilisées dans le soudage au laser. Il implique également l'identification des approches de contrôle de processus les plus pertinentes et la sélection des variables à réguler. De plus, le but est de sélectionner des stratégies de prédiction et d'optimisation qui contribueraient à atténuer les défis de qualité dans le processus de soudage au laser. Le second objectif s'articule autour de la mise en place d'une conception d'expérience méthodique, en conjonction avec des techniques éprouvées de traitement statistique. Cette démarche vise à analyser l'impact de divers paramètres opérationnels sur les caractéristiques géométriques du soudage au laser et ses caractéristiques microstructurales. Ces éléments influent sur les propriétés mécaniques du AA 6061, lorsqu'il est soudé pour former des joints à recouvrement avec l'AA 5052. Enfin, le troisième objectif de cette thèse est d'examiner l'influence des paramètres du modèle étudié dans la deuxième partie, mais en remplaçant l'AA 5052 par l'AA 5086 et de comparer les résultats des deux modèles. Il convient d'étudier les effets de la puissance, de la vitesse et de la distance focale sur la résistance à la traction, la micro-dureté et la microstructure en appliquant les modèles empiriques élaborés à partir de la méthode Taguchi.

Dans le cadre de cette recherche, nous avons proposé une méthode permettant de réguler les caractéristiques mécaniques en relation avec les paramètres de soudage au laser pour les tôles d'aluminium des trois alliages distincts. Les paramètres examinés comprennent

la distance focale, la vitesse de déplacement du foyer et la puissance de sortie du laser. Un apport majeur de cette étude est l'établissement de règles pour la gestion des paramètres de soudage au laser, permettant une anticipation efficace des caractéristiques mécaniques (mesures de micro-dureté et de résistance à la rupture) et des caractéristiques de la microstructure. La complexité de ce travail exige de prendre en compte l'équipement expérimental au niveau du laboratoire (cellule laser, machines de métallographie et dispositifs de mesure des caractéristiques mécaniques) pour la vérification des équations, des conclusions et des modèles. Afin de générer des graphiques de contour avec des plages de réponse changeantes en relation avec les variables de soudage au laser, la méthode de surface de réponse (RSM), une approche d'analyse statistique, est employée dans cette étude. Son adoption repose sur ses avantages clés, qui incluent sa facilité d'application et sa simplicité d'interprétation.

## 5. MÉTHODOLOGIE

Comprendre et identifier les relations entre les variables du processus de soudage au laser et la géométrie du joint soudé est essentiel pour maîtriser le procédé de soudage. La stratégie déployée pour réaliser les buts de ce mémoire se décline en trois phases distinctes. Ces phases concernent l'examen expérimental de la résistance ultime à la traction, l'évolution de la micro-dureté sur toute la surface de soudure des plaques, ainsi que les valeurs des mesures micro-structurelles des plaques soudées. L'évaluation va être conduite en utilisant l'analyse de variance (ANOVA) pour identifier les impacts des paramètres sur les procédures. Le schéma d'expérimentation s'appuie sur la méthode de planification d'expériences de Taguchi.

La phase initiale de cette tâche implique la réalisation d'une enquête approfondie sur l'évolution des technologies pertinentes pour les processus d'assemblage mécanique, avec une attention particulière portée au procédé de soudage au laser. Cette enquête couvre à la fois les systèmes de mesure susceptibles d'être utilisés afin d'acquérir les données requises à l'analyse du processus de soudage et les approches de surveillance en temps réel du processus

qui présentent un fort potentiel pour des applications dans des environnements industriels qui visent une grande productivité. L'objectif est de dresser la liste des principaux procédés de surveillance et de définir les paramètres potentiels à mesurer, suivre et contrôler durant le processus du soudage au laser. Le but est également d'identifier les systèmes intelligents applicables pour vérifier et anticiper la qualité ultime du produit. L'objectif de cet article est également de rechercher des outils et des capteurs utilisables, qui aideront à présenter une approche méthodologique pouvant peut-être formulée et ajustée en fonction de diverses applications, aussi bien dans l'industrie que dans un environnement de laboratoire. Elle récapitule les conclusions et les performances des systèmes et des approches similaires à celles des études antérieures qu'elle a évaluées.

La deuxième étape de ce travail vise à établir une approche de prédiction des caractéristiques mécaniques, fondée sur une évaluation statistique des résultats expérimentaux. Elle s'applique à un échantillon de plaque d'aluminium de type AA 6061, mesurant (150×40×1.6) mm, superposée à une plaque d'AA 5052 de dimensions (150×40×1.57) mm. Aucun gaz de protection n'est utilisé durant le procédé de soudage et l'écart entre les parties soudées est considéré comme nul. La distance focale, la puissance du laser et la vitesse de soudage, reconnues comme les facteurs les plus déterminants pour la qualité des soudures au laser, constituent le fondement des investigations proposées. Les aspects de la soudure à évaluer incluent la profondeur de pénétration, la microstructure, la résistance à la traction ultime et la micro-dureté. L'établissement des liens entre les variables et la qualité de la soudure vise également à fournir des données cruciales pour déterminer les variables clés en vue de la construction de modèles de prédiction précis et fiables.

La troisième phase de ce travail consiste à détecter et examiner les liens entre les paramètres du procédé de soudage, en employant la performance mécanique comme critère d'évaluation. Cette phase concerne le soudage de plaques d'aluminium de type AA 6061, mesurant (150×40×1.6) mm, en superposition avec l'alliage AA 5086, de dimensions identiques. Lors de ce processus, aucun gaz de protection n'est employé et l'intervalle de séparation entre les sections assemblées est considéré comme nul. Ce projet permet

d'examiner les impacts, les contributions et les interactions entre divers paramètres comme la distance focale, la puissance de soudage et la vitesse de soudage, tout en comparant ces résultats avec ceux obtenus dans la première expérience.

Les expérimentations sont effectuées sur des plaques d'aluminium de type AA 6061, soudées respectivement avec l'AA 5052 et l'AA5086. Un laser à fibre est employé pour cette recherche, émettant un rayon laser d'une longueur d'onde de 1070 nm avec une puissance maximale de 3000 watts. Une stratégie d'expérimentation en utilisant la méthode de Taguchi est sélectionnée afin de maximiser les résultats tout en minimisant le nombre d'essais. Les paramètres pris en compte incluent la distance focale, la puissance du laser et la vitesse de soudage. Les qualités de la soudure évaluées comprennent la microstructure, la micro-dureté et la résistance/force de traction ultime. Une fois la procédure du soudage terminée, les pièces sont soumises à une procédure métallographique classique, incluant le polissage, la gravure et l'observation microscopique. Les résultats sont ensuite analysés statistiquement par le biais d'une analyse de variance (ANOVA) pour déduire les impacts des paramètres considérés et leur influence sur la variation des attributs observés.

## **6. ORGANISATION DU MÉMOIRE**

Au-delà de cette introduction générale, ce mémoire est divisé en trois chapitres, chacun structuré comme un article académique, et elle se conclut par une synthèse générale. L'introduction générale offre une présentation du soudage en général, en mettant l'accent sur le soudage au laser, et se focalise sur la présentation des principes du processus de soudage au laser. Le premier chapitre établit le contexte de la recherche en exposant les principales méthodes d'assemblage mécanique, en accordant une attention particulière au soudage au laser. Il présente également les divers éléments et concepts pertinents à l'évaluation et au contrôle de la qualité du soudage au laser des alliages d'aluminium. De plus, ce chapitre propose un aperçu succinct des diverses approches et techniques utilisées pour la caractérisation, la prédiction, l'optimisation, ainsi que pour la surveillance continue et intelligente des processus de soudage. Le deuxième chapitre se focalise principalement sur

l'optimisation des attributs microstructuraux de la soudure qui influent sur les propriétés mécaniques des pièces soudées. Cette analyse est appliquée à un échantillon d'aluminium d'une épaisseur de 1.6 mm, composé des alliages AA 6061, AA 5052 et AA 5086, et formant des joints en chevauchement.

Le troisième volet de ce projet porte sur la détermination et l'examen des liens entre les paramètres du processus de soudage, en prenant en compte la performance mécanique comme critère de jugement. Ce segment met en scène le soudage de plaques d'aluminium de type AA 6061 avec l'alliage AA 5086, de dimensions comparables. Cela permet d'approfondir les impacts, les contributions et les interactions entre divers facteurs tels que la distance focale, la puissance de soudage et la vitesse de soudage. Les tests pour ce projet ont été structurés en suivant la méthode de Taguchi et les résultats ont été interprétés grâce à la méthode ANOVA. L'objectif de cette analyse est de déceler le meilleur modèle mathématique capable de prédire la réponse de manière appropriée dans le cadre des paramètres d'entrée. Ces résultats sont par la suite mis en parallèle avec ceux obtenus dans la première expérience afin d'évaluer et de comparer l'efficacité des deux processus de soudage. Pour conclure, cette étude donne une synthèse des buts que nous nous étions fixés et des résultats obtenus. Elle atteste des connexions existantes entre ces objectifs et résultats, en mettant en lumière l'importance cruciale de ce travail dans la compréhension des paramètres de soudage laser et leur impact sur la qualité de la soudure. L'importance de contrôler les paramètres du soudage laser pour atteindre les propriétés mécaniques souhaitées pour les alliages d'aluminium AA 6061, AA 5052 et AA 5086 est ainsi mise en évidence. Ce mémoire constitue aussi une fondation solide pour de futures recherches, en suggérant des directions d'études prometteuses pour optimiser les processus de soudage au laser, améliorer la performance des matériaux soudés et intégrer des techniques de contrôle plus avancées et efficaces. Les conclusions de ce travail, ainsi que les méthodes d'analyse employées, s'avéreront sans aucun doute précieuses pour la communauté scientifique et pour les professionnels de l'industrie souhaitant optimiser leurs procédés de soudage au laser et améliorer la qualité de leurs fabrications.

# **CHAPITRE 1**

## **EXPLORATION DES PROCÉDÉS DE SOUDAGE AU LASER : REVUE DES TECHNIQUES D'OPTIMISATION, SURVEILLANCE DE LA QUALITÉ EN TEMPS RÉEL ET RÔLE DE L'IA DANS LES APPLICATIONS INDUSTRIELLES DURABLES**

### **1.1 RÉSUMÉ EN FRANÇAIS DU PREMIER ARTICLE**

Cette revue est centrée sur l'importance croissante du soudage au laser dans diverses industries, mettant en lumière ses avantages et sa complexité intrinsèque en raison de phénomènes physiques délicats et de défis de surveillance et de contrôle. Le projet souligne la nécessité d'optimiser les processus de soudage au laser pour réduire les gaz à effet de serre, élément essentiel pour des pratiques de fabrication durables. Des matériaux légers, principalement les alliages d'aluminium, sont explorés comme une stratégie clé dans l'industrie automobile pour réduire le poids des véhicules, augmentant ainsi l'efficacité énergétique et diminuant les émissions.

L'étude examine plusieurs méthodes d'assemblage, y compris le collage adhésif, l'overlamination, l'assemblage mécanique, et le soudage, avec une revue complète des techniques de soudage au laser comme le soudage au laser hybride, le soudage au laser avec gaz de protection, et la réparation par fusion laser. Le document met également en lumière l'importance des processus de surveillance et de l'intelligence artificielle dans l'optimisation des paramètres de processus, la prévision des caractéristiques de jointure, le suivi de joint de soudure, la classification des défauts, et la validation des simulations.

Les technologies de capteurs et les techniques basées sur l'intelligence artificielle pour l'inspection de qualité en temps réel sont particulièrement mises en avant, la surveillance multi-capteurs et l'apprentissage profond dans la surveillance du soudage étant des domaines

de focus clés. La revue de littérature sert de ressource perspicace pour les chercheurs et les industries cherchant à optimiser leurs processus de soudage au laser et améliorer la qualité des produits, pointant vers l'avenir prometteur d'un système intelligent d'évaluation de la qualité.

## 1.2 CONTRIBUTION

Cet article initial, intitulé “*Exploring Laser Welding Processes: A Review of Optimization Techniques, Real-Time Quality Monitoring, and the Role of AI in Sustainable Industrial Applications*” a été principalement rédigé par son auteur principal, Abdessamad LAKHAL. Pedram Farhadipour, le deuxième auteur de cet article, a apporté des conseils pour affiner l'étude et a également participé à la révision de l'article aux côtés de Noureddine Barka. Ce dernier a supervisé le projet et joué un rôle clé dans l'amélioration de la version finale de l'article.

## 1.3 TITRE DU PREMIER ARTICLE

Exploring Laser Welding Processes: A Review of Optimization Techniques, Real-Time Quality Monitoring, and the Role of AI in Sustainable Industrial Applications

## 1.4 ABSTRACT

This review is all about how laser welding is becoming more important in many different fields. It talks about its benefits and how hard it is to monitor and control because of how complicated the physical processes are. The paper underscores the necessity of optimizing laser welding processes for the reduction of greenhouse gases, which is essential for sustainable manufacturing practices. Lightweight materials, primarily aluminum alloys, are explored as a key strategy in the automotive industry to reduce vehicle weight, thereby increasing fuel efficiency and decreasing emissions.

The study delves into several joining methods, including adhesive bonding, overlamination, mechanical joining, and welding, with a comprehensive review of laser

welding techniques such as hybrid laser welding, laser welding with backing gas, and laser fusion repair. The paper also illuminates the importance of monitoring processes and artificial intelligence in optimizing process parameters, predicting seam characteristics, tracking weld seams, classifying defects, and validating simulations.

Sensor technologies and AI-based techniques for real-time quality inspection are significantly highlighted, with multi-sensor monitoring and deep learning in welding monitoring being areas of key focus. The review paper serves as an insightful resource for researchers and industries seeking to optimize their laser welding processes and improve product quality, pointing towards the exciting future of an intelligent quality assessment system.

**Keywords:** Laser Welding, Real-Time Quality Monitoring, Artificial Intelligence, Sustainable Industrial Applications, Green Manufacturing, Lightweight Materials, Aluminum Alloys, Multi-Sensor Monitoring Technology, Deep Learning, Joining Methods, Hybrid Laser Welding, Monitoring Systems, Welding Sensors.

## 1.5 INTRODUCTION

Global warming, which is a recent problem that requires immediate attention, is a result of too much carbon dioxide (CO<sub>2</sub>) and other greenhouse gases in the Earth's atmosphere. These gases behave akin to an insulating layer that soaks up sunlight while gradually intensifying worldwide temperatures, with adverse implications for various ecosystems' sustainability [37].

To mitigate the consequences of climate change, it is crucial to engage in green manufacturing practices, which can reduce carbon emissions. Renewable energy options should be explored along with creating sustainable practices for minimizing waste and pollution. Better transportation systems also need to be adopted by countries for efficient travel while encouraging low-emitting modes (bikes, electric vehicles). Another key strategy

is enforcing regulations through mechanisms like cap-and-trade systems, which provide incentives for companies to prioritize their contribution to greener industrial processes. [1].

Even though global energy-related carbon dioxide emissions set a new high mark in 2018, few may fail to notice some underlying encouraging shifts. In fact, international statistics show that the rise of global carbon dioxide emissions has reduced over time, while specific countries and regions have successfully cut down their respective CO<sub>2</sub> discharge levels. Nonetheless, achieving significant reductions in overall global carbon output demands unity among nations. [2].

Sustainable economic development requires the utilization of environmentally friendly materials that decrease greenhouse gas emissions. Promoting environmentally friendly materials and technologies is a common goal, with initiatives and policies in place to support it. The automotive industry is exploring lightweight materials to achieve this. Vehicle weight reduction through lightweight materials can enhance fuel efficiency and decrease emissions, as well as efforts to reduce waste and increase recycling, which are also important components of sustainable economic development. [38]. Developed countries' economies greatly rely on the impact of the automotive industry, which should be optimized and improved continuously. Automobile producers have been cutting the weight of vehicles using sophisticated materials to enhance fuel efficiency and restrict emissions. Strict environmental regulations in the industry necessitate that vehicles meet high safety standards while limiting harmful emissions. To meet these requirements, reducing the weight of vehicles is essential, as demonstrated in Figure 5. Over the course of the previous few years, there has been a consistent growth in the production of light vehicles in all the market segments. As a result, research into lightweight manufacturing processes, such as sheet metal forming, has been a focus in recent years, with an emphasis on finding low-cost, innovative methods [39].

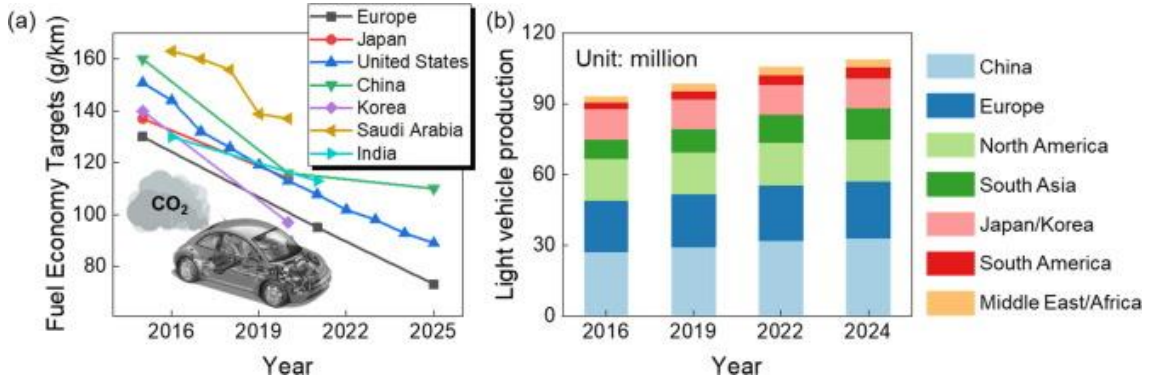


Figure 5: Strong demand for lightweight automobile materials. (a) Goals for fuel efficiency in various countries (passenger vehicles); (b) The number of light vehicles manufactured for the largest vehicle market [6]

Enhancing materials and manufacturing processes for the transportation sector can significantly cut energy consumption and emissions. Applications in transportation see a widespread use of aluminum alloys, from automobiles to the shipping and railway industries. Aluminum alloys are beneficial for their lightweight nature, which can help reduce the weight of vehicles and other transportation systems. This can lead to improved fuel efficiency and a reduction in emissions throughout the production chain of these industries. The increasing use of aluminum alloys in the transportation sector is therefore seen as a key strategy for promoting sustainable development and reducing the impact on the environment [40]–[42].

The automotive industry is an important contributor to the economies of many developed countries and continues to grow every year. In order to continue this growth and optimize the industry's performance, it is important for automotive manufacturers to make use of advanced materials that can help reduce the weight of vehicles. By combining different advanced materials, manufacturers can demonstrate the potential of these materials to contribute to weight reduction. As can be seen in Figure 6, the trend has shifted from using mostly one material for body structures to incorporating numerous materials (such as steel, aluminum, magnesium, and polymer composites) into complex designs (sheets, extrusions, and castings). Effective and efficient design methodologies can also play a role in achieving light-weighting goals. By using advanced materials and optimizing design, the automotive

industry can help improve fuel efficiency and reduce emissions while also maintaining or improving performance and safety [43].

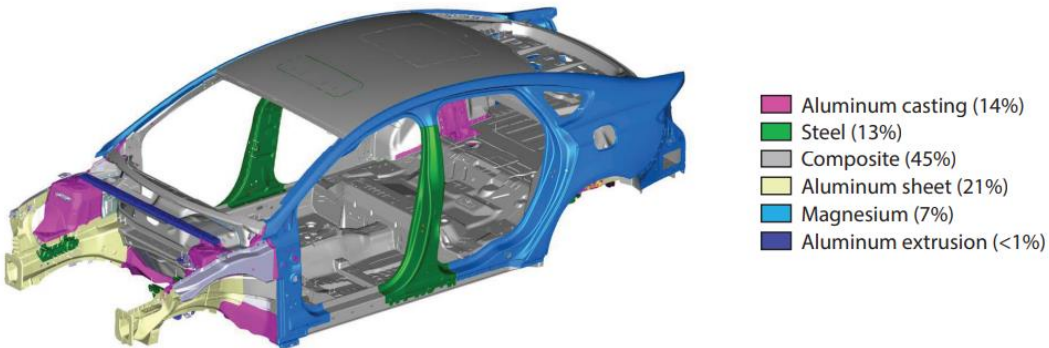


Figure 6: Vehicle composed of a variety of lightweight materials, Material distribution according to the Mach-II body-in-white [4]

During the car manufacturing process, there are certain stages where it is possible to replace traditional steel with lighter materials like aluminum alloys. Aluminum is a good material for reducing the weight of vehicles because it can decrease the weight by 20-30% compared to steel. This makes it a preferred choice for weight reduction in the automotive industry [44].

The development of lightweight cars is a major challenge, especially when it comes to creating hybrid components using a combination of aluminum alloys and steel grades, which are common in modern designs. In a competitive global automotive market, companies are looking for ways to reduce manufacturing costs, and using lightweight technology can be one way to achieve this. Light weighting can be accomplished through the use of new processes and equipment, and it is an important goal for many businesses [45].

One way to improve the sustainability of the industry is to use materials that have a positive environmental impact. In addition to choosing sustainable materials, it is also important to select the best joining method for a particular application in order to make the most effective use of the materials being used. There are various methods available for

joining materials, including overlamination, welding, adhesive bonding, mechanical joining, and hybrid joining, and each has its own strengths and limitations. By selecting the right joining method, manufacturers can optimize the performance and efficiency of their vehicles while minimizing waste and maximizing the use of materials. As is shown in Figure 7, additive manufacturing is not only cheaper for low-volume production, but it can also be used to make parts with more complicated shapes. This makes it possible to reduce weight even more by making true topology-optimized structures that can't be made with other methods [46].

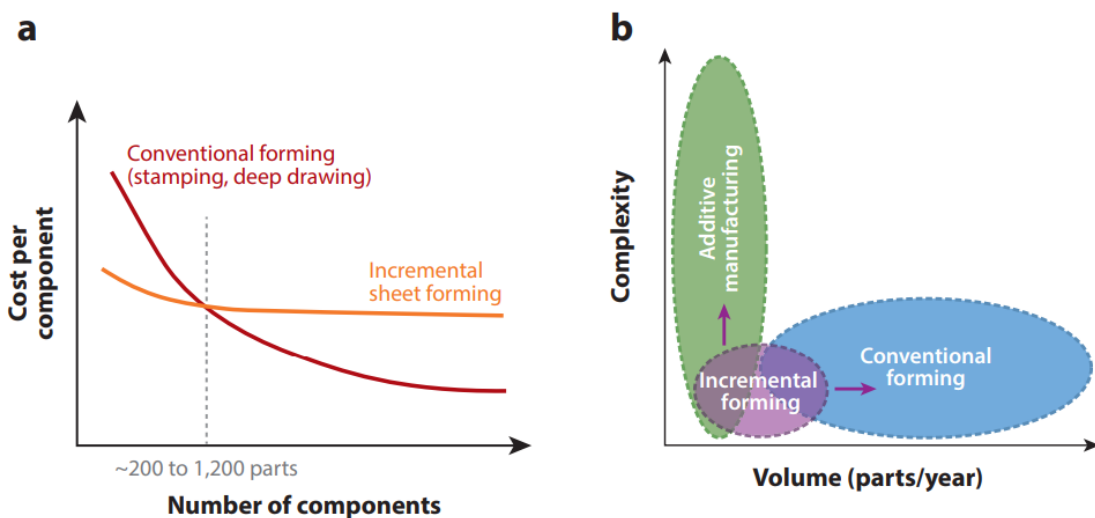


Figure 7: (a) Compared to traditional methods of forming, incremental forming is more cost-effective and can be done at low volumes. (b) Balance between part complexity and the number of parts made for each forming process [13]

This review paper presents a summary of the research that has been conducted on various joining approaches used in industries, with a focus on welding. The review looks at the various factors that can impact the effectiveness of welding, such as the materials being joined, the geometry of the parts being welded, the manufacturing processes being used, and the loading conditions the welds will need to withstand. By examining these factors, researchers can better understand the strengths and limitations of different welding techniques and identify opportunities for improvement.

## **1.6 JOINING METHODS:**

In recent decades, there has been significant progress in various industries, with researchers and professionals working to enhance the effectiveness, durability, and overall functioning of various structures. This has involved designing new approaches and optimizing current methods in order to create more effective and efficient designs. Various aspects should be taken into account while designing structures, such as the materials used, the types of loads the structures will need to withstand, and the operational requirements of the system. By constantly striving to improve the design and construction of various structures, researchers and industry professionals can help to ensure that these structures are as safe, efficient, and durable as possible [47], [48].

The fusion of materials is a significant aspect of manufacturing, as most products, machines, and structures are assembled from multiple parts that need to be fastened together. There are many different methods that can be used to join materials, including riveting, seaming, clamping, soldering, brazing, welding, and the use of adhesives. The most suitable method will depend on a variety of factors, including production economics, the mechanical properties of the materials being joined, and the desired level of reliability. Joining processes are generally divided into four main categories: overlamination, adhesive bonding, mechanical joining, and welding. It is important to choose the most appropriate process at every step in order to create highly reliable devices [49], [50].

### **1.6.1 Adhesive bonding**

Extensive research has been conducted over the last 80 years on adhesive joints, which are now widely employed for joining parts together. Adhesive joints consist of two main parts: the adhesive and the adherends, which are the materials being joined. Generally, parts can be joined in various ways, such as by forming a single or double lap joint or other possible configurations. An improper joint design can compromise its structural integrity. Therefore, a number of analytical models based on the materials used for the adhesive and adherends

have been suggested to address this issue. This can result in lighter constructions, as there is no need to drill holes or add additional hardware [51], [52].

Adhesive bonding allows for the formation of continuous and homogeneous joint lines on the bonding surface, which can lead to more uniform stress distribution, noise and vibration damping, and increased stiffness. Avoiding local stress concentrations, which can occur with other joining methods, is one of the main advantages of adhesive bonding. Overall, adhesive bonding is a versatile and effective method for joining a wide range of materials and has many potential applications in various industries [53].

Adhesive bonding is becoming a more popular option than mechanical fasteners in engineering applications, as it offers numerous advantages over conventional methods. For example, adhesively bonded joints distribute stress more uniformly along the bonded area, resulting in increased stiffness and load transmission, as well as reduced weight and cost. As depicted in Figure 8, a bonded joint can offer higher stiffness and a more even stress distribution compared to a riveted joint. Additionally, adhesives can bond materials with different coefficients of thermal expansion, as their flexibility can compensate for any differences. While adhesive bonding offers many advantages, there are also some drawbacks that require further research and development. For example, peeling and cleavage stress must be reduced as they concentrate the load in a small area, resulting in poor joint strength. Adhesives have limited resistance to extreme temperature and humidity conditions due to their polymeric nature. Moreover, bonding is not typically instantaneous, necessitating the use of tools to maintain the substrates in position, and the hardening process often requires elevated temperatures, which can be a significant economic disadvantage. To ensure a strong and durable joint, careful surface preparation is essential, such as solvent cleaning, mechanical abrasion, or chemical treatments. Quality control can be more challenging than with mechanical fasteners, as it is not possible to dismantle an adhesive bond. However, several non-destructive techniques are now available [54] – [57].

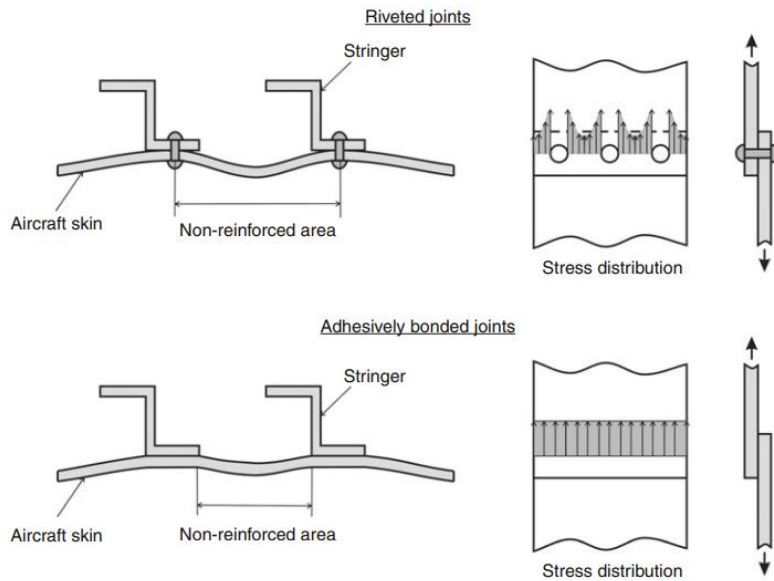


Figure 8: Comparison of Stiffness (Left) and Stress Distribution (Right) in Adhesively Bonded Joints Versus Riveted Joints [54]

### 1.6.2 Overlamination

Overlamination is a technique often used to connect parts using adhesives that are laminated directly onto the assembly. However, it is important to evaluate the stress distribution in such joints. Overlamination is a method used to improve the fatigue resistance of joints in thin-walled sandwich structures, which are lightweight composite structures made up of a low-density core sandwiched between two thin, stiff facings. These structures have high energy absorption properties, excellent stiffness-to-weight ratios, and superior ballistic resistance and are commonly used in the marine and naval industries. In figure 9, we have a variety of common materials and cross-sections employed in overlaminated joints. However, one of the main challenges in constructing these structures is joining the panels together and attaching them to other substructures. To address this challenge, the overlamination method has been developed. In general, an overlaminated joint consists of two parts that are bonded together through lamination. Overlaminated joints offer several advantages, including reduced fastening and assembly costs, lower primary structural weight, and faster construction times [58], [59].

There are several different types of cores that are commonly used in sandwich panels, including truss cores, foam cores, corrugated cores, and honeycomb cores. These cores have different structures and properties and are chosen for specific applications based on their strengths. Truss cores, honeycomb cores, and corrugated cores have periodically repeated inner structures and tend to have more empty volume in the core region compared to foam cores. Corrugated cores usually have open channels in one direction, while honeycomb cores are typically closed-cell structures with a variety of shapes, including hexagonal, square, and rectangular. In recent years, there has been a lot of research focused on developing new patterns and designs for these core structures [50].

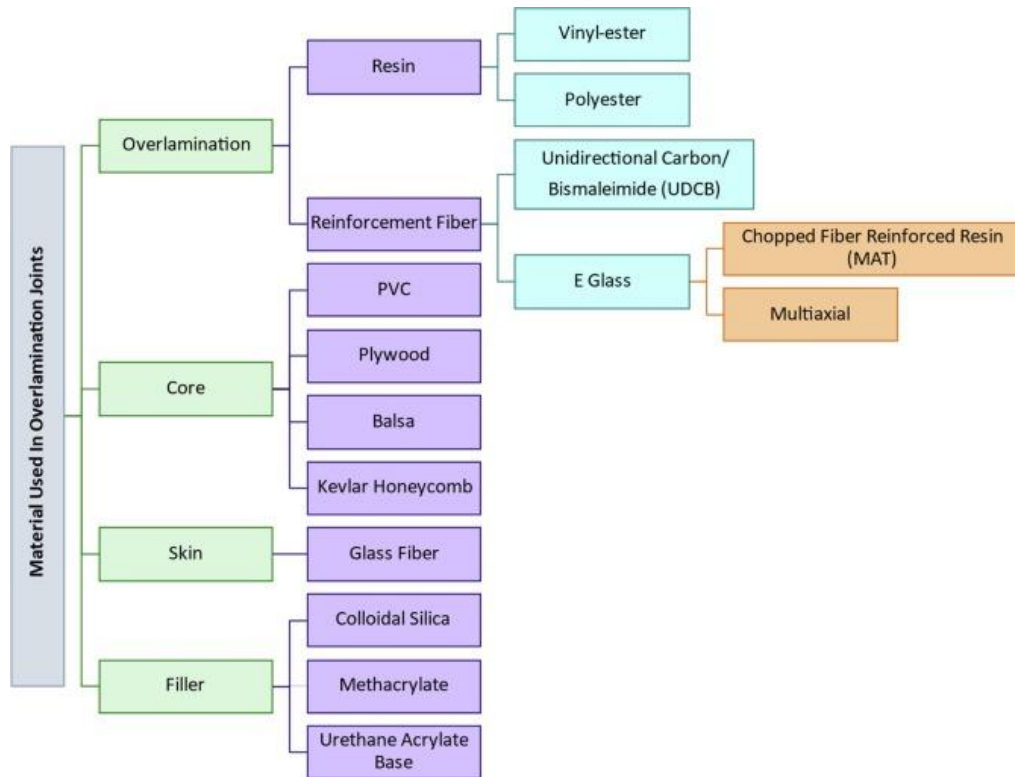


Figure 9: Variety of common materials and cross-sections employed overlaminated in joints [46]

### 1.6.3 mechanical joining

Joining is an essential aspect of manufacturing processes as it allows for easy, efficient, and cost-effective fabrication of products. Casting alone cannot produce complex or high-quality objects. Although costly casting methods like investment casting can be used for research or prototyping, they are not economical for large-scale production. Therefore, a basic-shaped object is first cast and then further processed to achieve the desired features and improve the surface finish and dimensional tolerance. Joining is a post-processing technique used to assemble individual components or structures to create a larger one. It is defined as the manufacturing process used to join two or more solid components, either temporarily or permanently. Joining can involve additional elements like filler metal, rivets, straps, nut-bolts, screws, cotters, keys, or external inputs like heat, pressure, or shockwaves. Joining is not limited to metals and can also be used for plastic, ceramic, and composite materials. There are various joining processes available that can be broadly classified into two categories: temporary joining and permanent joining, as shown in figure 10 [60].

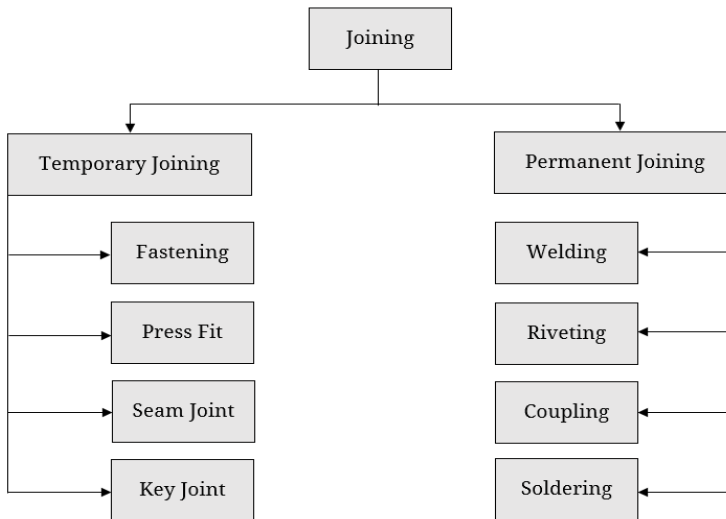


Figure 10: Categories of joining: temporary joining and permanent joining [27]

## **1.6.4 Welding**

The Iron Pillar of Delhi in India, established almost 1700 years ago, is one of the largest welds from that time. However, it was not until the 19th century that modern welding techniques, which involve creating a metallurgical bond between metallic materials, were invented. Today, various welding concepts such as laser transmission welding, friction stir welding, ultrasonic welding, and hot fusion resistance welding have replaced mechanical fastening and adhesive bonding. Ultrasonic welding is the most widely accepted process for plastic materials and can be automated. Numerous welding processes exist, and undoubtedly, more will be developed to meet the evolving demands of metalworking. Typically, welding processes can be categorized into two groups: fusion welding and solid-state welding, which encompass all the different welding techniques. We can join dissimilar materials using welding, such as metals and polymers. The main mechanism of joining is mechanical interlocking. There are several different welding techniques that can be used to join similar and dissimilar materials, including ultrasonic welding, induction heating joining, friction stir welding, and laser welding [61]–[63].

### **1.6.4.1 Friction welding**

Friction welding is a type of solid-state welding process where the material is plastically displaced and fused by applying a lateral force known as 'upset' while generating heat through mechanical friction between a moving component and a stationary one. As melting does not occur during this process, it is technically not a traditional welding method but rather a forging technique. Despite this distinction, the term 'welding' is still commonly used due to the similarities between the two processes. Friction welding is widely used in the aviation, automotive, and other similar industries for joining metals and even thermoplastics. There are various types of friction welding, such as the spin weld method, where the setup includes a fixed chuck and a rotating one, both of which are used to hold the two parts that will be welded together. As depicted in Figure 11, this method is alternatively referred to as inertia welding, rotational welding, or inertial friction welding. Linear friction welding shares

similarities with spin welding, although the moving chuck moves laterally rather than spinning. As a result, this technique requires the constant application of pressure and the use of high-shear strength materials. Friction surfacing welding is a process that is based on friction welding but differs in that it involves the application of a coating material to a substrate. A mechtrode, which is a rod made of the coating material, is rotated while under pressure, creating a plasticized layer at the interface between the rod and the substrate [63].

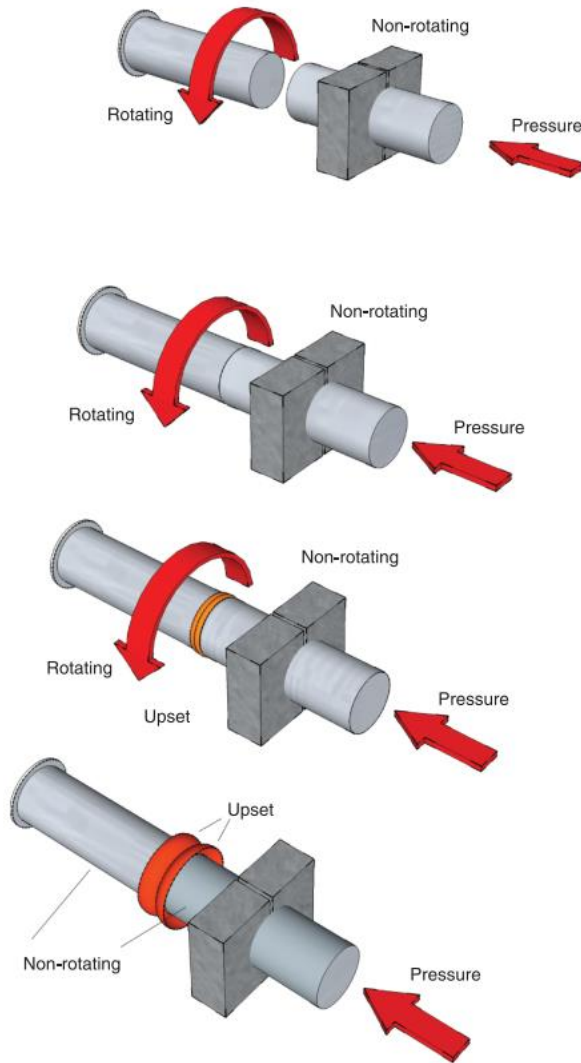


Figure 11: Conventional friction welding, also known as rotational welding [30]

Friction stir welding and friction stir processing are similar processes that are differentiated based on their applications. In friction stir welding, a non-consumable, rotating tool is inserted between the interfaces of two sheets to create diffusion at their edges, which results in the joining of materials, as shown in Figure 12. The advancing side in friction stir welding/processing is where the flow of materials has a higher temperature, while the retreating sides is the phase where the material flow has a lower temperature. Investigating the advancing and retreating side can differentiate between friction stir welding and friction stir processing. Figure 12(b) illustrates the basic schematic of friction stir processing, where stirring occurs in reversed processing directions. Friction stir welding overcomes the problem of void formation that occurs during arc welding. To carry out friction stir welding, a shoulder protruding with a pin, called a probe, is required. The shoulder arrangement creates frictional heating, while the pin probe facilitates stirring at the joint interface, as shown in Figure 12(a). The friction welding tool is a crucial component for the success of the process. It consists of a rotary round shoulder and a cylindrical pin with threads. Despite significant efforts to develop economic and reusable tools in the previous years, most of the attempts have been empirical in nature. Further work is required to refine the tool geometry for modifying the practice of friction stir welding for hard metals and alloys [64].

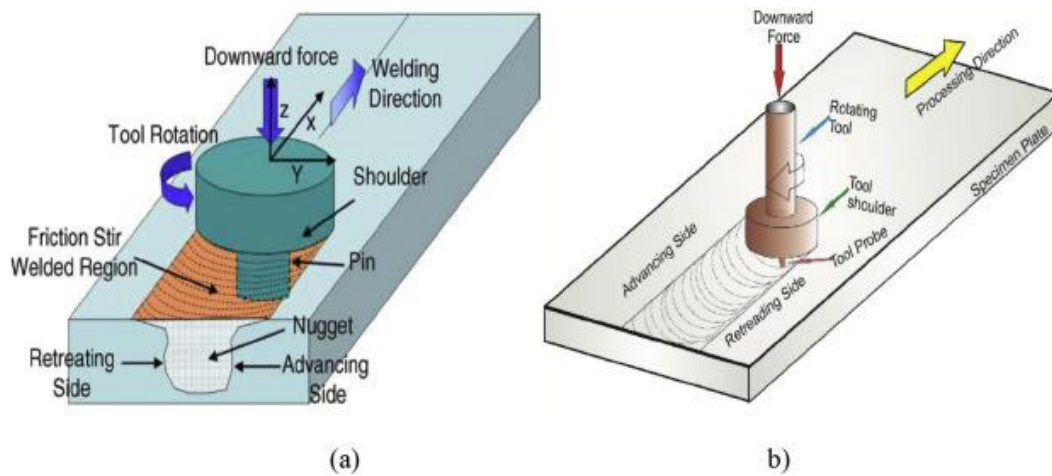


Figure 12: (a) Schematic illustration of friction stir welding; (b) Schematic illustration of friction stir processing [173], [174]

Friction stir welding process factors are tool rotational speed, welding speed, and axial load, which have a higher influence on joint characteristics. The selection of process parameters is the key to get sound joints without flaws. Generally, slower rotating speed and weld speed help provide higher heat input used for thick and difficult alloys. A combination of lower welding speed and faster rotational speed tends to enhance the heat supply and weld temperature. Although extremely low or high rotating speed and welding speed result in diverse mechanical qualities, therefore, it is significant to apply an optimal combination of process parameters to get superior joints [65].

#### 1.6.4.2 Ultrasonic welding

Ultrasonic welding is a technique that utilizes ultrasonic vibration to generate a solid-phase bond between objects by rubbing them together under the influence of static pressure. This vibration, which occurs at frequencies ranging from 20 kHz to several gigahertz, is fundamental to ultrasonic metal welding. The use of high frequency ultrasonic vibration can aid in promoting acoustic softening of materials during welding, akin to the process of thermal softening. However, research has demonstrated that the heat energy required to produce an equivalent softening effect is approximately 107 times greater than that of ultrasonic energy. As a result, ultrasonic metal welding requires less energy than other welding methods. During a typical ultrasonic metal welding process, specimens are pressed together and rubbed under the pressure of the horn, leading to plastic deformation and metallurgical reactions at the joint interface, resulting in permanent bonding facilitated by ultrasonic and thermal softening. While originally developed for plastic connections, advances in ultrasonic technology have enabled the application of this technique to metal bonding [66], [67].

Figure 13 depicts a typical ultrasonic welding system comprising an ultrasonic generator, transducer, booster, and horn. The generator supplies the excitation signal required for welding, while the transducer converts this signal into ultrasonic vibration. The booster amplifies the amplitude of the vibration, which is then transmitted to the horn. During

welding, the materials experience plastic deformation and generate frictional heat due to shear and frictional forces. Electrical energy is transformed into mechanical energy, which facilitates the formation of a stable connection at the welding interface. Prominent manufacturers of USMW equipment include Telsonic, Schunk, Branson, Sonics, Dukane, and Sonobond, among others. This section provides a review of the current state of research on ultrasonic generators, transducers, boosters, and horns, respectively [68]–[70].

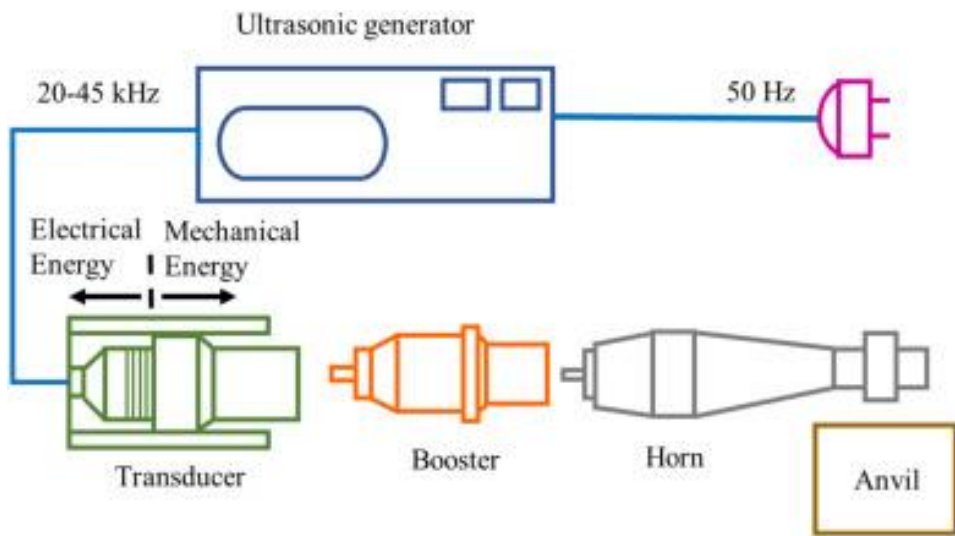


Figure 13: Diagrammatic representation of an Ultrasonic Welding System [35]

#### 1.6.4.3 Induction heating joining

In order to create a joint between metal and fiber-reinforced plastics using thermal techniques, one of the joining partners or a filler material must be partially or completely melted during the cooling phase of the process. Fiber-reinforced plastic components with a thermoplastic matrix are particularly suitable for thermal joining. The metallic component typically conducts thermal energy to the fiber-reinforced plastic component until the matrix melts, and the required heat can be generated using methods such as radiation, convection, friction, or electromagnetism. An additional fixture is usually needed to transmit the joining force. Conduction heating is an efficient way to generate heat in the joining zone since heat is produced directly at the surface of the metal component. Previous research has focused on

continuous and discontinuous process variants, with the latter consisting of heating, transport, and application of joining force in sequential steps. This variant is less flexible and energy-efficient than continuous variants due to longer process times. Current joining techniques for fiber-reinforced plastics and metal joints are not very productive due to the high number of process steps or the long process times required for curing the applied glue. Additionally, the complexity of the parts and surfaces that can be joined is limited, depending on the technique and its advantages or disadvantages. [71], [72].

#### 1.6.4.4     Laser Welding

Welding is the most practical and adaptable joining process used in the fabrication of goods across all industries. The energy required for welding is supplied by a concentrated beam in the process of laser welding. This method is extensively utilized in a variety of industrial settings and has a significant potential to join dissimilar materials. The laser power, the focus point, the pressure, and the welding speed are the most important characteristics to consider while doing laser welding [73]. There are a few different kinds of laser welding systems. CO<sub>2</sub> and Nd:YAG lasers are already in use. In the electronics, low power Nd:YAG lasers are used. Rapid technological progress means that diode lasers with enough power and power density to make good deep penetration welds are now affordable. Among the many laser-welded joints possible, butt- and lap-joints are among the most frequently welded with pulsed or continuous wave lasers [74]. CO<sub>2</sub> lasers have a wavelength of 10.6m and a power range of 1.5–6 kW, though some can work at 10 kW or more continuously. Metals don't have good absorption of the laser beam's energy, with an overall efficiency of up to 15%. However, the laser beam can transfer up to 0.8 of its energy to the workpiece. Mirrors and ZnSe lenses are what make up the optical system. These lasers are used for high-speed sheet welding [75]. The wavelength of a Nd:YAG solid-state laser is 1.06m. Most have an average power of a few hundred watts and a peak power of 1 to 10 kW. There are now lasers in the industry that have a continuous power of up to 3 kW. At this shorter wavelength, metals also absorb more light at the surface. In general, they are only about 3-5% effective. Because the beam's wavelength is shorter than that of CO<sub>2</sub> lasers, it can be guided through flexible glass

fibers. This makes it a good choice for 3D operations with robots that have arms that can move in different ways. This gives more flexibility, easier access, and lower costs [74]–[76].

In hybrid laser arc welding, both arc welding and laser welding are used at the same time in the same area. When a laser beam and an electric arc are used in the same weld pool, they work together to increase welding speed, penetration depth, and the ability to bridge gaps and keep the process stable [77].

## 1.7 REVIEW OF LASER WELDING TECHNIQUES

### 1.7.1 Hybrid laser welding

We can use a laser in combination with a second energy source to have better welding and combine the benefits of two methods like tungsten in-active gas, plasma, and metal inactive gas/metal active gas, but one problem with laser hybrid welding is that there are a number of variables that need to be carefully set and controlled [78].

Laser welding has become popular because the laser beam can be focused on a very small area and make a narrow and deep weld pool. The tight focus of the beam makes it possible to weld at a faster rate, which in turn reduces the amount of heat used and the chance that the welded parts will warp from the heat. But laser welding systems are more expensive, and most of them use a lot more electricity than they should. Laser welding isn't very good at filling gaps, so it takes a lot of care to line up the pieces and prepare the edges. Laser welding is also hard to do with materials that reflect a lot of light, such as aluminum, copper, gold, etc. On the other hand, arc welding processes are very good at bridging gaps, use electricity efficiently, and can join materials that are highly reflective. Arc welding systems are a lot less expensive than laser welding systems that can do the same job. But low energy density during arc welding slows the process down, which causes a lot of heat to be put into the weld zone and causes the part to warp. When both laser welding and arc welding are used

in the same weld pool, the hybridization effect makes up for the weaknesses of each process and builds on its strengths [79]–[88].

### **1.7.2 Laser welding with backing gas**

When a laser beam hits a piece of metal, it will quickly melt and even evaporate, leaving a keyhole on its surface. It makes laser welding penetrate deeper. The dynamic behavior of the keyhole and molten pool in laser welding shows a more complicated pattern. The behavior of the molten pool in full penetration laser welding with or without backing gas was studied, and it has been found that the backing gas makes the root hump form much better [89]. The use of side gas flow during full-penetration laser welding is a tried-and-true technique that can significantly enhance the quality of laser weld joints [90].

Weld porosities were diminished when nitrogen was utilized as a shielding gas, during high-power laser welding of 304 L stainless steel, the shielding gas composition had a substantial effect on the weld porosity [91]. Helium's strong ionization potential and thermal conductivity made it an ideal shielding gas for laser welding, increasing the weld width, the molten pool temperature, and the solidification time in ways that encouraged the bubbles to escape [92][93].

### **1.7.3 Laser welding trajectory**

The oscillating frequency is a reflection of the periodic movement speed of the laser spot as well as the degree of coincidence between beam trajectory and oscillation. Because of the greater oscillation frequency, there is a larger stirring effect, which causes the molten metal to behave differently in terms of its flow and its ability to solidify. Although the amplitude of the oscillation reflects the action range of the heat source, if you increase the value of this parameter, the laser beam will be able to cover a larger portion of the surrounding region. The trajectories of the lasers change depending on the particular oscillating mode that is being used, such as circular oscillating, transverse oscillating, infinite-shaped oscillating, and so on [94], [95].

Weld performance is enhanced by laser oscillating welding due to its ability to reduce grain size, increase gap tolerance, and decrease porosity defects [96]–[98]. Weld morphologies were enhanced by the beam oscillation, and the development of equiaxed grain was encouraged. The strongest weld was achieved with circular oscillation. The beam oscillation barely changed the weld's tensile strength, but it clearly improved its ductility. Welds with circular beam oscillation experienced greater strain than those without such motion. Reduced weld morphological flaws and more equiaxed grains were responsible for the ductility boost [99], [100].

#### **1.7.4    Laser fusion repair**

Laser fusion repair is a technology that may efficiently fix the surface collapse defect in a laser weld. While this is happening, the microstructure of the repaired weld is being refined as a result of the recrystallization that occurs during laser secondary fusion. As a result of this, the residual stress is being reduced and the fatigue performance is being enhanced. Additionally, resistance to tiredness is enhanced [101].

### **1.8    MONITORING PROCESSES AND AI**

#### **1.8.1    Monitoring processes**

Technology that can monitor processes in real time is essential for increasing productivity in welding and ensuring the quality of the final product. real-time welding quality monitoring through the use of sensors, cutting-edge tools, and AI-based methodologies now under development and study [102]. Figure 14 shows the process monitoring and feedback control experimental setup using a single-mode CW fiber laser.

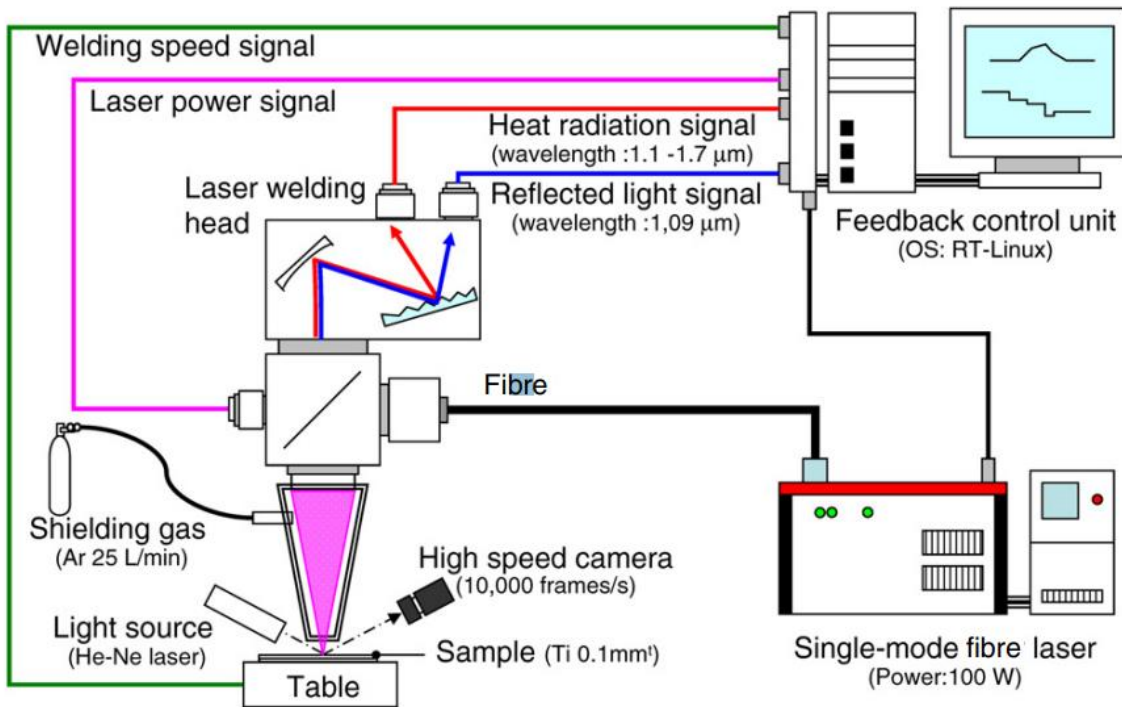


Figure 14: Process monitoring and feedback control experimental setup using a single-mode CW fiber laser [70]

In the process of laser welding, the keyhole, molten pool, plasma, and spatters all include various types of welding signals. These signals, which include the acoustic signal, the optical signal, the thermal signal, and others, are all intimately related to the quality of the welding. As a result, a sensor-based real-time monitoring system is able to effectively gather welding signals in the welding zone [103]–[106]. It has been shown that real-time monitoring of laser welding can significantly mitigate the damaging effects of a number of potential confounding variables on weld quality. There are three distinct phases to the monitoring procedure: the pre-processing scanning, the in-process monitoring, and the post-process diagnosing, as shown in figure 15 [107]–[109].

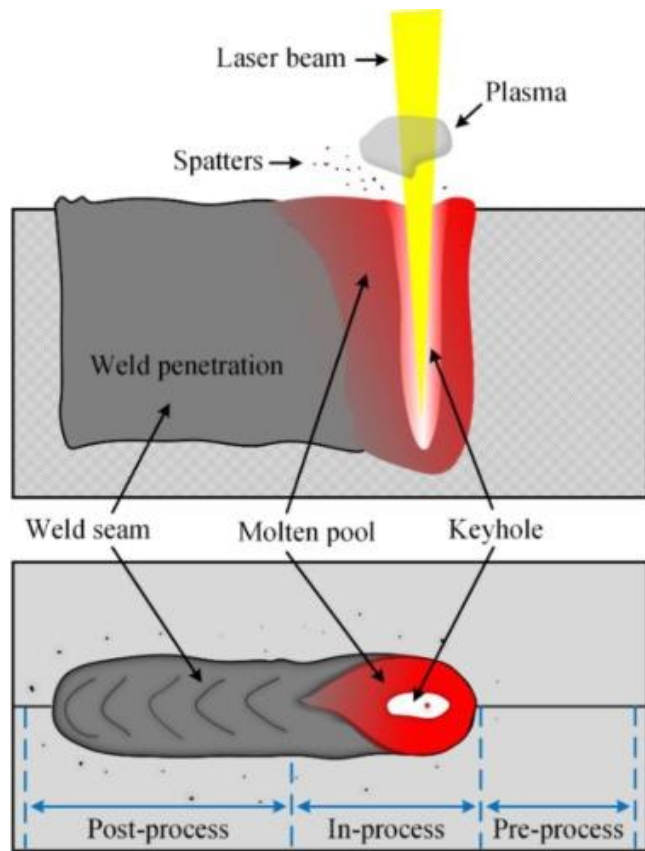


Figure 15: The diagram illustrating laser welding and the explanation of the distinct monitoring phases [110]

Pre-process scanning focuses on seam tracking by scanning the joint gap between workpieces to guarantee the laser beam spot focuses on the gap center for reliable joints. In-process monitoring monitors welding features such as keyholes, molten pools, plasma, and spatters in real time using various equipment [111]. Effective AI-based algorithms can predict and adapt weld seam quality by studying the dynamic changes of these variables. Post-process diagnostics covers defect diagnosis. Pores, cracks, spatters, surface collapse, underfill, and other weld product flaws are key indicators of weld seam quality. Defect diagnosis technology may detect weld faults in time to evaluate weld seam quality, improving product qualification rates [112]–[114]. The major monitoring goals, monitoring signals, and monitoring technology for various welding monitoring phases are summarized in Table 2.

Table 2: Monitoring objectives, monitoring signal, and monitoring technology in different monitoring stages

	<b>Monitoring objectives</b>	<b>Monitoring Signal</b>	<b>Monitoring technology</b>
<b>Pre-process</b>	Seam tracking Gap measuring	Optical signal	Machine vision Laser triangulation
<b>In-process</b>	Welding stability Defects monitoring Molten pool and keyhole geometry Feedback control Feature prediction	Acoustic signal Optical signal Electrical signal Thermal signal	See Figure 16
<b>Post-process</b>	Defects classification Weld geometry	Optical signal Acoustic emission	Machine vision Non-destructive inspection Metallographic test Laser triangulation

In order to comprehend the welding signal gathering procedure, the following section elaborates on the most popular multiple sensor fusion monitoring technology, in addition to discussing some of the most widely used sensors and unique monitoring approaches. Figure 16 depicts a taxonomy of monitoring sensors and methods.

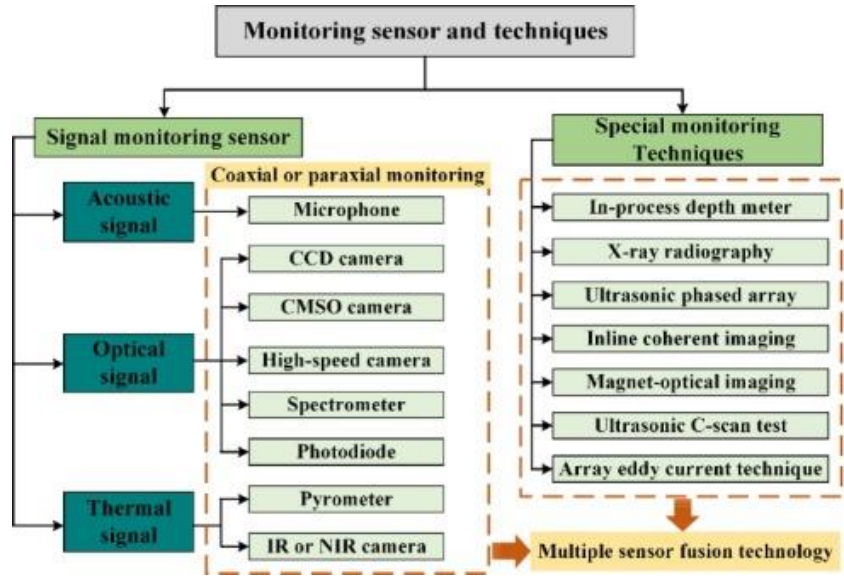


Figure 16: The categorization of sensors and methodologies [110]

### 1.8.2 Fundamental sensors utilized in monitoring

#### 1.8.2.1 Thermal signal

In the welding zone, the thermal radiation signal is particularly robust in the keyhole, the molten pool, and the high-temperature metallic vapor. Sensors like the pyrometer, and the infrared camera are frequently used to collect thermal data. The pyrometer's advantages are that it is less expensive and simpler to put together. The thermal signal was collected using a combination of ratio pyrometry and two-dimensional resolved measurement. It was demonstrated that two-dimensional temperature data had no effect on thermal radiation emissivity or attenuation. This innovative method might be used to determine the diameter of the molten pool, the latent heat, and to validate the simulation based on the Finite Element Method. Black body emission spectra at different temperatures are depicted in Figure 17 (a). The entire amount of radiation that is emitted is determined by the temperature, which is quite high in the welding zone, where the thermal radiation is also extremely powerful. Also, Figure 17 (b) shows a comparison of the pictures that were captured by a Si camera (on the

left) and an InGaAs camera (on the right) of the welding zone and its surroundings [115]–[120].

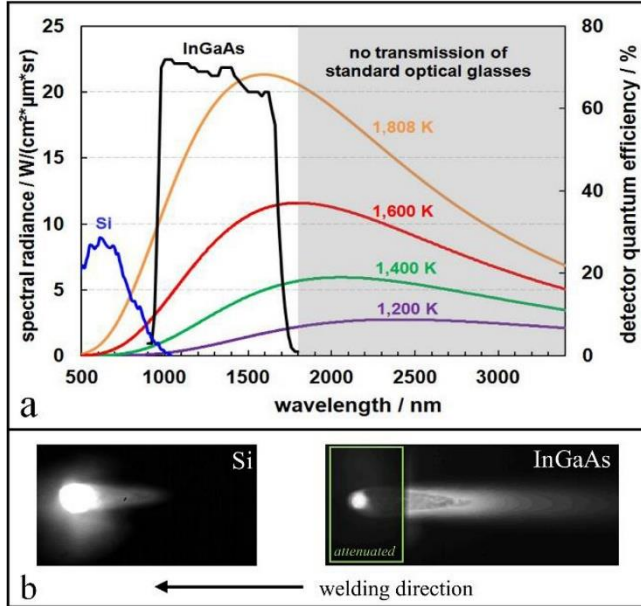


Figure 17: NIR camera-based online diagnostics. (a) Black body emission spectra based on Planck's law for different temperatures compared to Si and InGaAs detector sensitivity. (b) Comparison of images of the welding zone and its surroundings captured with a Si camera (left) or an InGaAs camera (right) [36], [121]

### 1.8.2.2 Optical signal

The major components of optical signal monitoring are optical radiation monitoring and optical vision monitoring. The laser beam and the welding zone are the primary sources of the optical radiation signal; also, strong optical radiation is being released from the molten pool, spatters, plasma, etc. [122], [123].

There are two types of optical radiation signals: one short and one long. The first group comprises radiation with a wavelength between 0.3 and 0.7 micrometers, including ultraviolet and visible light. The infrared spectrum, which spans 1.1 to 1.6 micrometers, is another option. An optical radiation signal can be gathered with the use of a spectrometer and a photodiode sensor. In order to collect independent information on the thermal status of

the molten pool (indicated by the T signal), the radiation from the plume (indicated by the P signal), and the reflected radiation of the laser beam (indicated by the R signal), three photodiode sensors were utilized. The R signal has a wavelength of approximately 1.0 micrometers, and a thorough illustration of optical radiation bands can be found in figure 18(a). Also, the monitoring system's architecture can be found in figure 18(b) [124], [125].

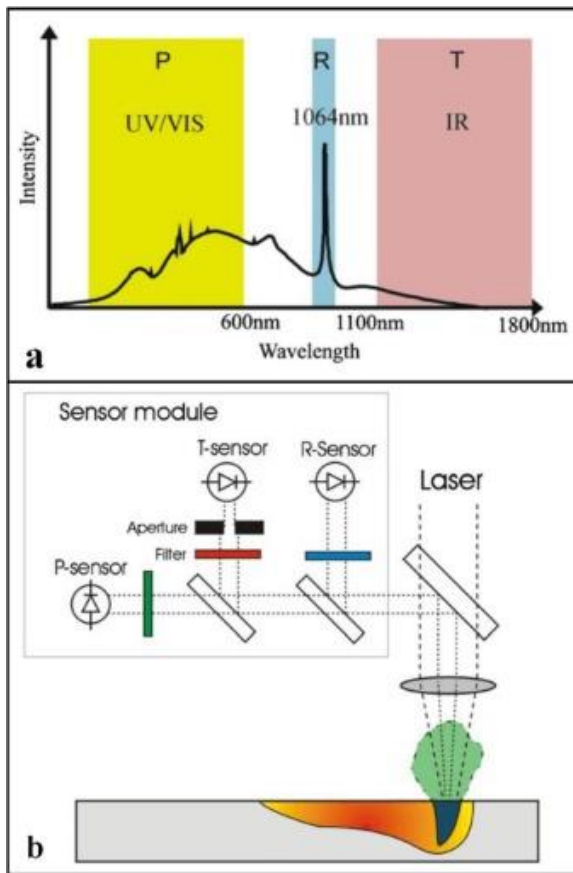


Figure 18: The spectral range for monitoring and the schematic diagram of this monitoring method [125]

Due to the high volume of accurate data that can be collected using optical vision monitoring, it has found widespread application. The keyhole, molten pool, spatters, plasma plume, and other morphological aspects are constantly shifting throughout the laser welding process. There is a direct relationship between the fluctuation of welding quality and these dynamic signals generated during the welding process. Using the image processing

technique, we can examine the dynamic behaviors of the keyhole under various welding settings. Figure 19 depicts the various sensor configurations used for visual monitoring during laser welding, including the CCD camera, high-speed camera, and CMSO camera, which are typically used for capturing images like plasma or molten pool, etc. Several filters and an auxiliary lighting system are used to dampen the effects of the intense visual radiation [126]–[136].

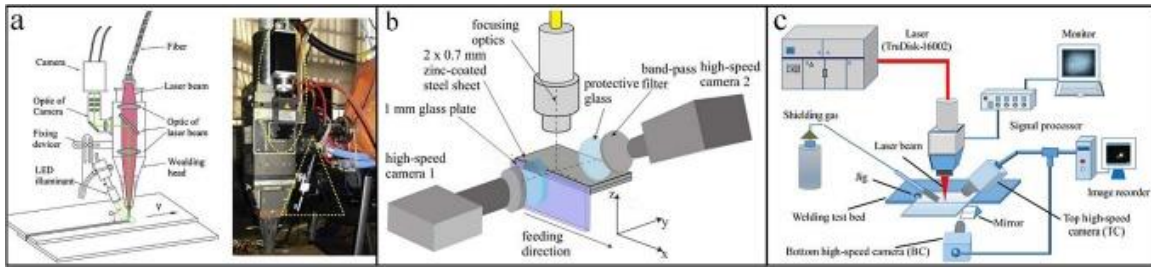


Figure 19: An alternative visual monitoring system. (a) A coaxial surveillance system that also has an auxiliary light source. (b) A system including two high-speed cameras for measuring melt velocities. (c) Observational system works on both the top and bottom [132], [137], [138]

#### 1.8.2.3 Acoustic emission signal

Due to their low price and ease of use, acoustic monitoring techniques have garnered a lot of attention. The acoustic signal is caused by pressure changes in the plasma being ejected through the keyhole, and it can be monitored noninvasively with a microphone or resonant sensor [139], [140]. Due to their low price and flexibility of use, acoustic monitoring techniques have garnered a lot of attention. In order to regulate the arc's length in real time, an automatic measuring and control system was developed to analyze the audio data. For accurate prediction of the molten pool's surface height, a linear fitting model was built based on the linear relationship between the arc sound and arc length. The characteristics of the acoustic signal that are brought on by the vapor flow during welding were modeled in a two-dimensional simulation. According to the simulations, the vapor flow speed is greatest right in the middle of the keyhole and decreases as one moves outside of the hole [141], [142].

Laser welding produces an ultrasonic signal that is very useful for non-destructive evaluation. In order to discover welding problems in aluminum sheets, researchers looked into ultrasonic phased array inspection technologies. This method of inspection was put to the test by comparing its detection results on weld seam quality to those of X-ray radiography and metallographic examinations. According to the findings, this technique successfully detected the presence of porosity. The electromagnetic acoustic transducer uses electromagnetic coupling to generate and detect ultrasonic waves, and it represents cutting-edge research in the area of non-destructive testing and inspection. Compared to more conventional methods of ultrasonic inspection, an electromagnetic acoustic transducer provides more reliable results. Penetration depths of the weld seam can be measured with the use of the laser electromagnetic acoustic transducer ultrasonic technology. The depth of the molten pool was determined using data from an ultrasonic phased array technology. The schematic representation of this examination technique is shown in Figure 20 [143]–[147].

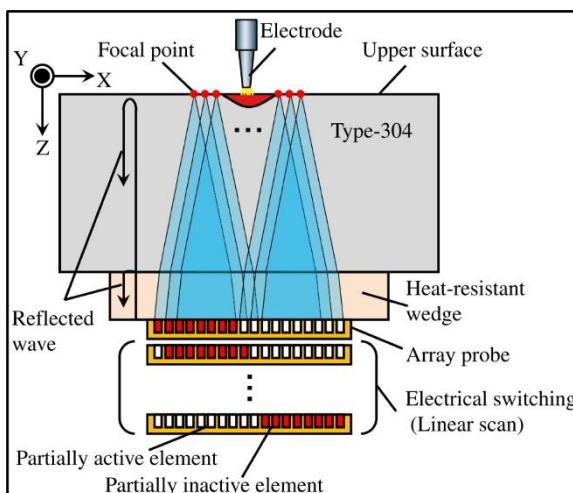


Figure 20: The figure depicts a schematic image illustrating the measurement of molten pool depth using an ultrasonic phased array system [143]

### 1.8.3 Monitoring methods

Certain typical sensors are subjected to the conventional methods of monitoring in order to track the welding process in coaxial or paraxial orientations. Coaxial monitoring

involves placing a spectroscope in the direction of the laser, allowing a view of the welding area. The optical and thermal signals that were obtained, are more stable and have less noise. Nevertheless, this approach lacks adaptability because of the difficulty involved in setting up the monitoring sensor. Seeing the keyhole and molten pool could be restricted by the reflected laser energy and plasma. Paraxial monitoring's strength is in the flexibility it affords in terms of adjusting the distance and angle at which the sensor is placed in relation to the welding area. The optimal monitoring site can be determined and recorded via repetitive calibration and comparison. Both coaxial and paraxial observation of the optical and thermal signals is possible. Common examples of paraxial assemblies include the microphone used for acquiring acoustic signals and the pyrometer used for detecting thermal ones [148]–[153].

Some new ways to keep an eye on things, like the X-ray imaging technique, inline coherent imaging, and magneto-optical imaging, have been recommended and have performed very well. Since its invention, the X-ray has found several uses as a non-destructive method of inspection. Information regarding the keyhole dimensions can be obtained in real time and in high spatial resolution with the use of in-situ X-ray videography applied to the welding process. Due to its excellent spatial and temporal resolution, X-ray technology can also be utilized to evaluate internal problems in a weld seam, examine the weld seam's microstructure and mechanical properties, and estimate the weld seam's residual stress distribution [154]–[156].

To extract the tomographic geometrical measurement data during the weld seam forming process, a monitoring device based on Fourier-domain optical coherence tomography was used. This technology is a novel sensor 3D measuring method for automated laser welding, and it can offer an industrial solution to inspect the keyhole depth in real-time. Inline Coherent Imaging Monitoring Innovation applies the principles of optical coherence tomography to laser processing metrology. Figure 21 (a) is a diagram of how the Inline Coherent Imaging system works. The Inline Coherent Imaging system is made up of a fiber-optic Michelson interferometer. To estimate the depth of a keyhole, an image beam is coaxially delivered with the laser beam. Figure 21 (b) is a graph that shows how the profile

of the weld penetration and the measured keyhole depth fit (green dots). It is clear to see that the curve that is made up of green dots follows the same pattern as the weld penetration [157]–[160].

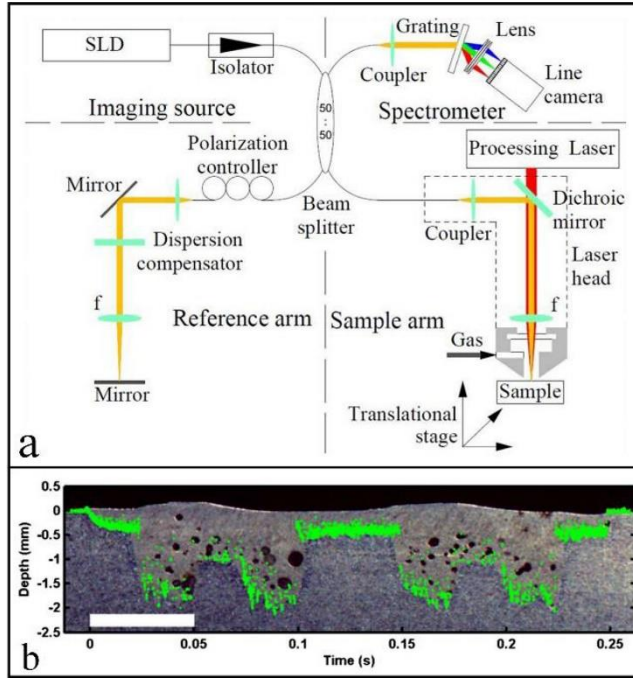


Figure 21: (a) Illustrates the schematic diagram of the ICI (Internal Control Instrumentation) system, (b) Displays the measured depths obtained using the ICI system, represented by green dots [161]

Complexity increases in the laser welding process whenever numerous laser beam reflections occur at the same time. Many of the signals from welding are indicative of the quality of the weld when monitored by a single sensor or technique. As a result, the suggested multi-sensor fusion technology can keep a closer eye on the welding process. As a result of their ability to provide detailed information about the weld area, vision sensors have quickly become an integral part of multi-sensor fusion systems. Most of the time, one or more vision sensors are part of the established monitoring system. A simplified diagram of the sensors used in a typical multi-sensor fusion system is depicted in Figure 22. Two photodiodes, a spectrometer, two video cameras, and an X-ray detecting system constitute the deployed sensors. In order to evaluate and simulate the laser welding process more deeply, the results

showed that this monitoring system could collect accurate and effective welding signals [162]–[165].

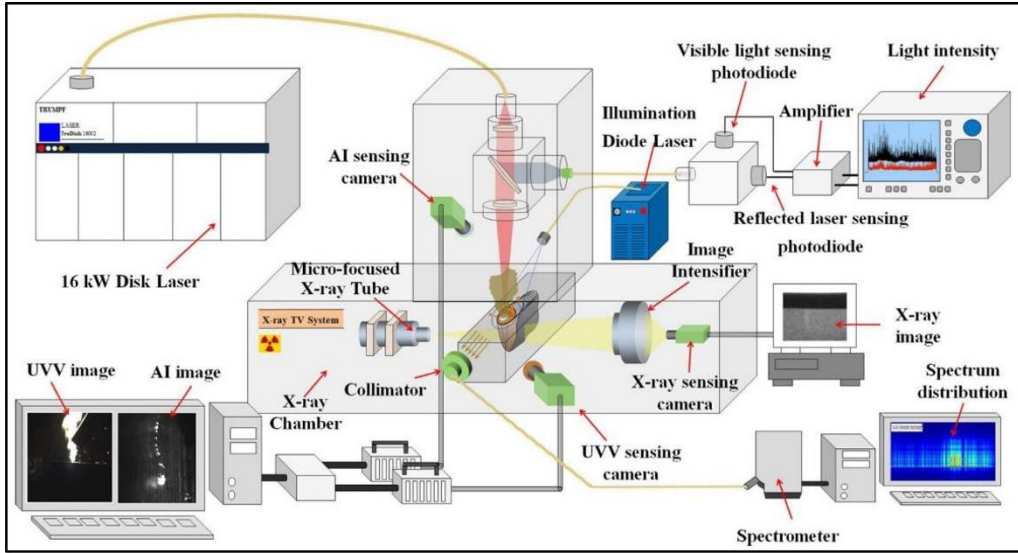


Figure 22: The sensing system comprised six distinct sensors, as shown in the setup [166]

## 1.9 DATA FUSION METHODS

The data from welding signals must be collected and analyzed as part of a comprehensive monitoring system. Data processing and analysis techniques, in particular those based on artificial intelligence (such as machine learning), are summed up in accordance with various monitoring targets. Figure 23 demonstrates the adaptability of AI-based methods in welding, from optimizing process parameters to predicting weld seam features to tracking the welding seam to adaptively controlling the welding process to categorizing weld problems and validating simulation results, etc. [167]–[172].

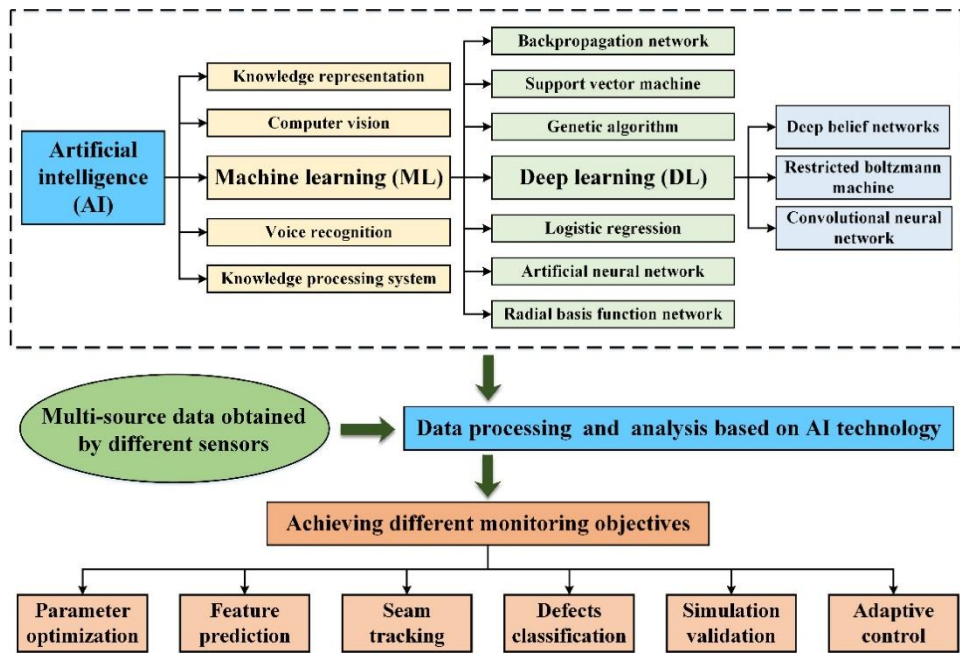


Figure 23: Different monitoring objectives are accomplished through the utilization of various AI-based technologies for data processing and analysis [110]

### 1.9.1 Optimization of the Process Parameters

For better quality welds, you need to set your process settings effectively. Optimization of welding settings is possible using both the Taguchi method and AI-based techniques, and a combination of the two can yield even better optimized solutions. The Taguchi method is popular for optimizing process parameters since it reduces the expense and time required for conducting experiments [173]–[176]. Welding settings were optimized using a combination of a back-propagation neural network (BPN) and an evolutionary algorithm (GA). The welding experiments were planned to use the Taguchi technique. The results showed the utility of the suggested procedure in improving the standard of the welded joint [177]. The laser welding process parameters were optimized in the presence of an external magnetic field using a radial basis function neural network (RBFNN) and GA. The influences of various welding factors, including the optimum parameters, on the appearance of the weld were investigated, and the results revealed that this technology had the potential to significantly reduce spatters [178].

### **1.9.2 Predicting Seam Characteristics**

The visual representation of the welding quality is the weld seam's visual appearance. Features of the weld seam, such as the weld seam's width and penetration depth, can be correctly anticipated by establishing a link with the monitoring signals [179], [180]. Weld seam features were predicted using a back-propagation neural network trained on real-time data from the acoustic signal. The outcomes of the prediction model were found to be in good agreement with the measured data of a real-world welding experiment. Because of its superior performance in spectral line identification, feature extraction, and redundancy elimination, the principal component analysis algorithm is widely employed in data processing [181]. Methods from deep learning and reinforcement learning were used to improve monitoring systems. This monitoring system is capable of learning and adjusting to various welding conditions. Multiple linear regression analysis and BPNN were compared for their effects, and the back-propagation neural network was found to be more effective [182], [183].

### **1.9.3 Tracking of the weld seam**

Effective laser beam placement on the workpiece is essential for the efficacy of the laser welding process, as it determines the welding trajectory and feed rate. In order to meet this need, researchers have spent a great deal of time exploring seam-tracking equipment and methods like infrared imaging technology, vision tracking (i.e., machine vision), and artificial vision technology. It is challenging to establish a steady weld seam when using a conventional teaching and playback robot for multi-pass welding [184]–[186]. The location and properties of the weld seam are extracted and analyzed in real time via a CCD camera-based seam tracking system. Welding trials confirmed and refined this automatic tracking system's recognition accuracy. The findings demonstrated the efficacy of the procedure in detecting seam gaps and tracing weld seams [187]. During butt joint welding, weld seam detection is accomplished using an effective algorithm applied to a single image. This

technique relied on a search of the remnant edge, utilizing an iterative edge detection and edge linking method to obtain the full weld seam [188].

#### **1.9.4 Defects classification**

The quality of weld products is diminished by external or internal welding flaws. Defects in the weld can be minimized with proper defect categorization and close inspection during the welding process. Weld faults, including hammering, cracking, spattering, underfilling, undercutting, blowout, etc., are typically detected using a vision-based detection system in conjunction with a classification model like a support vector machine or a non-destructive detection inspection method like ultrasonics [189]–[191]. The welding zone was monitored using a photodiode and a vision sensor, and faults in the weld were identified using a support vector machine. The findings confirmed the effectiveness of the method in detecting weld flaws. It was found that the ultrasonic phased array technology worked well for locating flaws in the welds of relatively thin sheets of aluminum. By using X-ray radiography equipment and the metallographic inspection method, this detection method can reliably identify the presence of clustered porosity. Weld flaws were detected by tracking and analyzing the radiation emitted by the electron-free plasma [192]–[194].

#### **1.9.5 Simulation validation**

With the aid of the laser welding numerical simulation model, the complex processes occurring in the welding zone may be revealed, allowing for improved comprehension and management of the welding process [195], [196]. The thermal phenomena experienced during the dynamic creation of the molten pool were studied using a combination of experimental data and the finite volume method [197]. The analytical model of the pool's surface temperature was refined using experimental data. Molten pool size and shape were adjusted in the experiment by measuring the three-dimensional topography data of the pool's surface. To regulate the welding process, the calibrated analytic model will supply information on the weld pool's perimeter and depth of penetration [198]. Figure 24 compares

simulation results to experimental data, enabling verification of the simulation model's efficacy. The numerical technique is also a good way to find the most important process parameters and minimize the number of possible weld defects [199].

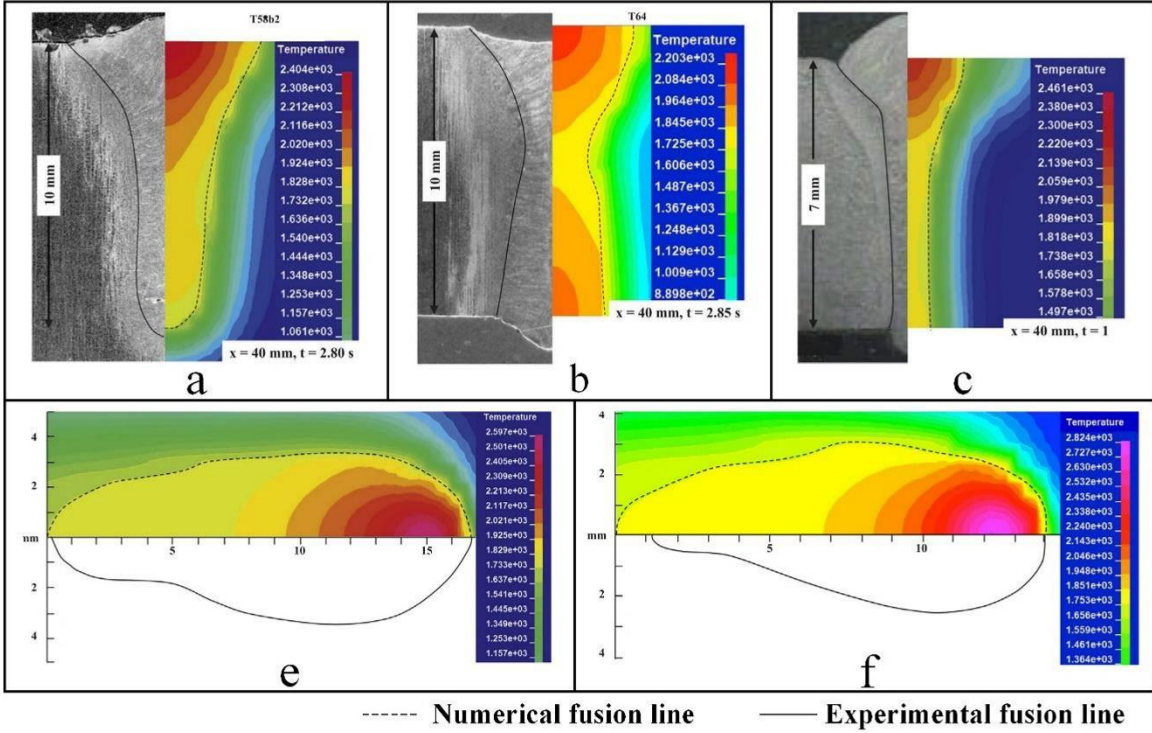


Figure 24: Welding experiment and numerical simulation results compared: (a) and (e) case I: partial penetration, (b) and (f) case II: full penetration, (c) case III: full penetration [209]

### 1.9.6 Command and control in processes

Due to the time required for monitoring signal capture, analysis, and transmission, there is a lag in the correction. But as technology gets better, it takes less and less time to process data. This makes real-time feedback control of the welding process possible [200]–[202]. To keep the width of the molten pool stable during the welding process, a CMOS camera-based control system was developed, using software algorithms to make instantaneous adjustments to the laser power. To adjust the laser welding process, a feedback control method was put in place. This method can optimize and control the focus of the laser beam. The proportional integral derivative algorithm for penetration feedback was provided by the penetration

model, which established a relationship between the weld penetration and the parent metal current. On the basis of this algorithm, a weld penetration monitoring system was developed and implemented. The viability of this approach was demonstrated by the aforementioned experiments. In order to build a smarter and more advanced control system to manage the penetration of the weld seam, in-depth research on the welding process of welders was undertaken. The adaptive neuro-fuzzy inference system mimicked the welding operation of a master welder. As an intelligent welding system, the three-dimensional vision sensing system was employed to continuously monitor the molten pool and record its unique parameters. This monitoring and adjusting mechanism makes the welding process more reliable, which enhances both the efficiency of welding and the quality of the result [203]–[208].

## 1.10 CONCLUSIONS

The application of laser welding processes is rapidly expanding in various industries; however, the implementation of monitoring systems presents a challenge, particularly in the optimization of process parameters and quality inspection of the final product. The laser welding technique provides significant advantages to industries, such as a minimized heat-affected zone that lessens geometrical distortion, increased energy efficiency, and a faster welding speed compared to traditional welding methods. Despite these advantages, laser welding remains a complex procedure due to the intricate physical phenomena involved and the difficulties in surveillance and control. As such, the study and definition of monitoring methods and technologies is a crucial area of focus for the enhancement and application of this solution.

This paper provides a detailed review of the development and exploration of sensors, new equipment, and AI-based techniques for real-time monitoring of welding quality. The process of monitoring welding quality is introduced, and in-process monitoring technology is identified as the most ideal method since it allows for adjustments to be made in real-time based on the monitoring information obtained during the welding process. Various types of

monitoring equipment are reviewed, with visual sensors being widely used due to their ability to provide comprehensive spatial information. The multi-sensor monitoring technology is identified as the most used method, as it compensates for the limitations of single sensors. Lastly, the paper summarizes the application of AI-based techniques in welding monitoring, with a particular focus on deep learning. AI technology has enormous potential in data processing and mining and can help achieve a range of monitoring objectives. Consequently, developing an intelligent quality assessment system is an exciting and challenging area of research.



## CHAPITRE 2

# **OPTIMISATION DES PROPRIÉTÉS MÉCANIQUES DANS LE SOUDAGE LASER D'ALUMINIUM HÉTÉROGÈNE : UNE ÉTUDE SUR LES ALLIAGES 6061 T6 ET 5052 H32**

### **2.1 RÉSUMÉ EN FRANÇAIS DU DEUXIÈME ARTICLE**

Cet article présente une étude approfondie sur l'optimisation des paramètres de soudage laser linéaire pour le soudage d'aluminium, en se concentrant spécifiquement sur les alliages 6061 T6 et 5052 H32. En appliquant une méthodologie basée sur l'analyse de la variance (ANOVA), nous avons examiné les effets de la puissance du laser, de la vitesse de soudage et de la position de focalisation sur la résistance mécanique des soudures. Les résultats ont révélé que la position de focalisation était le paramètre le plus important expliquant 52,81 % de la variance. Les résultats indiquent également que la vitesse de soudage est le deuxième facteur le plus influent, représentant 28,39 % des caractéristiques de la soudure. En utilisant la régression linéaire multiple et la méthode de la surface de réponse, nous avons réussi à élaborer un modèle permettant de prédire la charge de cisaillement par longueur de soudure. Notre étude fournit des informations précieuses pour améliorer la qualité et l'efficacité du soudage laser d'aluminium hétérogène.

### **2.2 CONTRIBUTION**

Cet article initial, intitulé "*Optimization of Mechanical Properties in Dissimilar Aluminum Laser Welding: A Study on 6061 T6 and 5052 H32 Alloys*", a principalement été rédigé par son auteur principal, Abdessamad Lakhal. Pedram Farhadipour, en tant que deuxième auteur, a fourni des conseils pour affiner l'étude et a également participé à la révision de l'article, aux côtés de Noureddine Barka. Ce dernier a supervisé le projet et joué un rôle clé dans l'amélioration de la version finale de l'article. De plus, Anas Ghazi Jerniti, Anas Kerbou, Asim Iltaf et Abderrahim Zilali ont apporté leur soutien dans la réalisation de plusieurs tests, la réalisation des expériences et l'analyse des résultats.

## **2.3 TITRE DU PREMIER ARTICLE**

Optimization of Mechanical Properties in Dissimilar Aluminum Laser Welding: A Study on 6061 T6 and 5052 H32 Alloys.

## **2.4 ABSTRACT**

The mechanical strength of laser-welded aluminum joints is of paramount importance in numerous industrial applications. This study presents a comprehensive investigation into the impacts of different laser welding parameters - focal position, speed, and laser power - on the mechanical strength of aluminum welds for AA 6061 and AA 5052 using overlap welding. Utilizing Analysis of Variance (ANOVA), multiple linear regression, and response surface methodology, we quantitatively evaluated the influence of each parameter. The results showed that the focal position contributes the most to the variance, indicating its profound impact on the weld's mechanical strength. Welding speed ranked second in importance, with laser power exerting the least influence. We also found that specific combinations of these parameters could optimize the mechanical strength of the welds, contributing valuable insights into the development of efficient laser welding processes for aluminum. These findings enhance our understanding of the laser welding process and provide practical guidelines for industrial applications demanding high-quality aluminum laser welds.

## **2.5 INTRODUCTION**

The characteristics of aluminum make it a highly appealing material in today's world, where sustainable development impacts all aspects of industry. As a metal, aluminum boasts solid mechanical strength, impressive resistance to corrosion, a lightweight nature, relatively low density, which results in a significant weight reduction in a car's body in white (BIW), excellent corrosion resistance, and appealing aesthetics. Moreover, aluminum alloys have demonstrated strong mechanical resistance, particularly in terms of rigidity [210]. The benefits of these properties are highly attractive to manufacturing sectors like the automotive

industry. They show a particular interest in the 5XXX alloy, as it can effectively reduce vehicle weight and, consequently, lower energy consumption. At the same time, the vehicles maintain a respectable lifespan.

Aluminum alloys are highly favored in various industries, such as automotive and aerospace, thanks to their exceptional corrosion resistance, lightweight nature, and outstanding mechanical properties [211]. At present, the vehicle body's weight is greatly impacted by dissimilar metal structures welded using various aluminum alloys. In contemporary manufacturing, key welding techniques utilized for joining different alloys include resistance spot welding, laser welding, friction stir spot welding, and the cold metal transfer (CMT) process [212]. Laser welding, offering benefits such as high power, precision, speed, efficiency, and minimal deformation, has become prevalent in metal joining applications and holds significant importance in industries like aeronautics, automotive, and electronics [213]. In the laser welding process, the key concern is the thermal behavior and dynamic nature of the molten pool, as these factors dictate the final microstructure and resulting mechanical properties. To gain a deeper understanding of laser welding, optimize process parameters, enhance microstructure, and boost the quality and attributes of the laser-welded joint, it is essential to investigate the mechanisms of heat transfer, fluid flow, and solidification characteristics of the molten metal [214], [215]. The 6XXX series AA6061-T6, a precipitation-hardened aluminum alloy (Al-Mg-Si), is commonly used in the production of aircraft fittings due to its excellent workability, high strength, and superior corrosion resistance. On the other hand, the 5XXX series AA5052-H32 (Al-Mg) is a non-heat-treatable alloy widely utilized in creating crash-sensitive marine components and ship cabinets, thanks to its impressive corrosion resistance in seawater environments [216]. Additionally, there is a significant challenge in finding a cost-effective welding technique for aluminum, with laser welding proving more profitable than other methods like resistance spot welding, which yields unsatisfactory outcomes due to the low resistivity of aluminum, or MIG welding, which leads to significant thermal distortion [217]. Undoubtedly, laser welding offers significant benefits in terms of weld shape, depth, and limited heat affected zone. It enables welding with outstanding precision and speed, and most importantly, it allows for the

possibility of automating the process, making it an excellent choice for improving productivity [218]. Defects like pores and cracks are common in aluminum laser welding, owing to the properties of the metal and its alloying elements. The low vaporization temperature of aluminum promotes the trapping of gas in the fused metal, while the high solidification rate increases the likelihood of cracks forming [219]–[221]. As a result of these imperfections, aluminum tends to lose its mechanical properties post-welding, particularly in terms of tensile strength. Studies have indicated that the tensile strength of AA 6013 drops to almost one-tenth of the maximum achievable strength for an aluminum alloy after autogenous laser welding. Consequently, researchers have suggested various methods to achieve better outcomes when welding aluminum with lasers. Post-welding heat treatments have yielded promising results as they enhance the properties of the weld by regulating residual stress intensity and allowing for the precipitation of specific phases in the melting zone and the thermally affected zone [222], [223]. However, the oscillation approach requires significant resources, particularly in industrial applications, and is only suitable for heat-treatable alloys like the 6XXX series (excluding AA 5052-H32). A new technique has emerged in the laser welding of aluminum alloys that involves oscillating the laser beam in a specific pattern. This method restrains the deterioration of aluminum properties during welding by limiting heat generation through energy distribution, as the beam follows a non-linear path during oscillation, as demonstrated by Vakili-Farahani et al. [224] on Ti6Al4. This also limits the loss of alloying elements.

Researchers have focused on studying the influence of laser power and welding speed, as they are considered the most significant parameters in laser welding. Ahn et al., who performed laser welding on 3 mm thick aluminum 2024-T3, examined the effects of laser power, velocity, focal length, and gas flow rate on the mechanical properties and microstructure of welded parts [225]. Kim et al. [226] conducted further research by optimizing laser welding of 1.4mm thick AA 5182 alloy, aiming to achieve the best tensile strength at specific values of laser power, welding speed, and wire feed rate. Meanwhile, Abioye et al. [227] developed a predictive model for the tensile strength of welded AA 5052-H32 based on laser power, welding speed, and focal distance. In continuation of these studies,

this work focuses on laser power and welding speed, given their importance as highlighted in previous research.

This study aims to analyze the impact of parameters during linear laser welding of aluminum alloy 6061-T6 with 5052-H32, utilizing the statistical tool of analysis of variance (ANOVA) to determine parameter effects. To obtain sufficient data for numerical calculation, a series of experiments must be conducted, involving systematic variations of parameters and combinations of numerous variations for each parameter. Therefore, an efficient design of experiments is crucial to collect rigorous data for analysis. A complete factorial design is created to quantify the effects of each parameter and exhibit the interaction between them. The study aims to develop a predictive model using linear regression to forecast mechanical properties obtained from a specific parameter set, followed by a response surface to highlight the values of the final parameters for the best tensile strength of the weld, which will be validated through tests.

## **2.6 EXPERIMENTAL PROCEDURE**

### **2.6.1 The materials**

AA6061-T6, an aluminum-based alloy containing Al, Mg, and Si, is a heat treatable alloy belonging to the 6000 family. It is commonly employed in the production of lightweight structures due to its advantageous strength to weight ratio and formability properties [228]. Good corrosion resistance, especially to saltwater, light weight and high strength, and machining capabilities are some of the properties of the AA5052-H32 alloys [229]. As a result, both 5052 and 6061 are extensively utilized in the automotive, aerospace, and transportation sectors [230]. In order to carry out the welding procedure, the specimens were machined to a size of 150 mm in length and 40 mm in width, with a thickness of 0.063 inch (around 1.6 mm) for Al 6061 and a thickness of 0.062 inch (around 1.575 mm) for Al 5052. Tables 3 and 4 display the nominal chemical composition and tensile strength properties of the base materials, respectively.

Table 3: Nominal chemical composition of 6061 T6 and 5052 H32 Al alloys used in this investigation

Material	Al (%)	Cr (%)	Cu (%)	Fe (%)	Mg (%)	Mn (%)	Si (%)	Ti (%)	Zn (%)	Others (%)
6061 T6	95.8 - 98.6	0.04 - 0.35	0.15 - 0.4	<= 0.7	0.8 - 1.2	<= 0.15	0.4 - 0.8	<= 0.15	<= 0.25	<= 0.15
5052 H32	95.7 - 97.7	0.15 - 0.35	<=0.1	<= 0.4	2.2 - 2.8	<= 0.1	<= 0.25	---	<=0.1 0	<= 0.15

Table 4: Tensile properties of 6061 T6 and 5052 H32 Al alloys used in this investigation

Material	Tensile Strength, Ult (Mpa)	Tensile Strength, Yield (Mpa)	Elongation (%)
6061 T6	310	276	17
5052 H32	228	193	12

## 2.6.2 Design of Experiments

The DOE (Design of Experiments) technique provides the most advantageous combination of input parameter values to assess their effects on the process response and achieve the best feasible outcomes given real-world conditions. In this particular study, the input factors include focal position, power, and speed, while the process response is the welding's tensile strength. For the experimental procedure, a three-level analysis was performed on the three factors, with Table 5 outlining the factors and levels and Table 6 presenting the experimental design obtained through the Taguchi method using Minitab software for the experiments.

The weldability area is established through initial tests that involve a sequence of welds, where parameters are adjusted using a trial-and-error approach. In the comprehensive factorial design, every combination of parameters that forms an experimental unit is replicated to gather sufficient samples for mechanical testing and microscopic examination.

Table 5: Factors and Levels for Experiment

Factor	Levels		
	1	2	3
Laser Power (kW)	2.5	2.7	2.9
Speed (m/min)	4	5	6
Focal position	+3	+5	+7

Table 6: Factors and Levels for Experiment

Experiment Number	Input parameters		
	Focal Position (mm)	Power (kW)	Speed (m/min)
1	+3	2.5	6
2	+3	2.7	5
3	+3	2.9	4
4	+5	2.5	5
5	+5	2.7	4
6	+5	2.9	6
7	+7	2.5	4
8	+7	2.7	6
9	+7	2.9	5

### 2.6.3 Welding and test plates

To create the weld, an Al 6061 sheet was overlapped completely on top of a Al 5052 sheet, with a length of 100 mm along the longitudinal direction at the center of the specimen. The length of the effective weld stitch was adjusted to 40 mm, ensuring that the welding surface area was similar across all the specimens that were tested. The plates are held firmly in place during the welding process by a specialized clamping system, with no gap between them.

The welding of the two plates creates a consolidated plate measuring 295 mm x 40 mm. A robotic fiber laser welding approach was utilized, utilizing a six-axis robotic system (FANUC M-710ic) and IPG Photonics YLS-3000 (Ytterbium Fiber Lasers) with a

wavelength of 1070 nm and a focal diameter of 0.25 mm (MCOL 14) for LWBs. The welding robot used for the experiment is depicted in Figure 25.

The specimens underwent welding using a linear laser beam without the use of shielding gas, as the study was concentrated on the enhancements brought about by the welding procedure's power and speed.

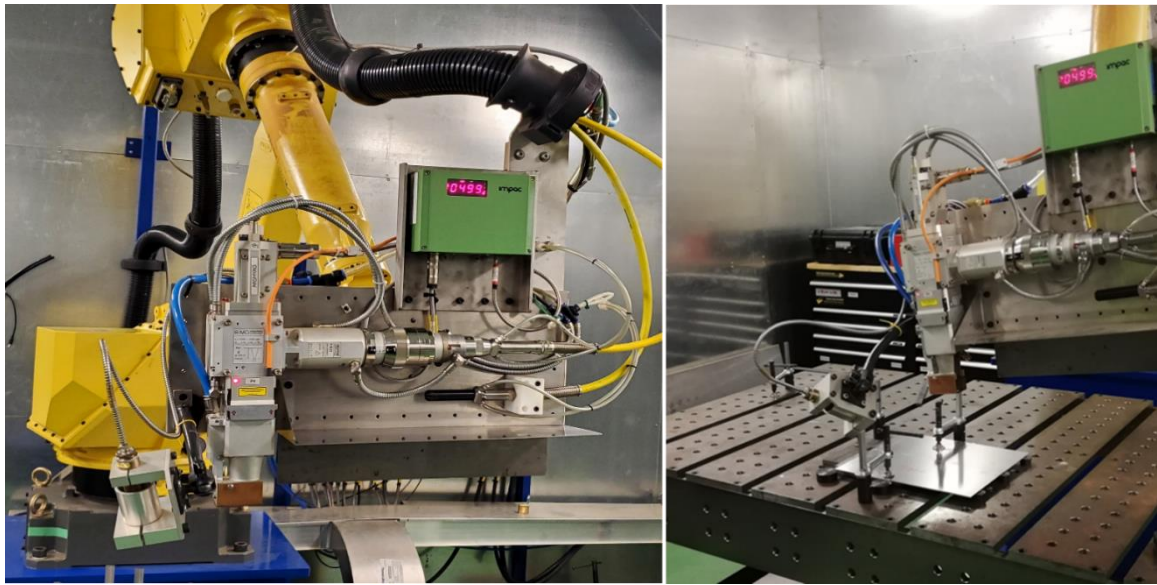


Figure 25: Automatic Fiber Laser System, six-axis-robotic system FANUC M-710ic with IPG Photonics YLS-3000 (Ytterbium Fiber Lasers)

## 2.7 CHARACTERIZATION OF WELD

Figure 26 shows a x5 magnification microscope observation of the welded portion of each specimen. All parts were well welded, and the laser was able to penetrate the first aluminum layer, reach the second material, and penetrate it as well. It can be seen that the parts with a focal length of +3 mm have a deeper penetration than those with a focal length of +5 mm, and similarly between those of +5 mm and +7 mm; moreover, the focal distance is bigger than the laser, which is further from the specimen, so the penetration is affected. The least penetrated part is number 8, with a focal distance of +7 mm, a power of 2.7 kW, and a speed of 6 m/min. The value of the focal distance is the largest, the value of the power

is medium, and the speed is the highest in the experiment. Test 3 is the most penetrated; we can even observe the weld on the other side of the part. For this test, we have the smallest value of focal distance (+3 mm), the largest value of power (2.9 kW), and the smallest value of speed (4 m/min).

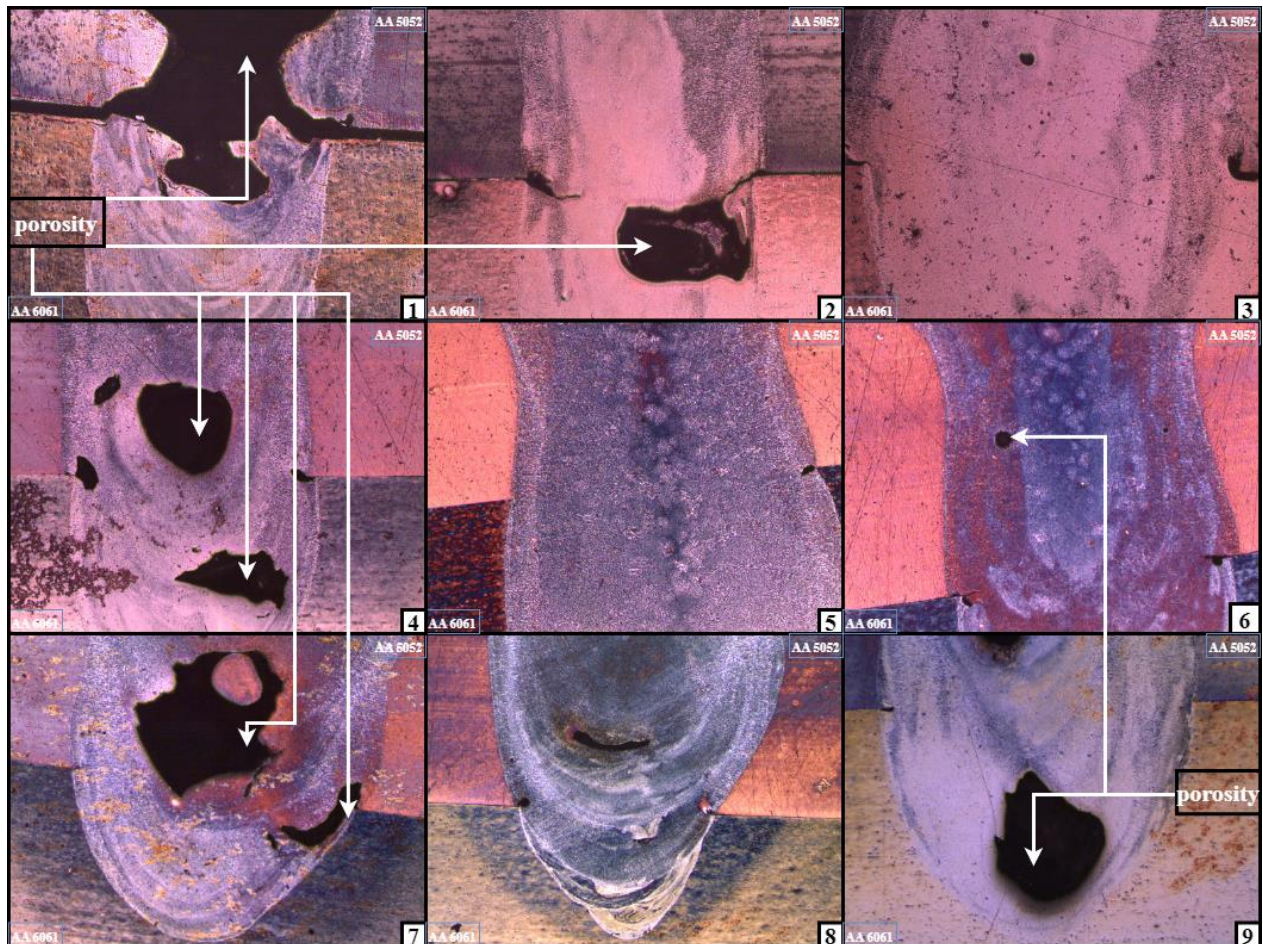


Figure 26: x5 magnification microscope observation of the welded portion of each specimen

Large defects such as porosities are also present; as for tests 1, 2, 4, 7, and 9, large porosities can be observed, and small porosities are visible in some places for tests 3, 5, 6, and 8. The primary causes of porosity can be attributed to two phenomena. The first is the trapping of hydrogen or vaporized metal in the keyhole. The second is the generation of irregularly shaped porosity in the weld due to keyhole instability, which can lead to the

formation of significant porosity [231]. Porosity is a common defect observed in some samples, and it appears to be caused by the entrapment of elements with low vaporization temperatures, including hydrogen, rather than keyhole instability. The porosity is typically observed at the center of the weld and has a spherical shape. In addition to porosity, hot cracking is also visible. Welding aluminum alloy often results in cracking due to its high coefficient of thermal expansion, which leads to severe contraction of the weld pool during solidification. Pores can often serve as the initiation site for cracking in such cases [232], [233]. Figure 27 presents a x100 magnification microscope to observe the microstructure of the welded portion for test 3. The picture shows the BM and Fusion parts of the welding.

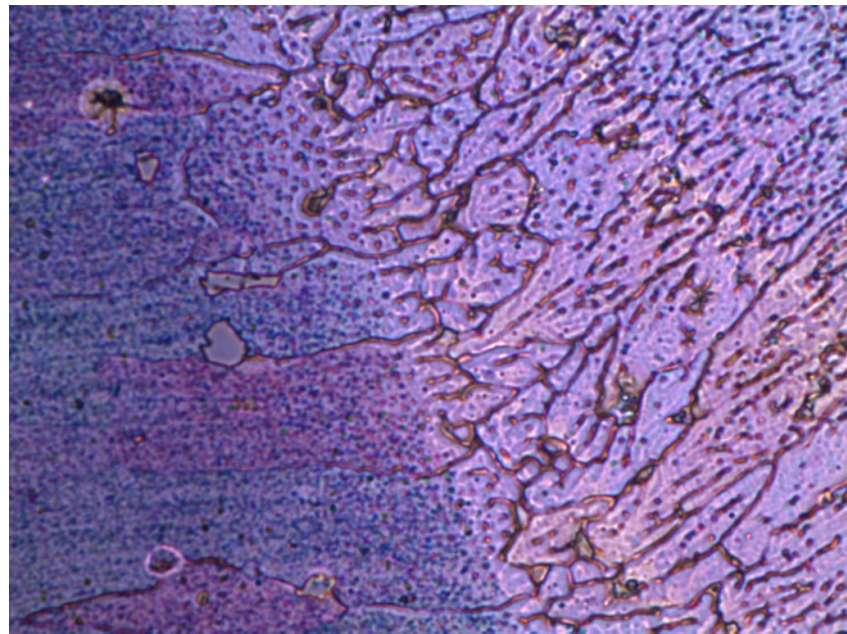


Figure 27: a x100 magnification microscope observation of the microstructure of the welded portion for test 3. The picture shows the BM and Fusion area

## 2.8 MECHANICAL PROPERTIES OF WELD

### 2.8.1 Micro hardness

Figure 28 shows the path followed for microhardness measurement, and the analysis indicates a consistent trend across all the welded specimens. Specifically, the hardness tends

to decrease in the melting zone as compared to the base metal, and this drop in hardness is more pronounced in the heat affected zone, where the minimum value is observed in each test. These findings are in line with the results of microhardness analyses carried out by various researchers in the field of laser welding. The decrease in hardness is typically attributed to the loss of some alloying elements resulting from the temperature increase in the fusion zone during the welding process, as well as the loss of cold work [225], [234], [235]. Nevertheless, the fusion zone exhibits superior hardness compared to the heat-affected zone. This can be attributed to the welding process being conducted at a high speed, which causes rapid cooling. This, in turn, leads to the creation of an exceptionally hard dendritic phase and a solid-solute strengthened  $\alpha'$  alloy after the melting and solidification process [232], [236], [237]. On the other hand, it appears that a drop in hardness is evident in the heat-affected zone, which could be attributed to the thermal cycle experienced during welding. This thermal cycle caused recrystallization and averaging, leading to the formation of larger, coarser grains [235].

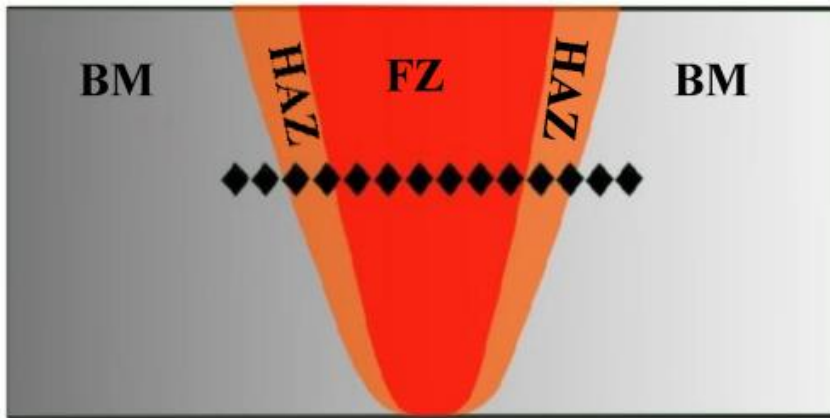


Figure 28: Hardness measurement path [238]

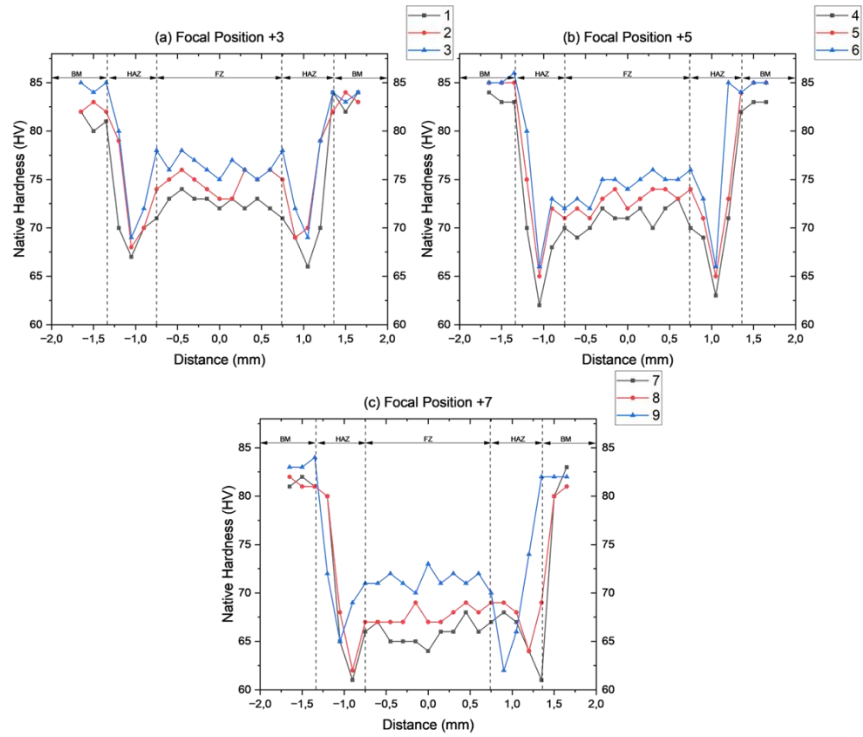


Figure 29: Hardness profile (a) Focal position +3mm, (b) Focal position +5mm, (c) Focal position +7mm

The hardness profiles of the heat-affected zone and fusion zone exhibit varying degrees of hardness drop depending on the parameter settings. This can be observed in Figure 29, which displays three sets of hardness profiles corresponding to three different focal positions. The three graphs are nearly identical, with the same width for the fusion and heat-affected zones. Regarding the microhardness values, it is noticeable that the tests conducted at a welding power of 2.9 kW exhibit lower microhardness values than the other profiles. Additionally, the higher the welding power and speed, the greater the microhardness in the fusion zone. It is also evident that the average microhardness value increases as the focal position decreases.

## 2.8.2 Tensile strength test

In overlap welding, we use the shear load per weld length ratio ( $r$ ),  $r (kN/m) = \frac{\text{the shear load (kN)}}{\text{weld legnt (m)}}$ , to analyze the data from the tensile test, the length of the weld is the same for every specimen examined, and from the same perspective,  $r_{\max}$  is the maximum shear load per weld length. To ensure the relevance of the results, each experiment in the tensile test is conducted three times as repetitions for every sample.

Figure 30 presents the shear load per weld length with displacement curves. We presented the curves with the best  $r_{\max}$  in the repetitions. It is crucial to note that failure occurred at the weld for all examined specimens, a typical outcome for aluminum alloys. Welding often diminishes the mechanical properties of the metal by causing alloying elements to vaporize and inducing cracks and porosities. Table 7 presents the maximum shear load per weld length for every test, as well as the maximum value and the average between the repetition results of each test. Figure 31 presents the maximum and average shear load per weld length for each specimen. As illustrated by the standard deviation values in Table 7 for each trial, the deviation from the mean tensile strength spans from 6.3% in Test 3 to 19.1% in Test 1. The best weld is related to test 3, with a shear load per weld length of 197 kN/m, which is set at +3 mm for focal position, 2.9 kW for power, and a speed of 4 m/min. On the other hand, the weak weld is the test 8, with a value of 106 kN/m for the shear load per weld length, with a +7 mm in focal position, 2.7 kW in power, and a speed of 6 m/min.

Table 7: The maximum shear load per weld length

Maximum shear load per weld length (kN/m)				Maximum	Average
Attempt	Rep 1	Rep 2	Rep 3		
1	159.8	110.0	152.1	159.8	$141 \pm 26.8$
2	191.3	157.3	158.7	191.3	$169 \pm 19.2$
3	211.0	187.4	192.6	211.0	$197 \pm 12.4$
4	162.3	115.1	138.9	162.3	$139 \pm 23.6$
5	186.3	158.8	173.1	186.3	$173 \pm 13.7$
6	160.1	135.8	146.4	160.1	$147 \pm 12.2$

7	137.8	116.3	120.8	137.8	$125 \pm 11.3$
8	118.7	92.1	108.0	118.7	$106 \pm 13.4$
9	152.9	134.9	133.5	152.9	$140 \pm 10.8$

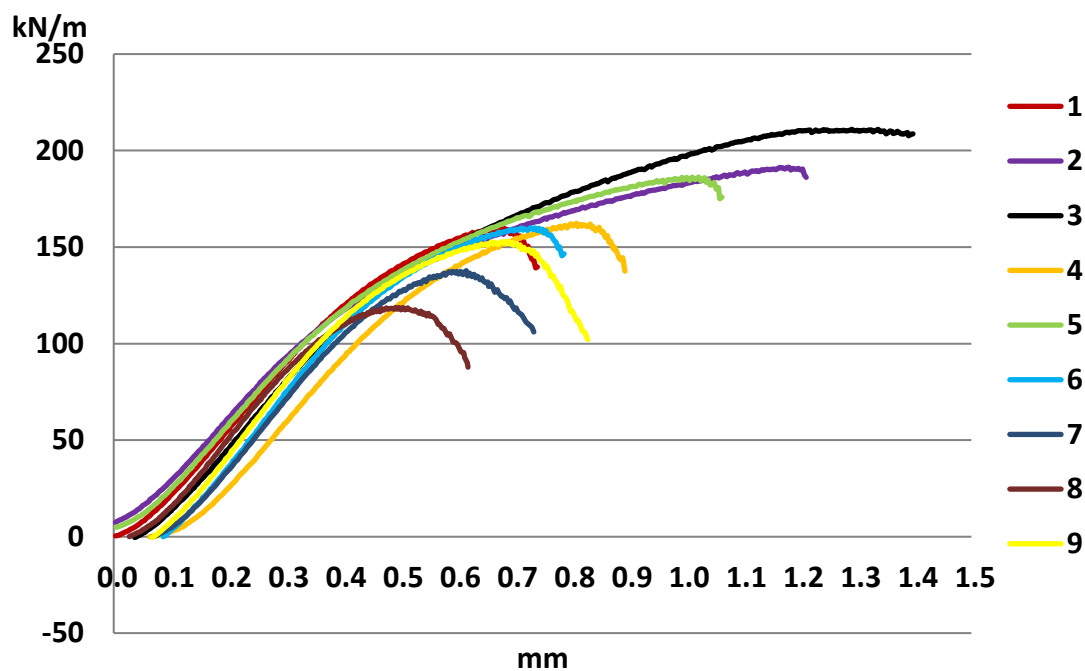


Figure 30: Shear load to welding length ratio (kN/m). Displacement (mm) curves for all the tested specimens

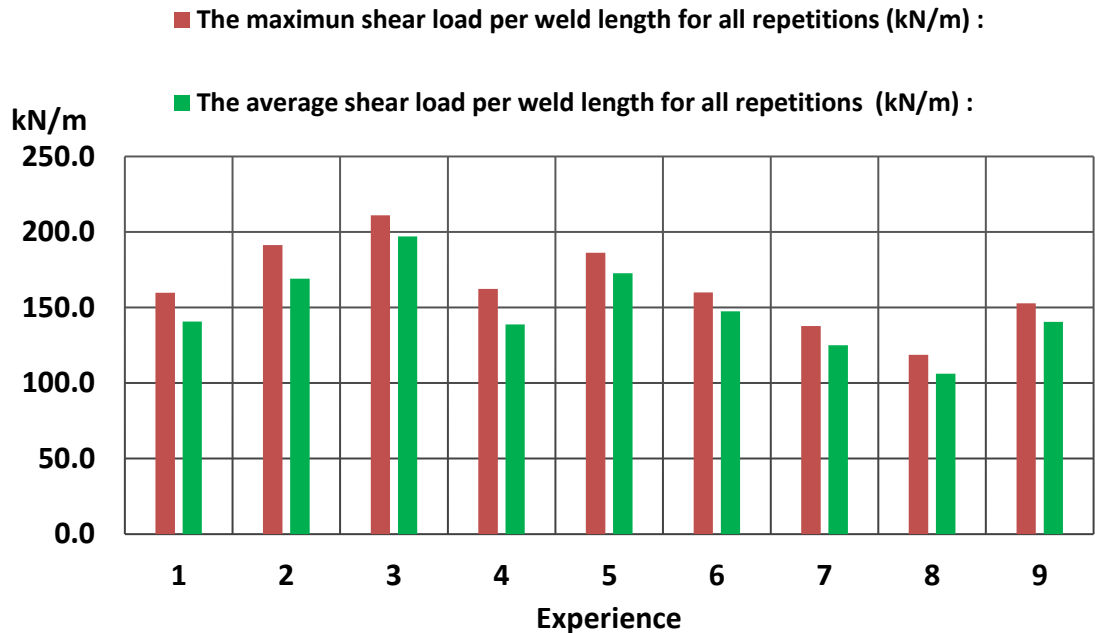


Figure 31: the maximum and the average shear load per weld length for each specimen

## 2.9 RESULT AND DISCUSSION

### 2.9.1 Analysis of Variance (ANOVA)

ANOVA, a statistical technique, is a useful tool for the effective interpretation of experimental data. It finds wide application in manufacturing industries to ensure quality control and process reliability [239]. The maximum shear load per weld length resulting from tensile tests on welded coupons is analyzed in relation to variable parameters designated by P, S, and FP, which represent laser power, speed, and focal position, respectively. The ANOVA results are presented in a table that summarizes numerical analysis data such as degree of freedom (DF), sum of squares (SS), and mean sum of squares (MS). The F-value and p-value, statistical terminology used in hypothesis testing, are also displayed in Table 8 to ensure the results are consistent and relevant. Table 8 demonstrates that the focal position is the most important parameter, accounting for 52.81 % of the variance and indicating the

most relevant factor, with a Fisher test value of 96.94. It is also clear that the value of the focal position has a negative effect on the mechanical strength of the welds. This is because an increase in the focal distance tends to decrease the mechanical resistance of the weld.

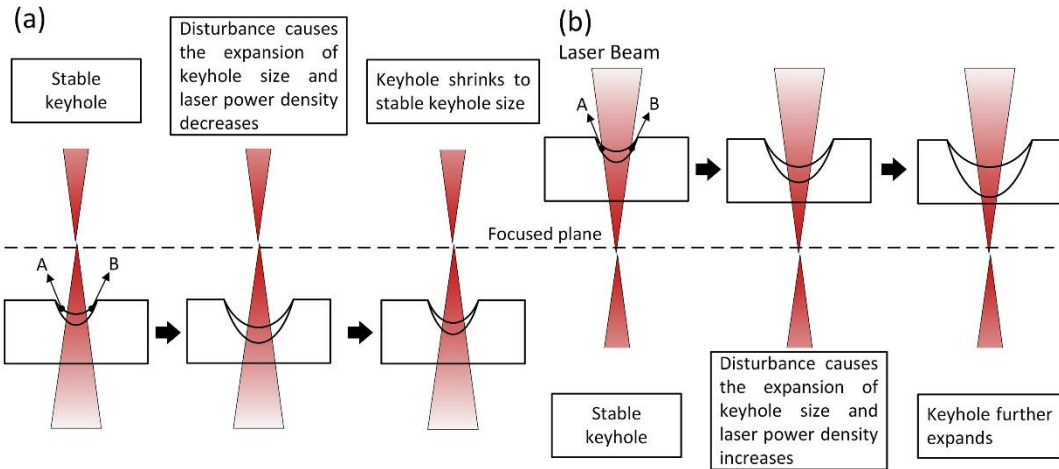


Figure 32: Depiction of keyhole dynamics in response to disruptions and laser beam engagement with the melted surface at both (a) positive and (b) negative defocusing locations [41]

This could be because the laser beam is being redirected vertically, which can cause the peak temperature to drop because there is less power density. This could be because, as Li et al. suggested [240], the back of the molten pool could be gathered and moved in the case of positive defocusing, as figure 32 shows. This would make the surface of the molten pool a good place for heat to move. This effect is less noticeable when the focal point goes deeper into the molten pool, which stabilizes the surface of the molten pool and keeps more heat inside the molten pool. Test 3 in the previous part has the best value of the maximum shear load per weld length and confirms these values. The speed parameter ranks as the second most crucial element, accounting for 28.39% of the weld's characteristics. Comparable to the focal distance, diminished welding speed adversely affects the welds' mechanical robustness. This occurrence is commonly seen in aluminum laser welding, where a reduced speed prolongs the beam exposure time, counterbalancing the heat dissipation caused by aluminum's high conductivity and reflectivity. Consequently, a more robust weld is produced, as the augmented linear energy enhances the weld's depth [241], [242]. The laser

power exhibits the lowest influence among the parameters in the ANOVA table, contributing 18.26%. Relative to the welds' ultimate tensile strength, the ANOVA provides a standard deviation of 4,0169.

Table 8: ANOVA table for the maximum shear load per weld length

Source	DF	Seq SS	Contribution	Adj SS	Adj MS	F-Value	P-Value
FP (mm)	2	3128.29	52.81%	3128.29	1564.15	96.94	0.010
P (kW)	2	1081.60	18.26%	1081.60	540.80	33.52	0.029
S (m/min)	2	1681.46	28.39%	1681.46	840.73	52.10	0.019
Error	2	32.27	0.4%	32.27	16.14		
Total	8	5923.62	100.00%				
S=4.0169 R-sq = 98.7% R-sq (adj) = 95.7% R-sq (pred) = 80.4%							

Figure 33 illustrates that an elevation in laser power generally improves the weld's mechanical resilience. The explanation for this is that greater energy delivery impacts the weld's depth [243]. However, the optimal tensile strength is attained with a laser power of 2900 W, which averts plate overheating at higher laser power levels, akin to the observations made by Chu et al. [244] in laser welding. The relationship between laser power and welding speed, measured as the specific point energy, has been the subject of a great deal of study. According to the findings of this research, the quality of the weld is significantly impacted by the interplay between laser power and welding speed, which is also a component of our project. Focal distance and laser power interact in a way that greatly affects welding quality, and this may be understood in terms of the influence of heat distribution, which emphasizes the significance of the laser beam in laser welding [227], [245], [246].

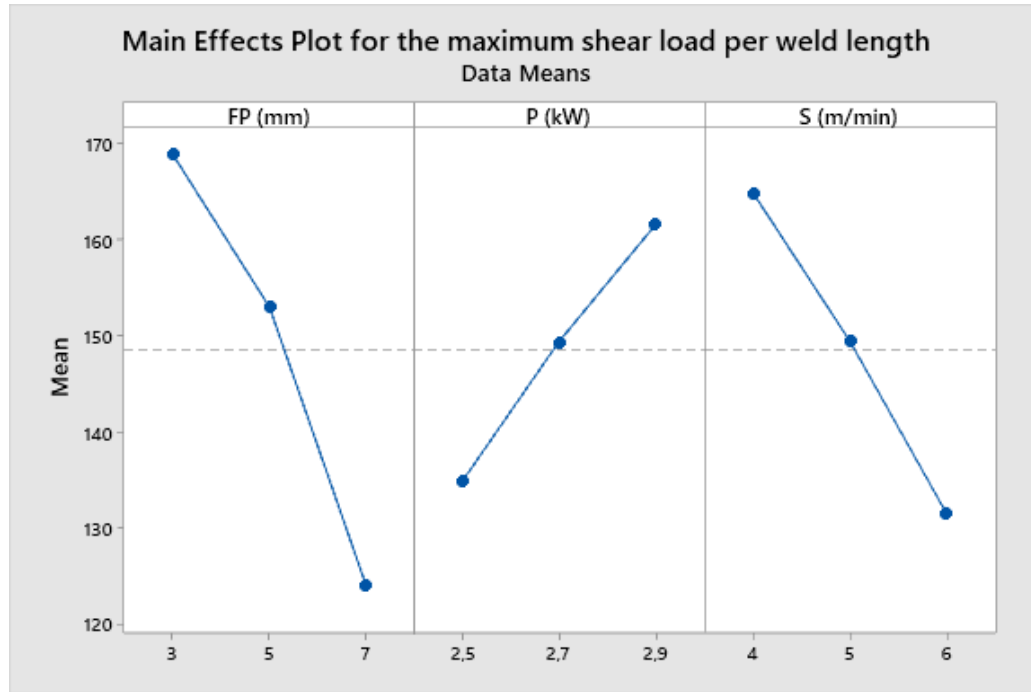


Figure 33: Parameters effect graph

### 2.9.2 The ANOVA analysis:

Through the examination of the gathered data, a model can be constructed to forecast outcomes based on input variables. The realm of modeling is vast, with numerous approaches for generating models for phenomena or experimental series. In this case, multiple linear regression was selected due to its simplicity in calculations and proven reliability, as demonstrated by various researchers who have employed it in their studies [247]–[249]. Multiple linear regression equations usually have an output that is generated from the input parameters and a coefficient that is found by using the least mean squares method:

$$\hat{y} = a_0 + a_1x_1 + a_2x_2 + a_3x_3 \dots \quad (1)$$

The derived model takes into account the three parameters acknowledged in the experimental design, namely focal position (FP), laser power (P), and speed (S). However,

we will disregard their interactions, resulting in a regression equation with the previous structure mentioned in (1). The model enables the prediction of the weld's shear load per weld length (SL) based on the individual parameter levels. It facilitates the identification or approximation of various attainable mechanical strength values by mapping them onto a response surface. The formula representing the developed model is provided below:

$$SL = 107,5 - 11,26 \cdot FP + 67 \cdot P - 16,72 \cdot S \quad (2)$$

Table 9 shows linear regression ANOVA results. Table 7 shows that the tensile strength model is appropriate at 96.63% confidence. The models' F-value of 77.50 indicates an expressive link, and their p-value approaching 0 suggests a relevant outcome. The model's coefficient of determination is 0.979, indicating a low error and strong dependability. Even the corrected R-square (0.966) and anticipated R-square (0.926) preclude overfitting. Figure 34 compares experimental data with linear regression model estimates to demonstrate the model's reliability. The residual errors have a range from -4.25 to +7.42 kN/m, with a mean error of -0.107, confirming the model's dependability.

Table 9: ANOVA of multiple linear regression model

Source	DF	Seq SS	Contribution	Adj SS	Adj MS	F-Value	P-Value
Regression	3	5798,9	97,89%	5798,9	1932,97	77,50	0,001
Error	5	124,7	2,11%	124,7	24,94		
Total	8	5923,6	100,00%				
R-sq = 97.89%      R-sq (adj) = 96.63%      R-sq (pred) = 92.63%							

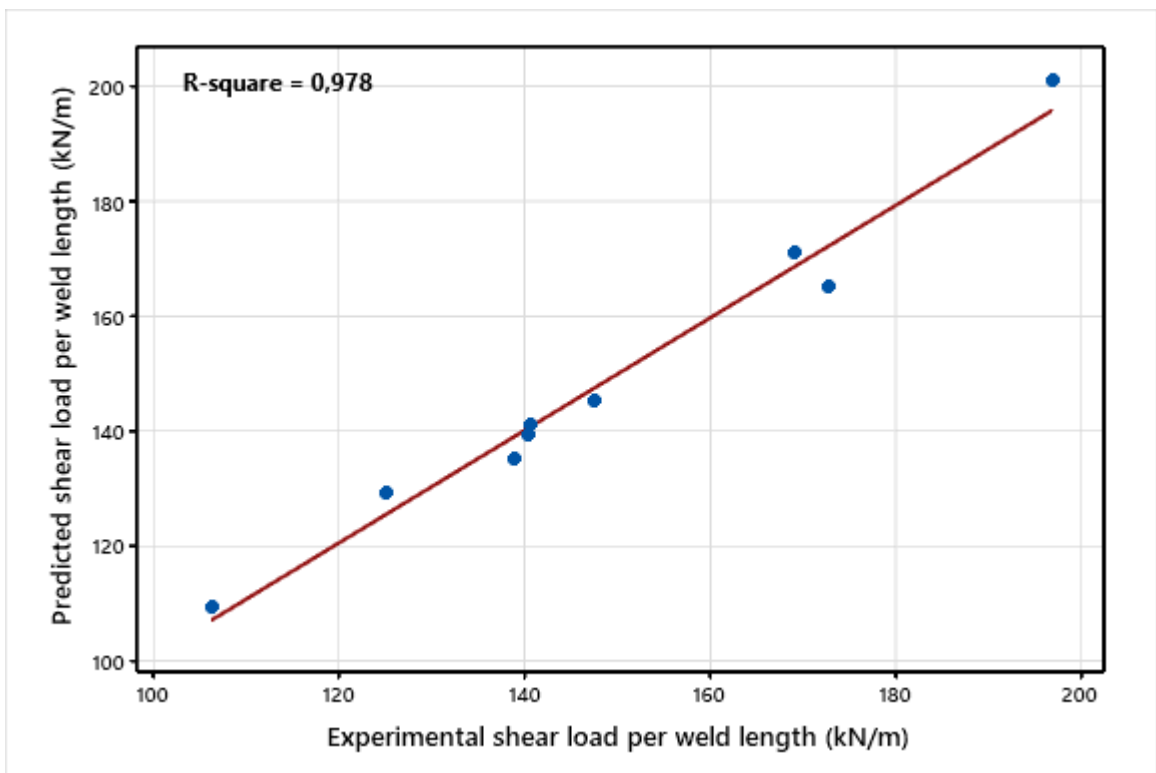


Figure 34: Experimental data vs Predicted value

### 2.9.3 Response surface method:

The response surface methodology stands out as a superior technique for predicting values in welding compared to alternative approaches [250]. It offers a mapping of anticipated values in relation to the parameters examined in the developed predictive model. Response surfaces are generated by maintaining a factor at a level that optimizes mechanical strength, as illustrated in Figure 33, which displays the impact of each parameter. As such, Figure 35 sets the focal position at 3 mm, while varying welding speed and power. The highest tensile value achieved is 201.14 kN/m, with a welding speed of 4 m/min and a laser power of 2.9 kW. Similarly, in Figure 36, the response surface predicts tensile strength based on focal position and laser power, with welding speed held constant at 4 m/min. This results in a minimum of 112.92 kN/m and a maximum tensile of 206.6 kN/m, attained with a focal position of 3 mm and a laser power of 2.9 kW. In Figure 37, the laser power is fixed at 2.9

kW, and the most durable weld is achieved with a focal position of 3.037 and a velocity of 4.01 m/min, characterized by a tensile strength of 200.6 kN/m.

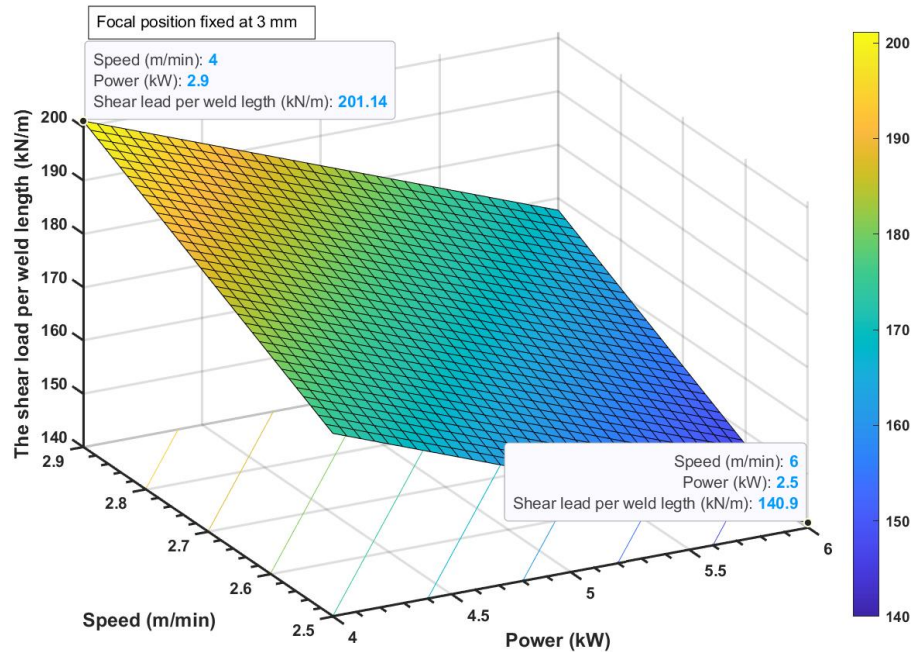


Figure 35: Response Surface for shear the load per weld length with Focal Position fixed at 3 mm

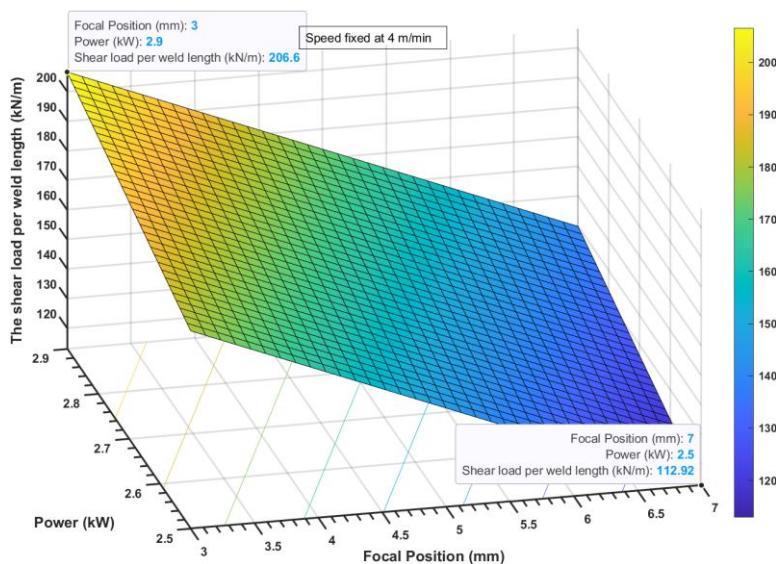


Figure 36: Response Surface for the shear the load per weld length with Speed fixed at 4 m/min

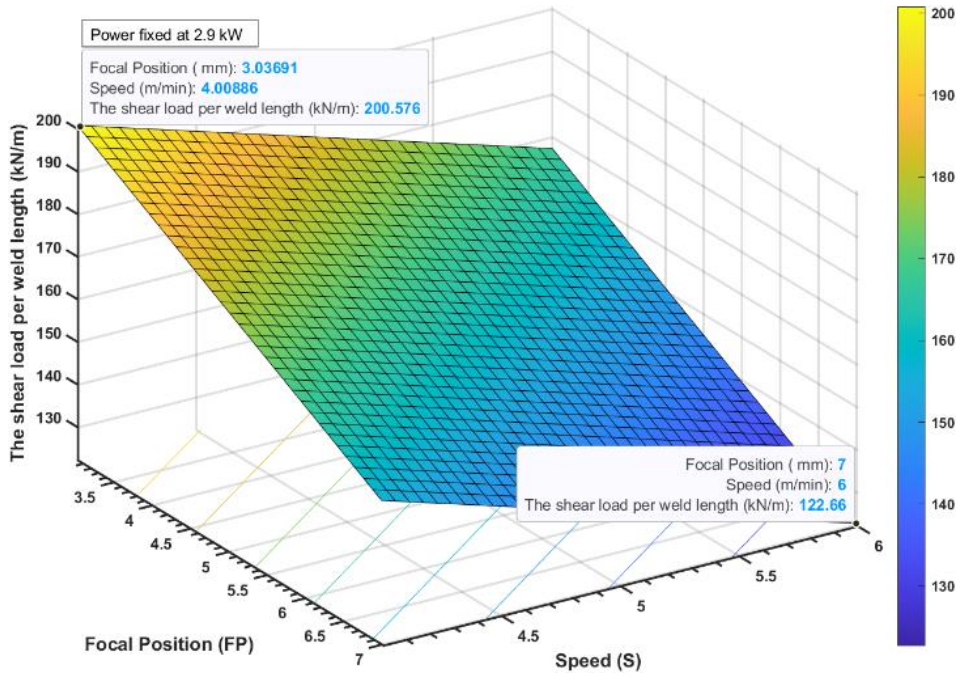


Figure 37: Response Surface for the shear the load per weld length with Power fixed at 2.9 kW

The findings corroborate the results of previous studies conducted on laser welding of aluminum, which suggest that reducing the welding speed leads to optimal tensile strength, as reported by Abioye, who also employed the response surface method [249]. The response surface reveals that maximum power is necessary for achieving the best mechanical strength, which is consistent with the findings of Kim et al., who conducted laser welding with different levels of laser power [247]. However, although the average parameter analysis indicates that a laser power of 2.9 kW produces a better weld, some strong welded parts are achieved by using a laser power of 2.7 kW, which is better than using 2.5 kW in laser power. For example, in test 5, we used less power (2.7 kW) and less speed (4 m/min), and we got a better result than in test 6, where we used 2.9 kW but more speed (6 m/min), and a focal position of 5 mm for both. This is likely because the slower speed is more beneficial for the weld, and using lower laser power prevents the weld from experiencing severe damage due to overheating [244].

## **2.10 CONCLUSION**

This study provides crucial insights into the laser welding of aluminum, demonstrating that the most influential parameters on the weld's mechanical strength are the focal position, speed, and laser power. Our ANOVA analysis, supported by multiple linear regression modeling and response surface methodology, underscored that the focal position accounted for the highest variance, thereby exerting the most substantial influence on the weld's mechanical strength. It was observed that a negative defocus resulted in a reduction of the weld's mechanical strength due to a decrease in power density and peak temperature.

Additionally, speed emerged as the second most important parameter, showing that a decrease in speed results in a more robust weld due to prolonged beam exposure time, which counters the heat dissipation effect of aluminum's high conductivity and reflectivity.

On the other hand, laser power, while still influential, had the least impact among the parameters. Nevertheless, an increase in laser power typically enhances the mechanical strength of the weld by impacting the weld's depth, with the optimal tensile strength achieved at 2900 W.

The study's findings suggest that proper adjustment and optimization of these parameters can significantly improve the quality and mechanical strength of aluminum laser welds. Further research could explore the impacts of other factors, such as laser wavelength and ambient conditions, to refine the understanding of laser welding dynamics.

In the face of rising demands for lightweight and high-strength materials in industries such as automotive and aerospace, these findings contribute valuable knowledge to the field of laser welding and present a stepping stone towards the development of more efficient and reliable laser welding processes.

## **CHAPITRE 3**

# **OPTIMISATION DES PARAMÈTRES DE SOUDAGE AU LASER POUR L'AMÉLIORATION DES PROPRIÉTÉS MÉCANIQUES DES ALLIAGES D'ALUMINIUM DISSEMBLABLES 6061 T6 ET 5086 H32.**

### **3.1 RÉSUMÉ EN FRANÇAIS DU DEUXIÈME ARTICLE**

Cet article examine l'optimisation des paramètres de soudage par laser pour améliorer les propriétés mécaniques des alliages d'aluminium dissemblables 6061 T6 et 5086 H32 dans le contexte d'un assemblage en recouvrement. Trois paramètres de soudage, la position focale (FP), la puissance du laser (P) et la vitesse de soudage (S), ont été identifiés comme étant d'une importance significative. Les résultats démontrent que la position focale a l'effet le plus significatif, suivie de la vitesse de soudage et de la puissance du laser. L'expérience a également démontré que l'augmentation de la distance focale et la réduction de la vitesse de soudage ont un effet négatif sur la résistance mécanique des soudures. Une méthode de régression linéaire multiple a été utilisée pour développer un modèle prédictif pour la charge de cisaillement par longueur de soudure en fonction de ces paramètres. De plus, la méthode de la surface de réponse a été utilisée pour visualiser et optimiser les paramètres de soudage. Les résultats de cette étude fournissent des informations précieuses pour améliorer la qualité et la fiabilité des procédés de soudage au laser des alliages d'aluminium dissemblables.

### **3.2 CONTRIBUTION**

Cet article initial, intitulé "*Optimizing Laser Welding Parameters for Enhanced Mechanical Properties of Dissimilar Aluminum Alloys 6061 T6 and 5086 H32*", a principalement été rédigé par son auteur principal, Abdessamad Lakhal. Pedram Farhadipour, en tant que deuxième auteur, a apporté des conseils pour affiner l'étude et a

également participé à la révision de l'article aux côtés de Noureddine Barka. Ce dernier a supervisé le projet et a joué un rôle clé dans l'amélioration de la version finale de l'article. De plus, Anas Ghazi Jerniti, Anas Kerbou, Asim Iltaf et Abderrahim Zilali m'ont apporté leur soutien dans la réalisation de plusieurs tests, dans la mise en œuvre de mes expériences, et dans l'analyse des résultats.

### **3.3 TITRE DU PREMIER ARTICLE**

Optimizing Laser Welding Parameters for Enhanced Mechanical Properties of Dissimilar Aluminum Alloys 6061 T6 and 5086 H32.

### **3.4 ABSTRACT**

In this research, we delve into a comprehensive analysis of the impact of varying parameters on overlap laser welding of aluminum alloys 6061-T6 and 5086-H32. The study concentrates on three critical parameters: laser power (P), speed (S), and focal position (FP). We assess the mechanical strength of the overlap welds, specifically the maximum shear load per weld length, utilizing tensile tests performed on welded coupons. The data obtained is subsequently scrutinized via Analysis of Variance (ANOVA), a reliable statistical method predominantly used in manufacturing industries for quality control and process reliability assessment. The focal position was found to significantly influence weld strength, accounting for approximately 49.19% of the variance, with increased focal distance resulting in weaker welds. The welding speed and laser power emerged as other impactful factors, with slower speeds and higher power generally improving the strength of the weld. Additionally, the study develops a reliable multiple linear regression model to predict the maximum shear load per weld length. We also use the response surface methodology to provide a visual representation of the influences of the investigated parameters. This investigation emphasizes the importance of precise parameter control in overlap laser welding of aluminum alloys and contributes valuable insights to the existing body of knowledge, paving the way for future research in this area.

### **3.5 INTRODUCTION**

In recent years, the automotive industry has experienced significant growth in electromobility and efforts to reduce energy consumption, with aluminum alloys often playing a crucial role in achieving these objectives [251]–[253]. Whether it concerns heat exchangers for thermal management in battery-electric motor systems or reducing overall vehicle weight, the mechanical and chemical properties of aluminum alloys make them the go-to materials for designing components in these systems. Classifications for aluminum metals range from 1XXX to 8XXX. This description is based on where it is used, how it is used, and what it is. Historically, flame brazing has been the primary method for joining aluminum alloy components in automotive applications such as air conditioning lines [251], [254]. Under the pressure of not only climate change (a company producing automotive components from aluminum alloys using flame brazing can emit up to 600,000 m<sup>3</sup> of CO<sub>2</sub> per year) but also the increasing complexity of component geometries (such as joints between parts with thin walls down to 0.5 mm or with significant differences in wall thickness), there has been a growing need for the development of laser welding [255], [256]. In comparison to other welding techniques, laser welding offers higher speed, greater precision, and increased flexibility [256]. Laser beam welding of aluminum alloys can be challenging due to defects related to melting, solidification, shrinkage, thermal expansion, hydrogen absorption, and other gas interactions [255]. The type and quantity of defects depend on the base and filler materials' chemical compositions as well as the welding parameters. Porosity and cracks are the most frequently observed defects during the welding process of these alloys. Some studies have reported crack initiations in aluminum alloys (6xxx series) with a broad solidification range between liquidus and solidus temperatures, while others have noted the formation of porosities in high-magnesium-content aluminum alloys, attributed to the lower melting temperature of Mg compared to Al [255]. Additional research has explored the effects of laser surface cleaning, sandblasting, shielding gas (argon) routing, or employing a two-spot laser beam during welding to reduce porosity and splatter [257], [258].

Aluminum is a metal characterized by its good mechanical strength, corrosion resistance, and low density. These properties are beneficial for manufacturing industries like the automotive sector, which has a particular interest in the 5XXX alloy. This alloy can reduce vehicle weight and energy consumption while maintaining a satisfactory lifespan [259]. Aluminum alloys are also widely used in other industries; for example, 2XXX and 7XXX alloys are commonly found in advanced sectors such as aerospace for manufacturing aircraft fuselages and wings. The 2024-T3 alloy is known for its high fatigue strength, excellent ductility, and suitability for use in extreme conditions. AA6061-T6, a precipitation-hardened aluminum alloy (Al-Mg-Si) belonging to the 6XXX series, is widely used in aircraft fittings production due to its exceptional workability, remarkable strength, and exceptional corrosion resistance. This series, in particular, is put to use in the production of bullet train cars. This series is favored in large part due to its high degree of weldability. For its strength and light weight, Al 6061 T6 alloy is used for some wagon parts on the German high-speed train Inter City Express (ICE). In addition to the magnesium and silicon found in the 6xxx series, 6061 T6 has also been subjected to heat treatment and artificial aging [260]–[262].

In cryogenic applications, Al-5086 distinguishes itself as the premier non-heat treatable aluminum alloy, as seen in Brazed Aluminum Heat Exchangers (BAHX). This is due to its cost-effective installation and exceptional performance, which require minimal maintenance [263], [264]. Al-5086 is the strongest aluminum alloy that cannot be treated with heat. It retains its integrity down to -196 degrees Celsius and is hence suitable for use in cryogenic applications. Welding aluminum alloys presents several challenges, as they possess high conductivity and tend to form a layer of brittle oxides. Welding thick plates of 5xxx series alloys can be particularly difficult, as their mechanical properties can be negatively impacted by welding defects such as porosity and spatter. Various welding methods, including electric arc, oxy-acetylene, TIG (tungsten inert gas), MIG or MAG (metal active gas), laser, and resistance welding, can be utilized for joining aluminum alloys. Each of these methods has its own set of advantages and disadvantages [265]. Among the issues encountered during welding, porosity is one of the most significant problems. Researchers have conducted studies to reduce the pore rate in the melting zone and the grain structure [266]. Other

complications, such as solidification cracks, hot cracks, and decreases in strength values in HAZ of Al 6061-T6 alloy have also been reported [267]. Microstructural changes and decreases in hardness values after welding are also important factors to be considered when designing welded joints for heat-treated Al alloys in the HAZ [261], [268]. Laser welding is currently preferred in industrial manufacturing due to its benefits such as low HAZ width, deep penetration, high welding speed, and low stress [268]. The issue of porosity during the welding of Al 6061 T6 alloy, specifically in the weld seam region, has been highlighted in numerous studies. In an effort to reduce the porosity rate in a 1 mm thick Al 6061 T6 alloy weld, Luca Pellon et al. [269] conducted a complete modification of the shielding gas.

Finding a cost-effective welding technique for aluminum presents a significant challenge. Compared to other methods like resistance spot welding or MIG welding, which yield unsatisfactory outcomes due to low resistivity and significant thermal distortion, laser welding has been found to be more profitable [270]. Laser welding provides several benefits, such as outstanding precision and speed, limited heat affected zone, and the possibility of automating the process, making it an excellent choice for improving productivity [271]. However, defects such as pores and cracks are common in aluminum laser welding due to the properties of the metal and its alloying elements. The low vaporization temperature of aluminum promotes gas trapping in the fused metal, while the high solidification rate increases the likelihood of cracks forming [272]–[274]. These imperfections tend to cause aluminum to lose its mechanical properties post-welding, especially in terms of tensile strength. For instance, the tensile strength of AA 6013 can drop to almost one-tenth of the maximum achievable strength for an aluminum alloy after autogenous laser welding. Researchers have therefore suggested various methods to achieve better outcomes when welding aluminum with lasers. Heat treatments after welding have been shown to be effective in improving the properties of welds by controlling residual stress and promoting precipitation of specific phases in both the melting and thermally affected zones [275], [276]. However, this method requires significant resources, particularly in industrial settings, and is only suitable for heat-treatable alloys such as the 6XXX series (excluding AA 5052-H32). A novel technique in laser welding of aluminum alloys involves oscillating the laser beam in

a specific pattern. This approach limits the deterioration of aluminum properties during welding by reducing heat generation through energy distribution. By following a non-linear path during oscillation, as demonstrated by Vakili-Farahani et al. [277] on Ti6Al4, this method also limits the loss of alloying elements.

Previous research has shown that laser power and welding speed are the most significant parameters in laser welding of aluminum alloys, and hence researchers have focused on studying their influence. For instance, Ahn et al. investigated the effects of laser power, velocity, focal length, and gas flow rate on the mechanical properties and microstructure of welded parts made of 3 mm thick aluminum 2024-T3 [278]. Similarly, Kim et al. optimized laser welding of 1.4 mm thick AA 5182 alloy to achieve the best tensile strength by selecting specific values of laser power, welding speed, and wire feed rate [279]. Abioye et al. developed a predictive model for the tensile strength of welded AA 5052-H32 based on laser power, welding speed, and focal distance [280]. Building on these studies, this work specifically focuses on the effects of laser power and welding speed, given their importance in previous research.

The objective of this research is to investigate the influence of parameters on linear laser welding of aluminum alloy 6061-T6 with 5086-H32, utilizing the statistical method of analysis of variance (ANOVA) to determine the impact of each parameter. To obtain a sufficient amount of data for numerical calculations, a series of experiments must be performed, involving systematic variations of parameters and combinations of numerous variations for each parameter. Therefore, an efficient design of experiments is essential to gather reliable data for analysis. A complete factorial design is created to quantify the effects of each parameter and display the interaction between them. The goal of this study is to create a predictive model using linear regression to estimate the mechanical properties obtained from a specific parameter set, followed by a response surface to determine the optimal values of the final parameters for the best tensile strength of the weld, which will be validated through tests.

### 3.6 EXPERIMENTAL SET-UP

AA 5086 and AA 6061 are aluminum alloys with high strength-to-weight ratios, good ductility, and corrosion resistance. AA 5086 is strain hardenable, while AA 6061 is age hardenable. Combining these two alloys results in a material with the combined properties of both, making it highly desirable in industries such as automotive, aerospace, and transportation [230], [281]. To perform the welding procedure, specimens of both alloys, with a size of 150 mm in length and 40 mm in width and a thickness of approximately 1.6 mm, were machined. The nominal chemical composition and tensile strength properties of the base materials are provided in tables 10 and 11, respectively.

Table 10: Nominal chemical composition of 6061 T6 and 5086 H32 Al alloys used in this investigation

Materials	Al (%)	Cr (%)	Cu (%)	Fe (%)	Mg (%)	Mn (%)	Si (%)	Ti (%)	Zn (%)	Others (%)
6061 T6	95.8 - 98.6	0.04 - 0.35	0.15 - 0.4	<= 0.7	0.8 - 1.2	<= 0.15	0.4 - 0.8	<= 0.15	<= 0.25	<= 0.15
5086 H32	93.0 - 96.3	0.05 - 0.25	<= 0.1	<= 0.5	3.5 - 4.5	0.2 - 0.7	<= 0.4	<= 0.15	<= 0.25	<= 0.15

Table 11: Tensile properties of 6061 T6 and 5086 H32 Al Alloys used in this investigation

Material	Tensile Strength, Ult (Mpa)	Tensile Strength, Yield (Mpa)	Elongation (%)
6061 T6	310	276	17
5086 H32	290	207	12

The welding apparatus includes a FANUC robot, as mentioned in figure 38, equipped with an IPG Photonics YLS-3000 laser source, which is a Yb:YAG laser operating at a wavelength of 1070 nm. The laser head is a BIMO High YAG model, which provides a laser focus diameter of 0.25 mm. The use of a robot arm is necessary in laser welding due to the hazardous nature of the process, which requires an automated workstation.



Figure 38: Automatic Fiber Laser System, six-axis-robotic system FANUC M-710ic with IPG Photonics YLS-3000 (Ytterbium Fiber Lasers)

As mentioned earlier, the specimens were welded using a linear laser beam. The study specifically focuses on the impact of focal position improvement, and thus, no shielding gas is used during the experiments. Multiple welds are carried out by varying the laser power, welding speed, and focal position. A complete factorial design with three factors and three levels is employed, as outlined in table 12, to arrange the variation of parameters. The complete factorial design is advantageous since it allows for the consideration of all possible combinations between the different levels of the three parameters, defined as the limit of the weldability zone, to prevent overheating or maintain the welding in a conduction mode. Additionally, the complete factorial design can reveal the effect of interaction between parameters, which is significant for this study since the parameters under consideration are related to the characteristics of the laser welding machine, as shown in table 13.

Table 12: Factors and Levels for Experiment

Factor	Levels		
	1	2	3
Laser Power (kW)	2.5	2.7	2.9
Speed (m/min)	4	5	6
Focal position	+3	+5	+7

Table 13: Experimental Design

Experiment Number	Input parameters		
	Focal Position (mm)	Power (kW)	Speed (m/min)
1	+3	2.5	6
2	+3	2.7	5
3	+3	2.9	4
4	+5	2.5	5
5	+5	2.7	4
6	+5	2.9	6
7	+7	2.5	4
8	+7	2.7	6
9	+7	2.9	5

To join the Al 6061 and Al 5052 sheets, they were overlapped completely with a length of 100 mm along the longitudinal direction at the center of the specimen, and a 40 mm effective weld stitch was utilized to ensure similar welding surface area across all the specimens. During welding, a specialized clamping system firmly held the plates in place, without any gaps between them.

The weldability zone was determined through preliminary tests involving a sequence of welds, with parameter adjustments using a trial-and-error approach. In the comprehensive factorial design, each combination of parameters forming an experimental unit was replicated to obtain sufficient samples for mechanical testing and micrographic analysis.

After the welding processes were completed, samples for tensile testing were prepared. Samples for microstructure analysis underwent preparation procedures involving cutting with a rotary saw machine, coating with epoxy, and polishing prior to scrutinization for weld defect observation. Vickers microhardness testing was then performed using a 200 lbf load, a dwell time of 10 seconds, and a 150 µm interval between each indentation to assess the weld hardness.

### **3.7 CHARACTERIZATION OF WELD**

Figure 39 displays microscope observations of the welded section of each specimen, taken at x5 magnification. The welding process resulted in well-welded parts, with the laser penetrating both the first and second material layers. The penetration depth varies among the specimens, depending on the focal position. Specimens with a focal distance of +3 mm exhibit deeper penetration compared to those with a focal distance of +5 mm, and similarly between those of +5 mm and +7 mm. As the focal distance increases, the laser is further from the specimen, leading to a reduction in penetration. The least penetrated specimen is number 8, with a focal distance of +7 mm, a power of 2.7 kW, and a speed of 6 m/min. This specimen had the largest value of focal distance, a medium value of power, and the highest speed in the experiment. In contrast, Test 3 displayed the highest penetration, with the weld even visible on the other side of the part. This test had the smallest value of focal distance (+3 mm), the largest value of power (2.9 kW), and the smallest value of speed (4 m/min).

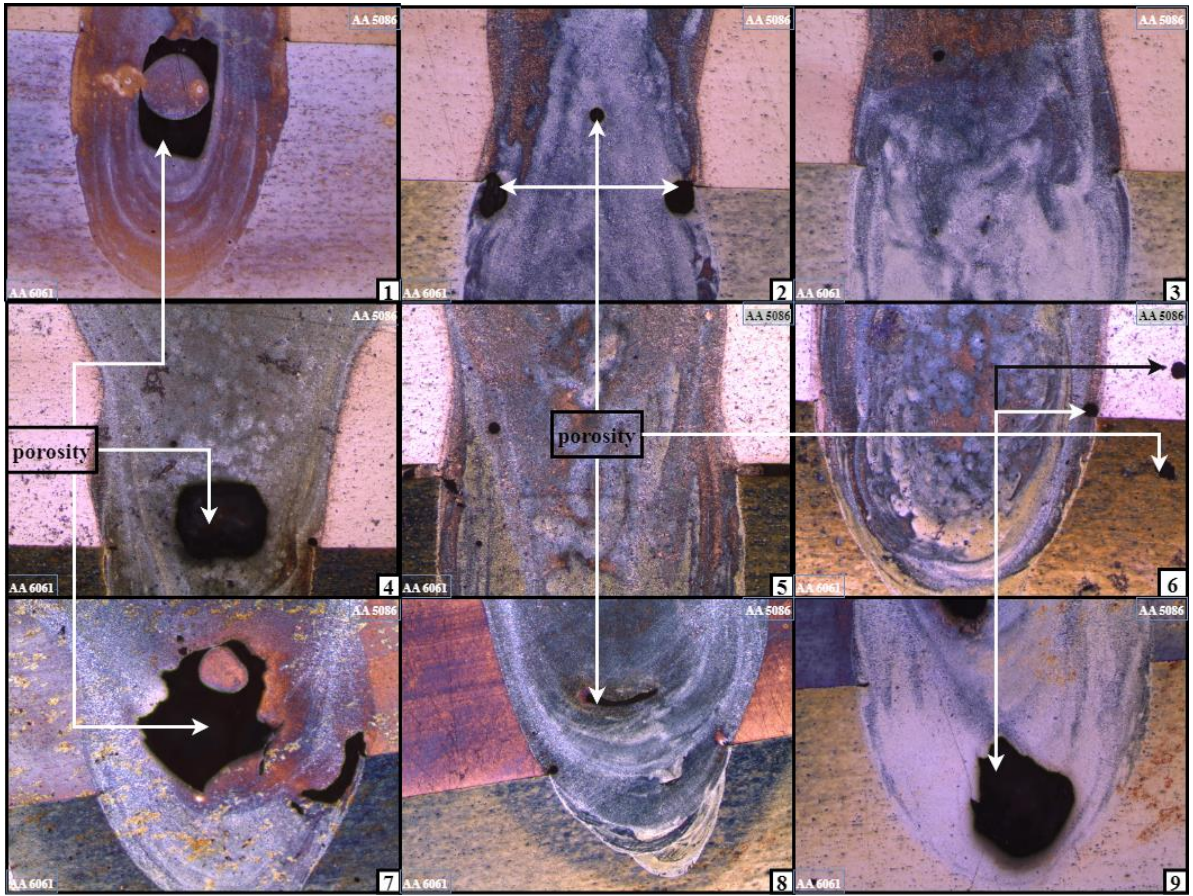


Figure 39: x5 magnification microscope observation of the welded portion of each specimen

Large defects, such as porosities, are present in the samples. Tests 1, 4, 7, and 9 show significant porosities, while small porosities are observed in some areas of tests 2, 3, 5, 6, and 8. The primary causes of porosity can be attributed to two phenomena. The first is the trapping of hydrogen or vaporized metal in the keyhole, and the second is the generation of irregularly shaped porosity due to keyhole instability, which can lead to significant porosity formation [231]. Porosity is a commonly observed defect caused by the entrapment of low vaporization temperature elements such as hydrogen, rather than keyhole instability. Spherical porosity is often observed at the center of the weld. In addition to porosity, hot cracking is also visible. The high coefficient of thermal expansion of aluminum alloy often leads to cracking due to severe contraction of the weld pool during solidification. Pores can

also serve as the initiation site for cracking in such cases [232], [233]. Figure 40 presents a microscope observation with x100 magnification of the microstructure of the welded portion of test 3, showing the base metal and fusion zone.

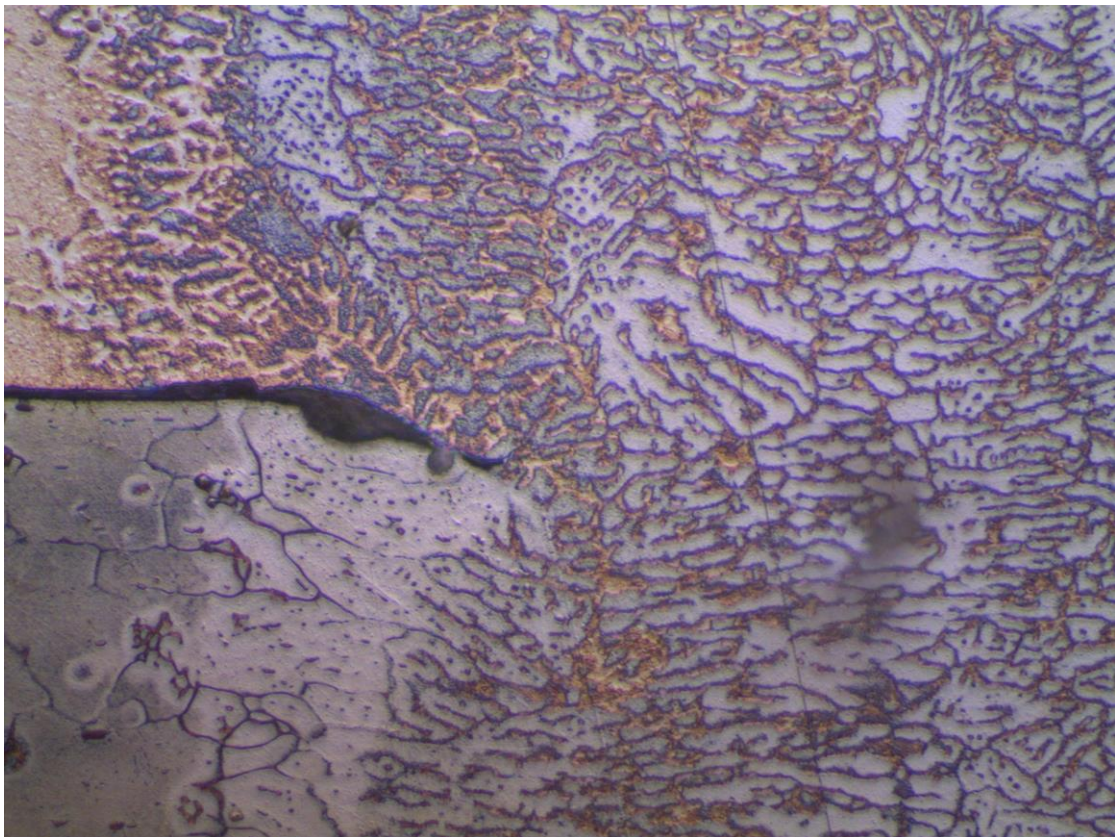


Figure 40: A x100 magnification microscope observation the microstructure of the welded portion for test 3, the picture shows the BM and Fusion part

### 3.8 MECHANICAL PROPERTIES OF WELD

#### 3.8.1 Hardness profile

The microhardness measurements, as shown in Figure 41, indicate a consistent trend among all tested welded specimens. Specifically, a decrease in hardness is observed in the melting zone compared to the base metal, with the heat-affected zone exhibiting a more pronounced drop in hardness, reaching a minimum value in each test. These findings are

consistent with previous studies in the field of laser welding and are attributed to the loss of some alloying elements and cold work during the welding process [266], [275], [276].

However, the fusion zone exhibits higher hardness compared to the heat-affected zone due to the high welding speed that causes rapid cooling, resulting in the formation of a hard dendritic phase and a solid-solute strengthened  $\alpha'$  alloy after the melting and solidification process [273], [277], [278]. The heat-affected zone, on the other hand, experiences a drop in hardness due to the thermal cycle during welding, causing recrystallization and the formation of larger, coarser grains [276].

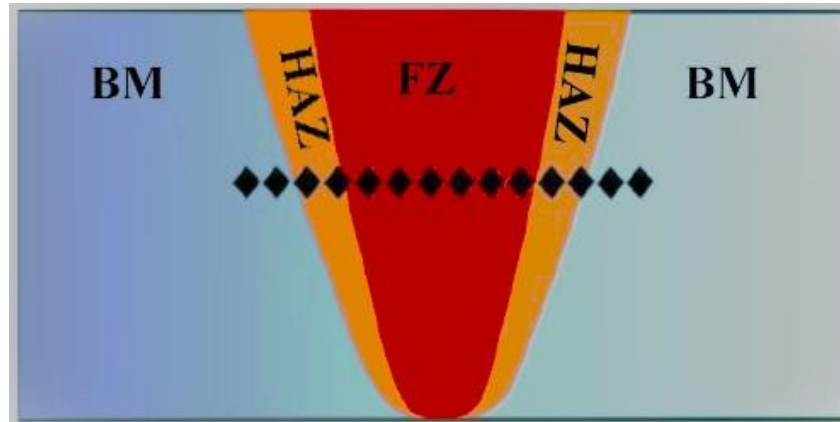


Figure 41: Hardness measurement path

Figure 42 shows that the degree of hardness drop in the heat-affected zone and fusion zone varies depending on the parameter settings. The graph displays three sets of hardness profiles corresponding to different focal positions, and they exhibit a similar width for both the fusion and heat-affected zones. The microhardness values differ across the profiles, with the tests conducted at a welding power of 2.9 kW showing lower microhardness values than the others. The microhardness in the fusion zone increases with higher welding power and speed. Moreover, the average microhardness value rises as the focal position decreases.

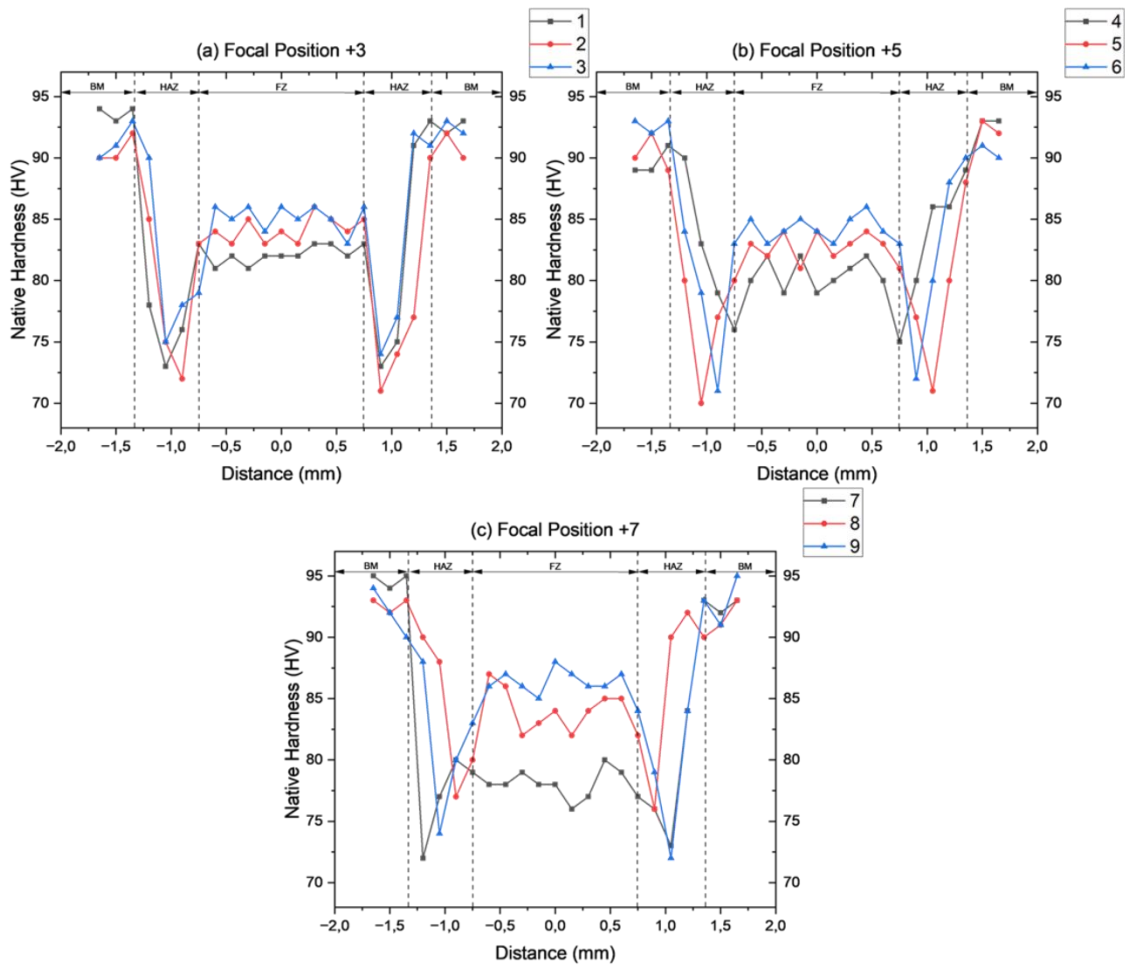


Figure 42: Hardness profile (a) Focal position +3mm, (b) Focal position +5mm, (c) Focal position +7mm

### 3.8.2 Tensile strength test:

To analyze the data from the tensile test in overlap welding, the ratio of shear load per weld length ( $r$ ) is used, where  $r$  (kN/m) equals the shear load (kN) divided by the weld length (m),  $r$  (kN/m) =  $\frac{\text{the shear load (kN)}}{\text{weld legnt (m)}}$ .  $r_{\max}$  is the maximum shear load divided by the weld length, and the weld length is constant throughout all specimens. To ensure the reliability of the results, each experiment in the tensile test is repeated three times for each sample.

Table 14: The maximum shear load per weld length

5086 - Maximum shear load per weld length (kN/m)				Maximum	Average
Attempt	Rep 1	Rep 2	Rep 3		
1	155.1	120.1	153.8	155.1	$143 \pm 19.9$
2	186.4	152.7	169.1	186.4	$169 \pm 16.9$
3	200.2	194.3	204.6	204.6	$200 \pm 5.2$
4	145.8	145.1	132.2	145.8	$141 \pm 7.7$
5	179.3	175.0	174.4	179.3	$176 \pm 2.7$
6	145.7	161.7	149.7	161.7	$152 \pm 8.4$
7	127.2	129.5	129.5	129.5	$129 \pm 1.4$
8	97.4	97.6	137.4	137.4	$111 \pm 23.0$
9	149.5	133.0	154.8	154.8	$146 \pm 11.4$

Figure 43 shows the shear load per weld length with displacement curves. We showed the curves with the best  $r_{max}$  in the repetitions. It is important to note that all of the examined specimens broke at the weld, which is normal for aluminum alloys. Most of the time, welding weakens the metal's mechanical qualities by making the alloying elements evaporate and creating cracks and holes. Table 14 shows the maximum shear load per length of weld for each test, as well as the highest value and the average of the results from each test's repetitions. In Figure 44, the highest shear load and the average shear load for each specimen's length of weld are shown. The difference from the mean tensile strength ranges from 1.1% in Test 7 to 20.8% in Test 8. This is shown by the standard deviation numbers in Table 14 for each test.

The best weld is related to test 3, with a shear load per weld length of 199.7 kN/m, which is set at +3 mm for focal position, 2.9 kW for power, and a speed of 4 m/min. On the other hand, the weak weld is test 8, with a value of 110.8 kN/m for the shear load per weld length, with +7 mm in focal position, 2.7 kW in power, and a speed of 6 m/min.

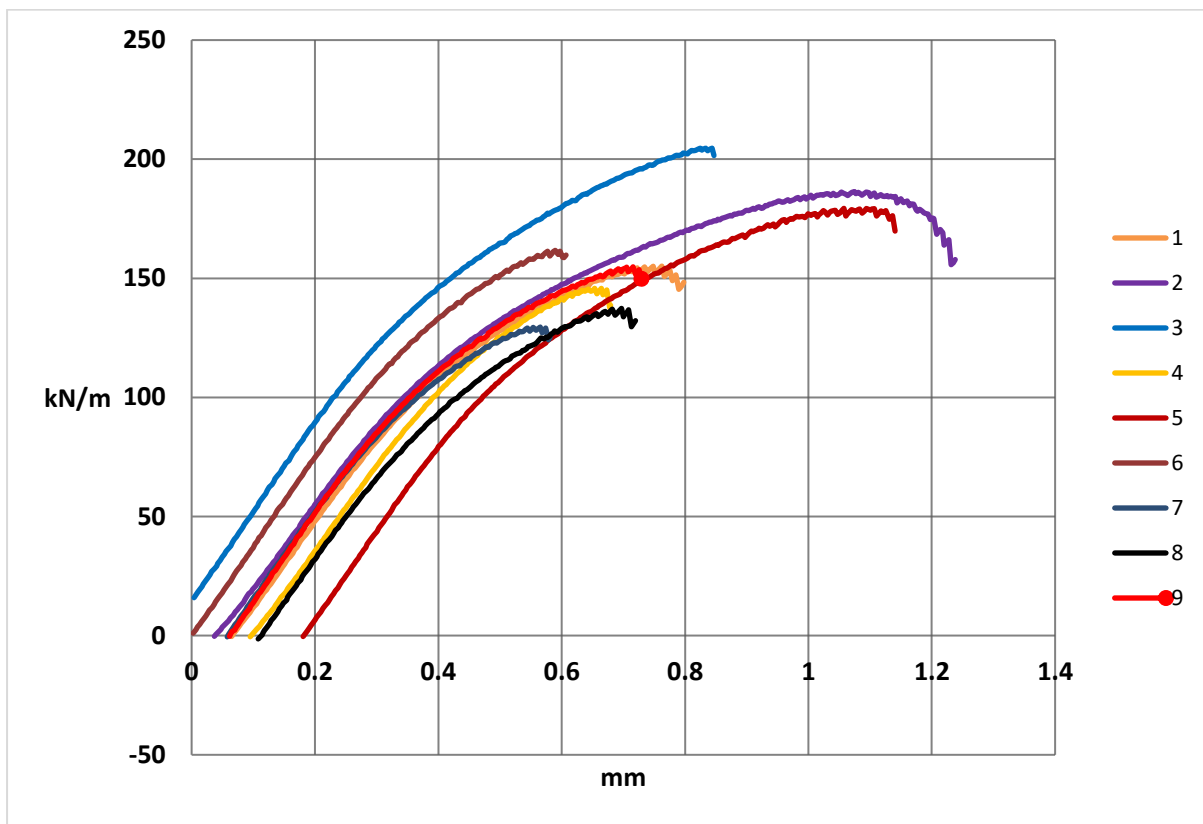


Figure 43: Shear load to welding length ratio (kN/m). Displacement (mm) curves for all the tested specimens

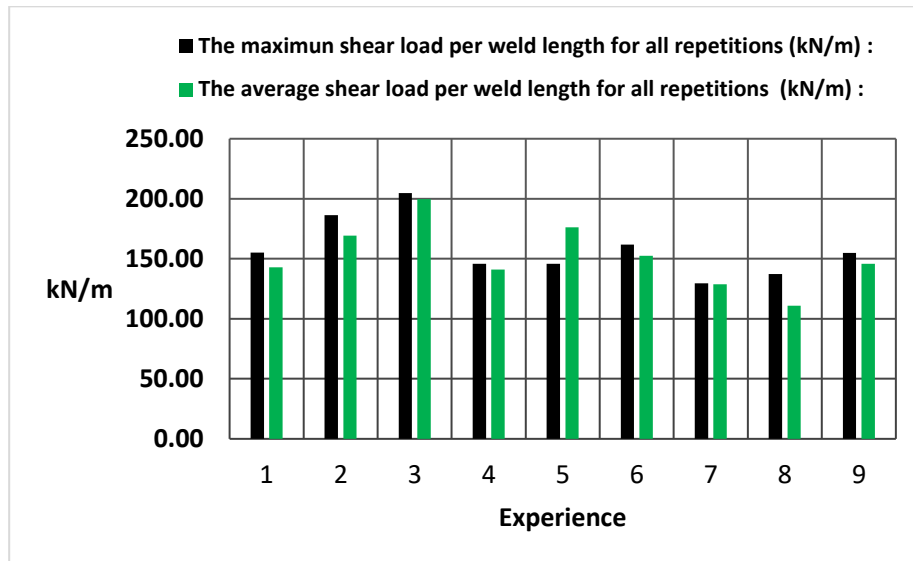


Figure 44: The maximum and the average shear load per weld length for each specimen

## 3.9 RESULTS AND ANALYSIS

### 3.9.1 Analysis of Variance

The statistical method known as ANOVA is a valuable tool for accurately interpreting experimental data, particularly in manufacturing industries where quality control and process reliability are crucial considerations [239]. In this study, the maximum shear load per weld length resulting from tensile tests on welded coupons is analyzed in relation to the variable parameters of laser power (P), speed (S), and focal position (FP). ANOVA results are presented in a table that provides important numerical analysis data such as degree of freedom (DF), sum of squares (SS), and mean sum of squares (MS), as well as statistical terminology such as F-value and p-value for hypothesis testing. The data in Table 15 clearly indicates that focal position is the most important parameter, accounting for 49.19% of the variance and showing the highest Fisher test value of 63.86. Furthermore, the data indicates that an increase in focal distance has a negative effect on the mechanical strength of the welds since it tends to decrease their resistance.

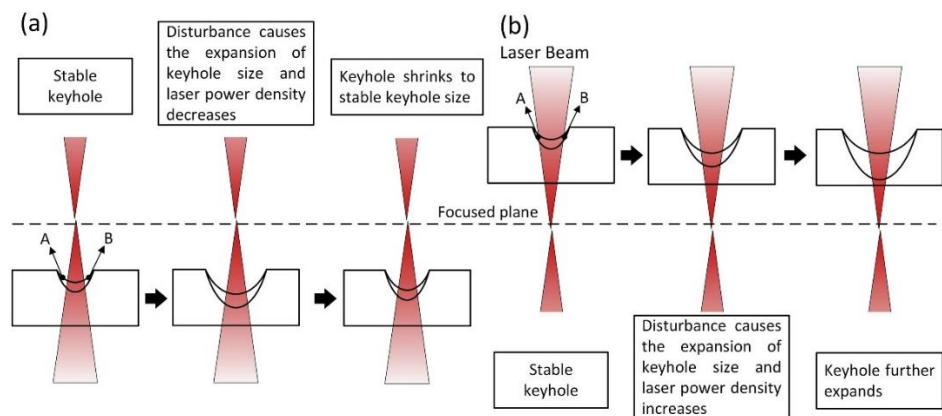


Figure 45: Depiction of keyhole dynamics in response to disruptions and laser beam engagement with the melted surface at both (a) positive and (b) negative defocusing locations [282]

The drop in peak temperature may be attributed to the laser beam being redirected vertically, resulting in a lower power density. Li et al. [240] suggested that positive defocusing may cause the back of the molten pool to accumulate and move, as depicted in Figure 45, making the molten pool surface an ideal place for heat transfer. However, this effect is less noticeable when the focal point penetrates deeper into the molten pool, stabilizing the surface and retaining more heat within the molten pool. Test 3 in the previous section yielded the highest maximum shear load per weld length, validating these findings. The speed parameter is ranked second in importance, contributing to 28.69% of the weld's properties. Reduced welding speed, similar to focal distance, negatively affects the weld's mechanical strength. This is frequently observed in aluminum laser welding, where lower speeds prolong beam exposure time, offsetting heat dissipation due to aluminum's high conductivity and reflectivity. As a result, a stronger weld is produced, as increased linear energy enhances weld depth [241], [242]. In the ANOVA table, laser power exhibits the lowest influence among the parameters, accounting for 21.35%. The ANOVA provides a standard deviation of 4.66335 concerning the weld's ultimate tensile strength.

Table 15: ANOVA table for the maximum shear load per weld length

Source	DF	Seq SS	Contribution	Adj SS	Adj MS	F-Value	P-Value
FP (mm)	2	2777.66	49.19%	2777.66	1388.83	63.86	0.015
P (kW)	2	1205.69	21.35%	1205.69	602.84	27.72	0.035
S (m/min)	2	1619.74	28.69%	1619.74	809.87	37.24	0.026
Error	2	43.49	0.77%	43.49	21.75		
Total	8	5646.59	100.00%				
S=4.66335 R-sq = 99.23% R-sq (adj) = 96.92% R-sq (pred) = 84.40%							

The mechanical strength of the weld is generally enhanced by an increase in laser power, as shown in Figure 46. This is due to the greater energy delivery that affects the weld's depth, as reported in previous studies [243]. However, the optimal tensile strength is achieved at a laser power of 2900 W, which prevents overheating of the plate at higher power levels,

as observed by Chu et al. [244] in their laser welding experiments. The interplay between laser power and welding speed, quantified as the specific point energy, has also been extensively studied as a crucial factor affecting the quality of the weld, and it is also a consideration in our project. The focal distance and laser power have a significant impact on welding quality, as they interact in a manner that affects heat distribution. This underscores the importance of the laser beam in laser welding, as emphasized by previous research [245], [246], [249].

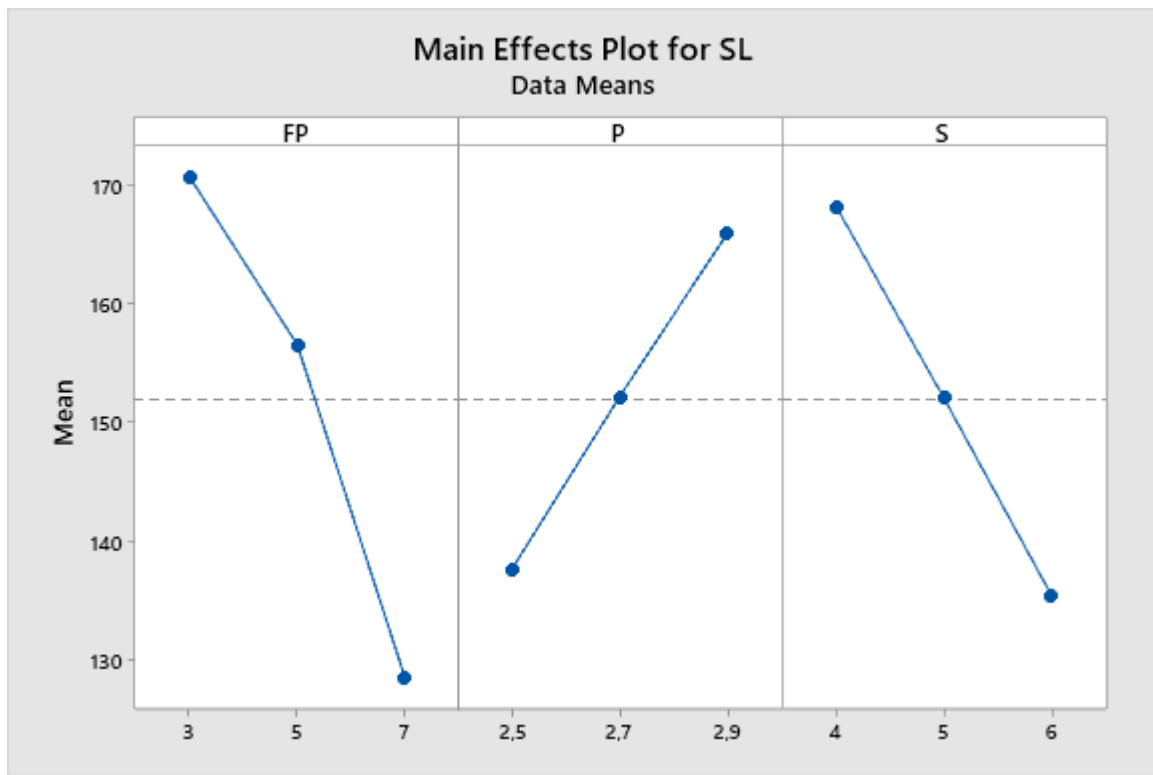


Figure 46: Parameters effect graph

### 3.9.2 The ANOVA analysis:

By analyzing the collected data, a model can be developed to predict outcomes based on input variables. The field of modeling is vast and offers various methods for generating models for phenomena or experimental series. For this particular study, multiple linear regression was chosen due to its simplicity in calculations and proven reliability. Many

researchers have employed this method in their studies, as demonstrated by previous research works [227], [247], [248]. Multiple linear regression equations typically have an output generated from input parameters and a coefficient determined using the least mean squares method:

$$\hat{y} = a_0 + a_1x_1 + a_2x_2 + a_3x_3 \dots \quad (1)$$

The model developed considers the three parameters identified in the experimental design, namely focal position (FP), laser power (P), and speed (S). However, for simplicity, their interactions will not be considered in the regression equation, which will have the same structure as equation (1). The model predicts the shear load per weld length (SL) based on the individual levels of each parameter. It maps various possible mechanical strength values onto a response surface, allowing for identification or estimation of these values. The formula representing the developed model is given below:

$$SL = 107.5 - 11.26 \cdot FP + 67. P - 16.72 \cdot S \quad (2)$$

The ANOVA results of the linear regression model are presented in Table 16. The table reveals that the model for predicting tensile strength is accurate with 96.63% confidence. The model's F-value of 65.00 indicates a strong correlation, and its p-value near 0 implies a significant result. The coefficient of determination, 0.975, signifies low error and high reliability. Moreover, the corrected R-square (0.96) and predicted R-square (0.919) rule out overfitting.

Figure 47 displays a comparison of the experimental data and the estimates from the linear regression model, indicating the model's validity. The residual errors range from -4.3 to +7.9 kN/m with a mean error of 0, validating the model's reliability.

Tableau 16: ANOVA of multiple linear regression model

Source	DF	Seq SS	Contribution	Adj SS	Adj MS	F-Value	P-Value
Regression	3	5505.4	97.50%	5505.4	1835.14	65.00	0.001
Error	5	141.2	2.50%	141.2	28.23		
Total	8	5646.6	100.00%				
R-sq = 97.5%		R-sq (adj) = 96.00%			R-sq (pred) = 91.92%		

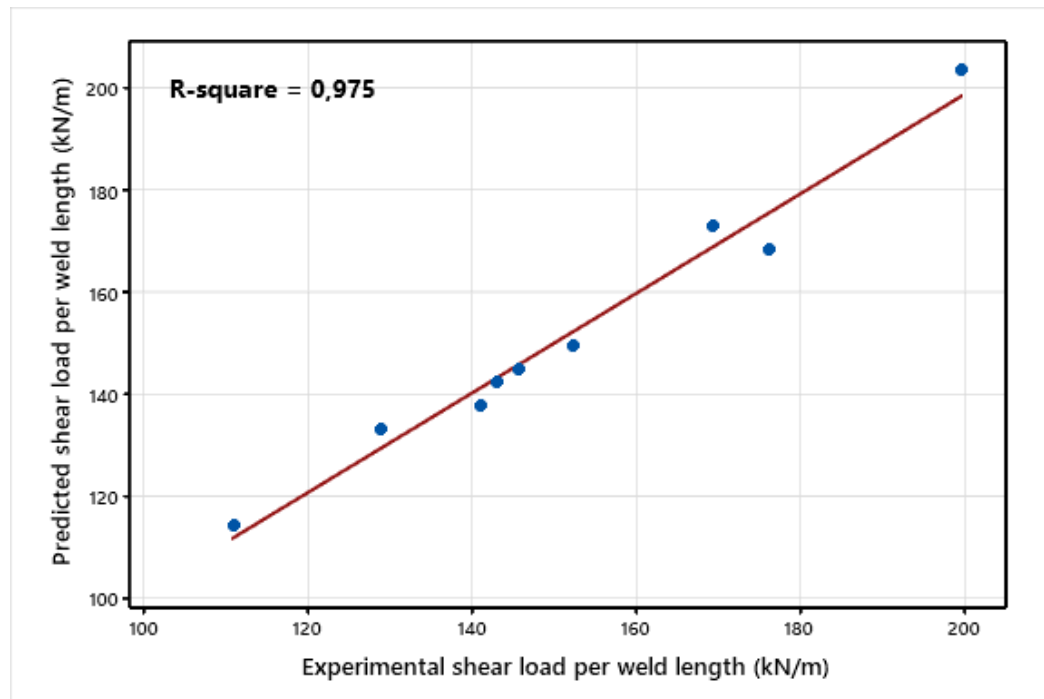


Figure 47: Experimental data vs Predicted value

### 3.9.3 Response surface method:

Compared to other methods, response surface methodology is considered a superior technique for predicting welding values [250]. It provides a visual representation of expected values based on the parameters examined in the developed predictive model. Figure 46 illustrates the impact of each parameter by keeping a factor at a level that optimizes mechanical strength, which generates response surfaces. Figure 48 sets the focal position at 3 mm while varying welding speed and power, with a maximum tensile value of 203.68 kN/m

attained at a welding speed of 4 m/min and a laser power of 2.9 kW. Similarly, in Figure 49, the response surface predicts tensile strength based on focal position and laser power, with welding speed held constant at 4 m/min. This results in a minimum of 115.46 kN/m and a maximum tensile of 209.54 kN/m, achieved with a focal position of 3 mm and a laser power of 2.9 kW. Figure 50 fixes the laser power at 2.9 kW, and the most durable weld is achieved with a focal position of 3.145 and a velocity of 4 m/min, characterized by a tensile strength of 199.5 kN/m.

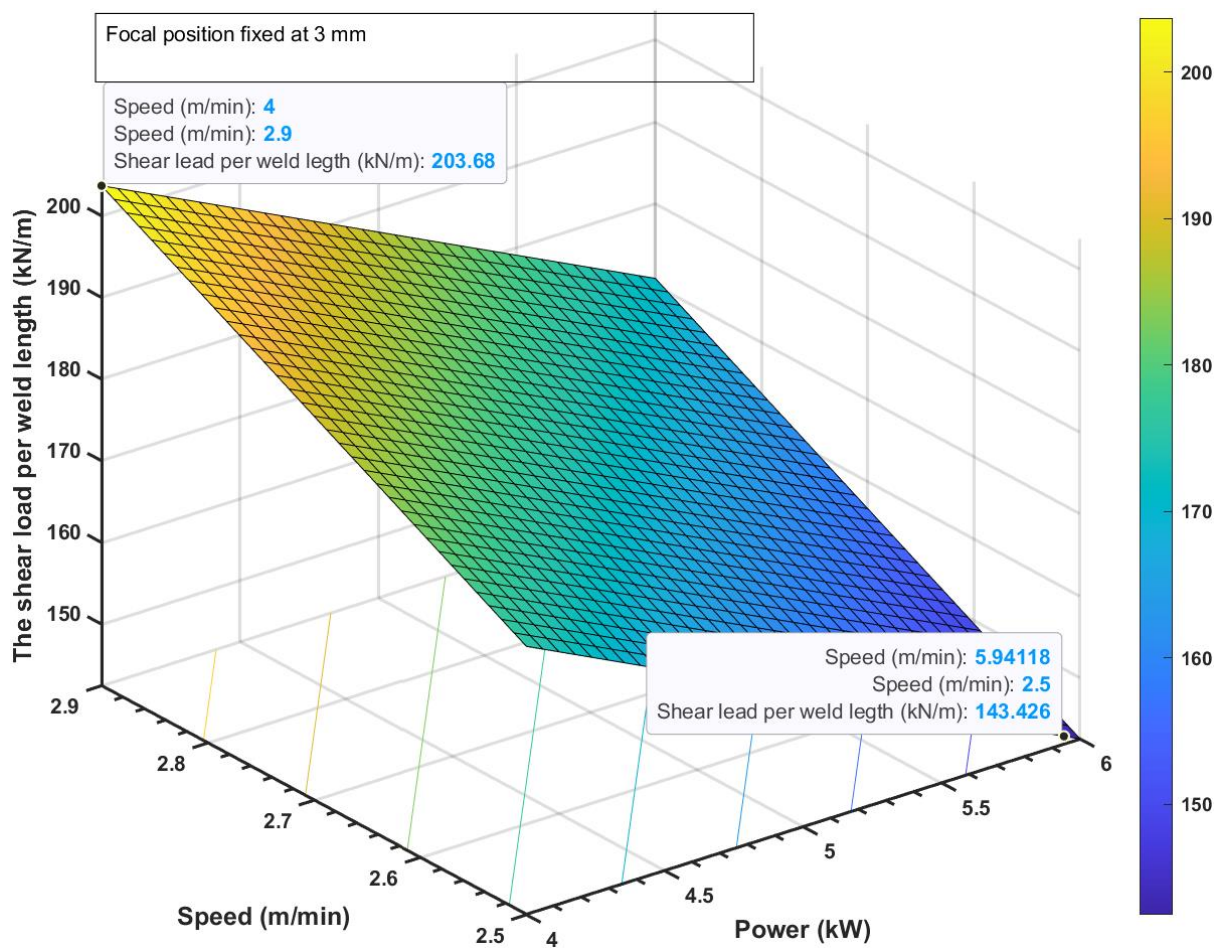


Figure 48: Response Surface for shear the load per weld length with Focal Position fixed at 3 mm

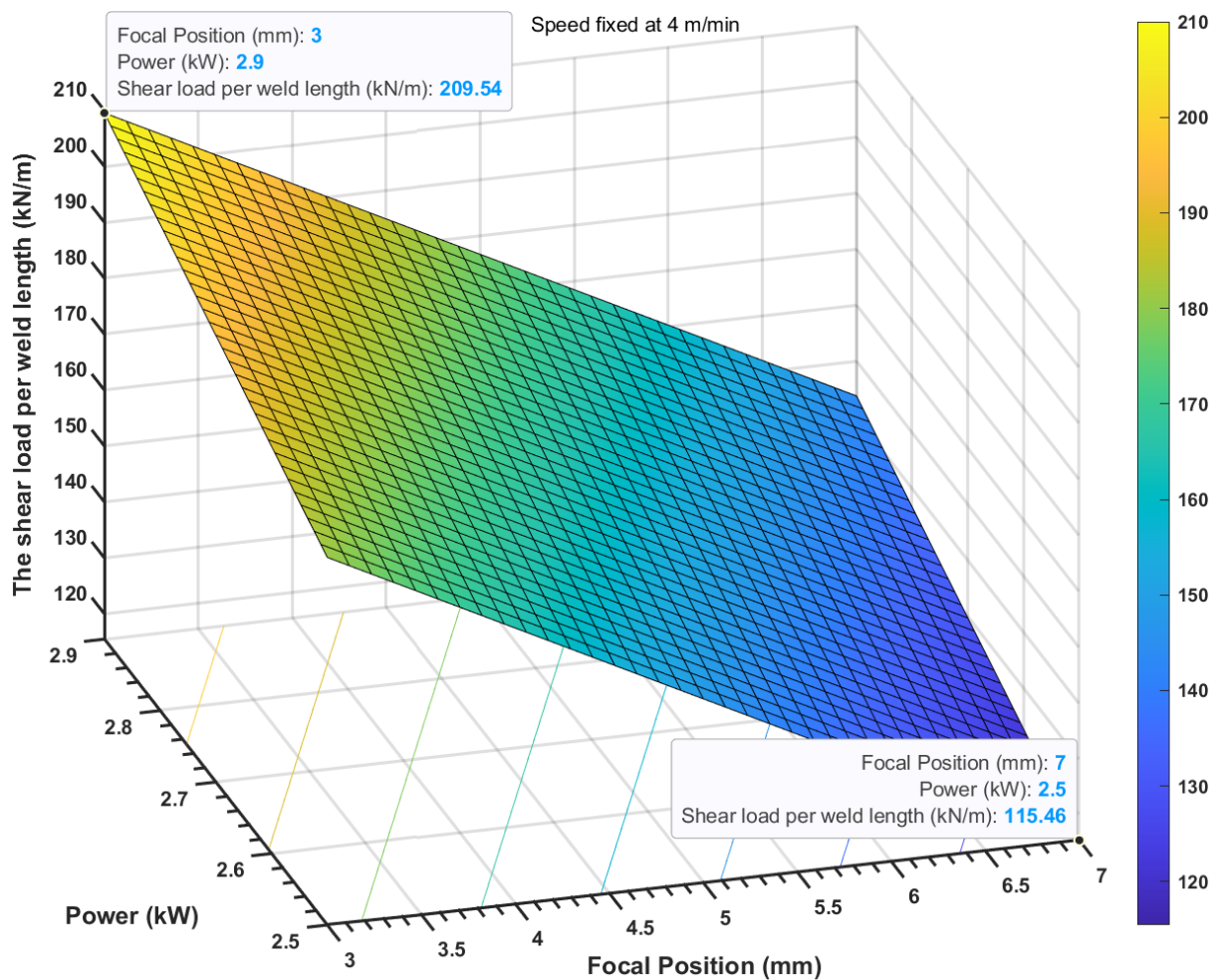


Figure 49: Response Surface for the shear the load per weld length with Speed fixed at 4 m/min

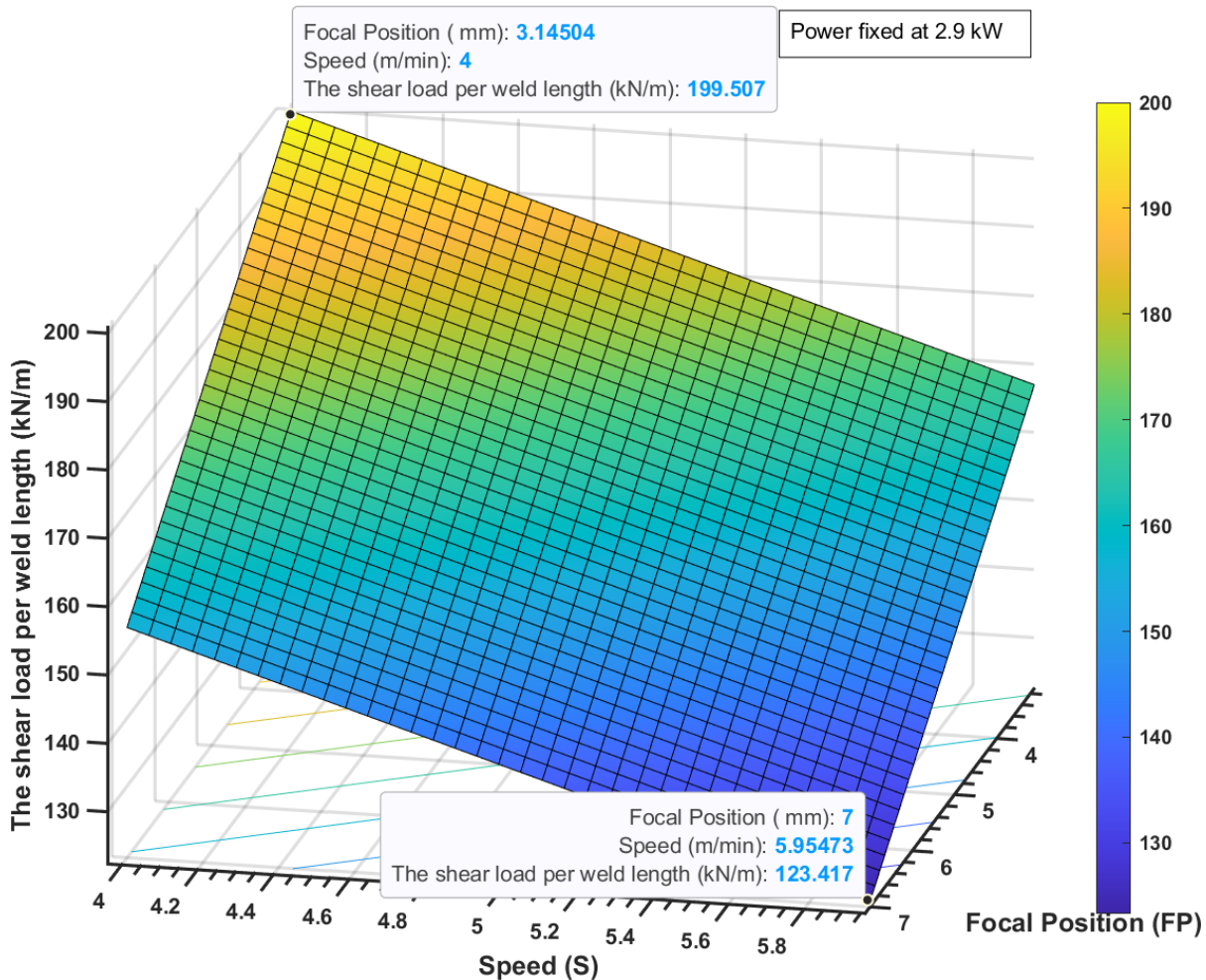


Figure 50: Response Surface for the shear the load per weld length with Power fixed at 2.9 kW

The results support previous studies that also employed the response surface method in laser welding of aluminum, indicating that reducing welding speed leads to optimal tensile strength [249]. The response surface analysis shows that maximum power is required to achieve the best mechanical strength, which is consistent with the literature on laser welding at various laser power levels [226]. However, although an average parameter analysis suggests that a laser power of 2.9 kW produces a better weld, some strongly welded parts are obtained by using lower laser power. For instance, in test 5, where less power (2.7 kW) and a slower speed (4 m/min) were used, better results were achieved than in test 6, where more power (2.9 kW) and a higher speed (6 m/min) were employed, with both tests having a focal

position of 5 mm. This is probably because the slower speed is more beneficial for the weld, and using lower laser power prevents severe damage to the weld due to overheating [244].

### 3.10 CONCLUSION

The focus of this study has been to investigate the influence of varying laser parameters on the mechanical properties of aluminum laser welds, with particular attention to laser power (P), speed (S), and focal position (FP). A thorough analysis using statistical methods, notably ANOVA, has allowed for a significant understanding of how these parameters interact and impact the quality of the welds produced.

Through this investigation, focal position has emerged as the most influential parameter, accounting for 49.19% of the variance in weld strength. We've found that increased focal distance tends to weaken the weld, suggesting that precise control of this aspect of the welding process is paramount to ensuring optimal results. Welding speed also plays a significant role, contributing 28.69% of the variance, with slower speeds leading to stronger welds due to increased beam exposure time. While laser power had the least influence among the parameters tested, it nonetheless affected 21.35% of the weld's properties.

Further, a reliable linear regression model has been developed to predict the maximum shear load per weld length, with accuracy confirmed through a strong F-value and low p-value. This model facilitates the prediction of weld strength based on the individual levels of the key parameters.

In addition to the regression model, a response surface methodology was employed to visualize the effects of each parameter on weld strength, further confirming the importance of focal position, speed, and laser power.

This comprehensive study supports previous findings in the field of laser welding of aluminum while offering additional depth in the analysis of the interplay between key parameters. It underscores the significance of precise parameter control in achieving high-quality, reliable welds and suggests a direction for further investigation in the quest for optimizing the laser welding process.





## **CONCLUSION GÉNÉRALE**

Au terme de cette étude approfondie sur le soudage au laser de l'aluminium 6061 avec les alliages 5052 et 5086, plusieurs conclusions importantes peuvent être tirées. Premièrement, la revue de la littérature a mis en évidence l'importance et l'efficacité du soudage au laser en tant que technique d'assemblage dans l'industrie. Les méthodes de surveillance des procédés ont été identifiées et ont montré leur pertinence pour contrôler les paramètres clés du soudage au laser, en particulier pour la prédition et l'optimisation de la qualité du soudage. Deuxièmement, grâce à un plan expérimental rigoureux et à l'application d'outils d'analyse statistique, nous avons pu déterminer l'influence significative de divers paramètres de procédé. L'étude des effets de la puissance, de la vitesse et de la distance focale sur la résistance à la traction, la micro-dureté et la microstructure a confirmé la pertinence des schémas basés sur des observations pratiques développés à partir de la méthode Taguchi.

Le déploiement du soudage au laser se répand rapidement dans divers secteurs industriels. Néanmoins, l'implémentation de systèmes de surveillance, l'amélioration des paramètres de la procédure et l'assurance de la qualité du produit achevé restent des défis importants. Malgré sa complexité due à la nature des phénomènes physiques engagés et aux obstacles en matière de contrôle et de surveillance, le soudage au laser offre des atouts significatifs tels qu'une efficacité énergétique supérieure et une vitesse de soudage plus rapide comparée aux techniques traditionnelles. De ce fait, l'exploration et la détermination de méthodes et technologies de surveillance deviennent cruciales pour l'élaboration de solutions solides et fiables. Dans le contexte actuel marqué par l'essor de l'industrie 4.0, des outils innovants sont mis à disposition pour répondre à ces problématiques de surveillance et de contrôle des paramètres du procédé. L'intégration de solutions basées sur l'intelligence artificielle et les algorithmes d'apprentissage automatique peut permettre d'assurer une

qualité optimale et un emploi plus efficient des matières premières. Dans le cadre de ce mémoire, une revue de littérature a été réalisée sur l'importance et l'efficacité du soudage au laser en tant que technique d'assemblage industriel. Les méthodes de contrôle du procédé ont été identifiées et analysées pour leur capacité à réguler les paramètres essentiels du soudage au laser, notamment pour la prédiction et l'optimisation de la qualité du soudage à l'aide d'intelligence artificielle. Ce mémoire propose ainsi des orientations technologiques qui mettent en lumière les méthodes les plus performantes pour la surveillance en temps réel du soudage au laser.

Au cours de cette recherche, nous avons mis en avant une stratégie visant à réguler les propriétés mécaniques en fonction des paramètres du soudage au laser pour les plaques d'aluminium. Les paramètres examinés incluent la distance focale, la vitesse ainsi que la puissance de l'émission de l'énergie laser. L'une des contributions majeures de cette étude réside dans l'établissement des directives pour la régulation des paramètres du soudage au laser, permettant ainsi une prédiction précise des propriétés mécaniques, telles que la microdureté, la résistance à la rupture et la force de rupture, ainsi que l'observation de la microstructure. La complexité de ce travail demande la prise en compte des équipements expérimentaux au niveau du laboratoire, tels que la cellule laser, les appareils de métallographie et les machines d'évaluation des propriétés mécaniques, pour la vérification des formules, des résultats et des modèles. Afin de générer des courbes de niveau avec des intervalles de réponse variables basés sur les paramètres du soudage au laser, cette étude fait appel à l'analyse expérimentale RSM (méthode de la surface de réponse). Cette technique d'analyse statistique a été choisie en raison de sa facilité d'application et de son interprétation aisée. Ce travail a démontré que les paramètres de soudage, ainsi que les dispositions et les modèles de soudage, ont une influence notable sur les propriétés mécaniques et la microstructure des plaques d'aluminium, résultant ainsi en des propriétés distinctes pour le métal soudé. Pour organiser les expériences en tenant compte du nombre de paramètres et des divers niveaux associés à chacun d'eux, la méthode de Taguchi a été employée.

L'analyse des résultats a été effectuée en utilisant la méthode ANOVA, dans le but d'obtenir un modèle mathématique optimal permettant de prédire avec précision de nouvelles observations. La première phase du projet visait à évaluer l'impact des différents paramètres du processus sur la forme de soudure et les caractéristiques microstructurelles des composants soudés en aluminium, spécifiquement l'alliage 6061 et l'alliage 5052, formant des joints à recouvrement. Les découvertes de cette phase initiale comprenaient :

- En exploitant trois paramètres de soudage (distance focale, puissance de soudage et vitesse de soudage), chacun ayant trois niveaux pour souder deux plaques d'aluminium de différents alliages en position de chevauchement, les plus grandes valeurs de contrainte ont été obtenues en maximisant la puissance de soudage et en minimisant la vitesse de soudage ;
- Une faible vitesse de soudage permet une pénétration totale de la soudure, tandis que des niveaux plus élevés entraînent des éclaboussures variables le long de la ligne de soudure ;
- Concernant la microdureté, elle est maximale dans le matériau de base, puis diminue dans la zone affectée par la chaleur pour finalement augmenter à nouveau dans la zone de fusion, tout en restant inférieure à celle du matériau de base. De plus, il a été observé que les essais effectués à la puissance de soudage maximale présentaient des valeurs de microdureté inférieures aux autres profils. Plus la puissance et la vitesse de soudage augmentent, plus la microdureté dans la zone de fusion est élevée. Il est également apparent que la valeur moyenne de la microdureté augmente lorsque la position focale diminue ;
- L'examen de la structure transversale de la microstructure de chaque éprouvette soudée a révélé que la vitesse de soudage est en relation inverse à la profondeur de soudure, la désignant comme le paramètre principal affectant la profondeur de soudure. De la même manière, la distance focale est inversement proportionnelle à la

profondeur de soudure, tandis que la puissance de soudage y est directement proportionnelle ;

- Les graphiques d'effet principal de la force de traction ultime ont permis de conclure que la puissance de soudage est directement proportionnelle à la force de traction ultime, tandis que la vitesse de soudage ainsi que la distance focale y sont inversement proportionnelles. En outre, les paramètres de soudage les plus efficaces se sont révélés être la distance focale, suivie de la vitesse, puis de la puissance ;
- Tous les points de rupture lors des essais de traction étaient localisés dans la zone soudée ;
- Une analyse des résultats de la force de traction ultime des échantillons soudés a montré que les forces les plus élevées peuvent être obtenues en utilisant une puissance de soudage élevée et une vitesse de soudage moyenne ;
- Les résultats de contrainte ont été analysés par la méthode ANOVA et un modèle mathématique a été élaboré pour des prédictions dans le même espace de conception ;

La phase finale de cette étude a révélé des résultats comparables à ceux de la première phase, avec un comportement quasi-identique observé entre les deux matériaux sous les mêmes paramètres et conditions de soudage. Bien qu'il y ait des différences minimes en raison de la variation de la composition des deux alliages - le 5052 et le 5086 - ces variations n'ont pas significativement affecté les résultats. Par conséquent, il est possible d'utiliser n'importe lequel des deux alliages, en choisissant celui qui convient le mieux en fonction de ses caractéristiques spécifiques, sans craindre d'impact négatif sur le produit final.

Ces conclusions suggèrent de procéder à faire plus d'études concernant le soudage au laser dans des applications nécessitant une automatisation. Le soudage et le traitement de surface d'un grand éventail de matériaux d'ingénierie pourraient être explorés, en utilisant des études statistiques pour affiner les paramètres et prédire les meilleures performances

mécaniques des pièces soudées dans plusieurs configurations. Ainsi, ces résultats peuvent servir d'inspiration aux chercheurs et ingénieurs afin de confronter et d'élargir les travaux précédents grâce à de nouvelles études qui intégreront des concepts novateurs de soudage à l'avenir.

En termes de recommandations pour les travaux futurs, il serait intéressant d'étudier l'effet de la trajectoire du soudage sur les propriétés mécaniques du matériau soudé. L'ajout d'un gaz, comme l'argon, pourrait également être envisagé. Par ailleurs, l'utilisation de modèles intelligents basés sur l'intelligence artificielle pour améliorer la qualité du soudage pourrait s'avérer fructueuse. Dans la même perspective, l'accélération de la transition numérique a favorisé l'utilisation de techniques et méthodes intelligentes de surveillance, de contrôle, de prédiction et d'optimisation. Pour améliorer la précision du modèle de classification et la prédiction de la porosité, il serait judicieux d'optimiser les performances de l'algorithme d'apprentissage automatique. L'exploration et l'analyse de différentes techniques pour résoudre les problèmes de déséquilibre pourraient également être envisagées dans les recherches futures.

Au terme de cette étude exhaustive sur le soudage au laser des alliages d'aluminium 6061 avec les alliages 5052 et 5086, plusieurs conclusions significatives émergent, en établissant un solide lien entre les objectifs initiaux de ce mémoire et les résultats obtenus.

Premièrement, la revue de la littérature a souligné l'efficacité du soudage au laser comme technique d'assemblage dans l'industrie. Les méthodes de surveillance des procédés ont été identifiées et évaluées pour leur capacité à contrôler les paramètres clés du soudage au laser, offrant des perspectives précieuses pour la prédiction et l'optimisation de la qualité du soudage grâce à des approches basées sur l'intelligence artificielle.

En appliquant rigoureusement un plan expérimental et des outils d'analyse statistique, nous avons pu déterminer l'influence significative de divers paramètres de procédé. L'étude approfondie des effets de la puissance, de la vitesse et de la distance focale sur les propriétés mécaniques a confirmé la pertinence des schémas basés sur des observations pratiques développés à partir de la méthode Taguchi.

Bien que le déploiement du soudage au laser se généralise rapidement dans divers secteurs industriels, les défis persistent, notamment en termes d'implémentation de systèmes de surveillance, d'amélioration des paramètres de procédure et d'assurance de la qualité du produit final. Malgré la complexité inhérente à cette technique, ses avantages en termes d'efficacité énergétique et de vitesse de soudage demeurent indéniables.

Ces résultats confirment l'importance de développer des méthodes et des technologies de surveillance pour consolider et optimiser l'application du soudage au laser. Dans le contexte actuel de l'industrie 4.0, l'intégration d'outils innovants basés sur l'intelligence artificielle offre des opportunités prometteuses pour garantir une qualité optimale et une utilisation plus efficiente des matières premières.

De plus, cette étude a fourni des directives précises pour réguler les propriétés mécaniques en fonction des paramètres du soudage au laser pour les plaques d'aluminium. Ces conclusions offrent des pistes d'amélioration claires pour la prédiction des propriétés mécaniques, telles que la microdureté, la résistance à la rupture et la force de rupture, ainsi que pour l'observation de la microstructure.

En envisageant des recherches futures, l'étude de l'effet de la trajectoire du soudage sur les propriétés mécaniques du matériau soudé, l'introduction de gaz complémentaires, comme l'argon, et l'optimisation des modèles d'apprentissage automatique pourraient enrichir davantage ces résultats. Ces recommandations offrent des pistes concrètes pour une continuation fructueuse de ce projet.

Cette conclusion générale renforce le lien entre les objectifs initiaux de ce mémoire, les résultats obtenus et les perspectives d'amélioration future, offrant ainsi une synthèse explicite et cohérente de ce travail de recherche.



## RÉFÉRENCES BIBLIOGRAPHIQUES

- [1] J. Zhu, Y. Lu, Z. Song, X. Shao, et X.-G. Yue, « The choice of green manufacturing modes under carbon tax and carbon quota », *J Clean Prod*, vol. 384, p. 135336, janv. 2023, doi: 10.1016/J.JCLEPRO.2022.135336.
- [2] J. Zheng *et al.*, « Combination method of multiple molding technologies for reducing energy and carbon emission in the foundry industry », *Sustainable Materials and Technologies*, p. e00522, déc. 2022, doi: 10.1016/J.SUSMAT.2022.E00522.
- [3] A. Giampieri, J. Ling-Chin, Z. Ma, A. Smallbone, et A. P. Roskilly, « A review of the current automotive manufacturing practice from an energy perspective », *Appl Energy*, vol. 261, p. 114074, mars 2020, doi: 10.1016/J.APENERGY.2019.114074.
- [4] J. G. (John G. Kaufman, E. L. Rooy, et American Foundry Society., « Aluminum alloy castings : properties, processes, and applications », p. 340, 2004, Consulté le: 16 mai 2023. [En ligne]. Disponible à: [https://www.asminternational.org/aluminum-alloy-castings-properties-processes-and-applications/results/-/journal\\_content/56/05114G/PUBLICATION/](https://www.asminternational.org/aluminum-alloy-castings-properties-processes-and-applications/results/-/journal_content/56/05114G/PUBLICATION/)
- [5] D. K. Koli, G. Agnihotri, et R. Purohit, « Advanced Aluminium Matrix Composites: The Critical Need of Automotive and Aerospace Engineering Fields », *Mater Today Proc*, vol. 2, n° 4-5, p. 3032-3041, janv. 2015, doi: 10.1016/J.MATPR.2015.07.290.
- [6] K. K. Sankaran et R. S. Mishra, « Aluminum Alloys », *Metallurgy and Design of Alloys with Hierarchical Microstructures*, p. 57-176, 2017, doi: 10.1016/B978-0-12-812068-2.00004-7.

- [7] W. Cassada, J. Liu, et J. Staley, « Aluminum alloys for aircraft structures », *Advanced Materials & Processes*, vol. 160, n° 12, p. 27-30, déc. 2002, Consulté le: 17 mai 2023. [En ligne]. Disponible à: <https://go.gale.com/ps/i.do?p=AONE&sw=w&issn=08827958&v=2.1&it=r&id=GALE%7CA95594296&sid=googleScholar&linkaccess=fulltext>
- [8] E. Georgantzia, M. Gkantou, et G. S. Kamaris, « Aluminium alloys as structural material: A review of research », *Eng Struct*, vol. 227, p. 111372, janv. 2021, doi: 10.1016/J.ENGSTRUCT.2020.111372.
- [9] J. Fathi, P. Ebrahimzadeh, R. Farasati, et R. Teimouri, « Friction stir welding of aluminum 6061-T6 in presence of watercooling: Analyzing mechanical properties and residual stress distribution », *International Journal of Lightweight Materials and Manufacture*, vol. 2, n° 2, p. 107-115, juin 2019, doi: 10.1016/J.IJLMM.2019.04.007.
- [10] Z. Huang, W. Wang, Y. Zhang, et J. Lai, « Low speed impact properties of 5052 aluminum alloy plate », *Procedia Manuf*, vol. 50, p. 668-672, janv. 2020, doi: 10.1016/J.PROMFG.2020.08.120.
- [11] I. Pashby, « Joining techniques for aluminium spaceframes used in automobiles », *J Mater Process Technol*, janv. 2000, Consulté le: 17 mai 2023. [En ligne]. Disponible à: [https://www.academia.edu/81509671/Joining\\_techniques\\_for\\_aluminium\\_spaceframes\\_used\\_in\\_automobiles](https://www.academia.edu/81509671/Joining_techniques_for_aluminium_spaceframes_used_in_automobiles)
- [12] G. Meschut, V. Janzen, et T. Olfermann, « Innovative and highly productive joining technologies for multi-material lightweight car body structures », *J Mater Eng Perform*, vol. 23, n° 5, p. 1515-1523, avr. 2014, doi: 10.1007/S11665-014-0962-3/FIGURES/12.

- [13] T. A. Barnes et I. R. Pashby, « Joining techniques for aluminum spaceframes used in automobiles. Part II - adhesive bonding and mechanical fasteners », *J Mater Process Technol*, vol. 99, n° 1, p. 72-79, mars 2000, doi: 10.1016/S0924-0136(99)00361-1.
- [14] P. Briskham, N. Blundell, L. Han, R. Hewitt, K. Young, et D. Boomer, « Comparison of self-pierce riveting, resistance spot welding and spot friction joining for aluminium automotive sheet », 2006.
- [15] T. A. Barnes and I. R. Pashby, « Joining techniques for aluminium spaceframes used in automobiles », *J Mater Process Technol*, janv. 2000, Consulté le: 17 mai 2023. [En ligne]. Disponible à: [https://www.academia.edu/81509671/Joining\\_techniques\\_for\\_aluminium\\_spaceframes\\_used\\_in\\_automobiles](https://www.academia.edu/81509671/Joining_techniques_for_aluminium_spaceframes_used_in_automobiles)
- [16] R. Qiu, J. Li, H. Shi, et H. Yu, « Characterization of resistance spot welded joints between aluminum alloy and mild steel with composite electrodes », *Journal of Materials Research and Technology*, vol. 24, p. 1190-1202, mai 2023, doi: 10.1016/J.JMRT.2023.03.069.
- [17] Y. Xu *et al.*, « Welding seam tracking in robotic gas metal arc welding », *J Mater Process Technol*, vol. 248, p. 18-30, oct. 2017, doi: 10.1016/J.JMATPROTEC.2017.04.025.
- [18] B. T. Gibson *et al.*, « Friction stir welding: Process, automation, and control », *J Manuf Process*, vol. 16, n° 1, p. 56-73, janv. 2014, doi: 10.1016/J.JMAPRO.2013.04.002.
- [19] Q. Li, Z. Mu, M. Luo, A. Huang, et S. Pang, « Laser Spot Micro-Welding of Ultra-Thin Steel Sheet », *Micromachines 2021, Vol. 12, Page 342*, vol. 12, n° 3, p. 342, mars 2021, doi: 10.3390/MI12030342.
- [20] K. Weman et Klas. Traduction de : Weman, « Procédés de soudage », p. 344.

- [21] D. Y. You, X. D. Gao, et S. Katayama, « Review of laser welding monitoring », <http://dx.doi.org/10.1179/1362171813Y.0000000180>, vol. 19, n° 3, p. 181-201, 2014, doi: 10.1179/1362171813Y.0000000180.
- [22] S. Katayama, « Introduction: fundamentals of laser welding », *Handbook of Laser Welding Technologies*, p. 3-16, janv. 2013, doi: 10.1533/9780857098771.1.3.
- [23] A. Gorkič, M. Jezeršek, J. Možina, et J. Daci, « Measurement of weldpiece distortion during pulsed laser welding using rapid laser profilometry », <https://doi.org/10.1179/174329306X77065>, vol. 11, n° 1, p. 48-56, févr. 2013, doi: 10.1179/174329306X77065.
- [24] K. Hao, G. Li, M. Gao, et X. Zeng, « Weld formation mechanism of fiber laser oscillating welding of austenitic stainless steel », *J Mater Process Technol*, vol. 225, p. 77-83, nov. 2015, doi: 10.1016/J.JMATPROTEC.2015.05.021.
- [25] J. Stavridis, A. Papacharalampopoulos, et P. Stavropoulos, « Quality assessment in laser welding: a critical review », *The International Journal of Advanced Manufacturing Technology* 2018 94:5, vol. 94, n° 5, p. 1825-1847, mai 2017, doi: 10.1007/S00170-017-0461-4.
- [26] P. Wang, X. Chen, Q. Pan, B. Madigan, et J. Long, « Laser welding dissimilar materials of aluminum to steel: an overview », *International Journal of Advanced Manufacturing Technology*, vol. 87, n° 9-12, p. 3081-3090, déc. 2016, doi: 10.1007/S00170-016-8725-Y/METRICS.
- [27] S. Katayama, S. Kawaguchi, M. Mizutani, Y. Kawahito, et T. Tarui, « Welding phenomena and in-process monitoring in high-power YAG laser welding of aluminium alloy », <http://dx.doi.org/10.1080/09507110902836929>, vol. 23, n° 10, p. 753-762, oct. 2009, doi: 10.1080/09507110902836929.

- [28] S. Kuryntsev, « A Review: Laser Welding of Dissimilar Materials (Al/Fe, Al/Ti, Al/Cu)&mdash;Methods and Techniques, Microstructure and Properties », *Materials* 2022, Vol. 15, Page 122, vol. 15, n° 1, p. 122, déc. 2021, doi: 10.3390/MA15010122.
- [29] Y. Kawahito, M. Kito, et S. Katayama, « In-process monitoring and adaptive control for gap in micro butt welding with pulsed YAG laser », *J Phys D Appl Phys*, vol. 40, n° 9, p. 2972, avr. 2007, doi: 10.1088/0022-3727/40/9/045.
- [30] S. Katayama, « Formation Mechanisms and Preventive Procedures of Laser Welding Defects », *Topics in Mining, Metallurgy and Materials Engineering*, p. 87-111, 2020, doi: 10.1007/978-981-15-7933-2\_5/COVER.
- [31] Y. Huang, Y. Yuan, L. Yang, D. Wu, et S. Chen, « Real-time monitoring and control of porosity defects during arc welding of aluminum alloys », *J Mater Process Technol*, vol. 286, p. 116832, déc. 2020, doi: 10.1016/J.JMATPROTEC.2020.116832.
- [32] H. M. M. A. Rashed, « Control of Distortion in Aluminium Heat Treatment », *Fundamentals of Aluminium Metallurgy*, p. 495-524, janv. 2018, doi: 10.1016/B978-0-08-102063-0.00013-8.
- [33] H. Murakawa, « Residual stress and distortion in laser welding », *Handbook of Laser Welding Technologies*, p. 374-400e, janv. 2013, doi: 10.1533/9780857098771.2.374.
- [34] C. L. Tsai et D. S. Kim, « Understanding residual stress and distortion in welds: an overview », *Processes and Mechanisms of Welding Residual Stress and Distortion*, p. 3-31, janv. 2005, doi: 10.1533/9781845690939.1.3.
- [35] W. Cai, J. Z. Wang, P. Jiang, L. C. Cao, G. Y. Mi, et Q. Zhou, « Application of sensing techniques and artificial intelligence-based methods to laser welding real-time monitoring: A critical review of recent literature », *J Manuf Syst*, vol. 57, p. 1-18, oct. 2020, doi: 10.1016/J.JMSY.2020.07.021.

- [36] W. Cai, J. Z. Wang, P. Jiang, L. C. Cao, G. Y. Mi, et Q. Zhou, « Application of sensing techniques and artificial intelligence-based methods to laser welding real-time monitoring: A critical review of recent literature », *J Manuf Syst*, vol. 57, p. 1-18, oct. 2020, doi: 10.1016/J.JMSY.2020.07.021.
- [37] H. Ben Ameur, X. Han, Z. Liu, et J. Peillex, « When did global warming start? A new baseline for carbon budgeting », *Econ Model*, vol. 116, p. 106005, nov. 2022, doi: 10.1016/J.ECONMOD.2022.106005.
- [38] A. Taub, E. de Moor, A. Luo, D. K. Matlock, J. G. Speer, et U. Vaidya, « Materials for Automotive Lightweighting », <https://doi.org/10.1146/annurev-matsci-070218-010134>, vol. 49, p. 327-359, juill. 2019, doi: 10.1146/ANNUREV-MATSCI-070218-010134.
- [39] P. K. Mallick, « Advanced materials for automotive applications: An overview », *Advanced Materials in Automotive Engineering*, p. 5-27, févr. 2012, doi: 10.1016/B978-1-84569-561-3.50002-8.
- [40] M. Graudenz et M. Baur, « Applications of laser welding in the automotive industry », *Handbook of Laser Welding Technologies*, p. 555-574, janv. 2013, doi: 10.1533/9780857098771.4.555.
- [41] H. Wang, « Applications of laser welding in the railway industry », *Handbook of Laser Welding Technologies*, p. 575-595, juin 2013, doi: 10.1533/9780857098771.4.575.
- [42] X. Wang, X. Zhou, Z. Xia, et X. Gu, « A survey of welding robot intelligent path optimization », *J Manuf Process*, vol. 63, p. 14-23, mars 2021, doi: 10.1016/J.JMAPRO.2020.04.085.
- [43] J. M. Sánchez Amaya, M. R. Amaya-Vázquez, et F. J. Botana, « Laser welding of light metal alloys: Aluminium and titanium alloys », *Handbook of Laser Welding Technologies*, p. 215-254, juin 2013, doi: 10.1533/9780857098771.2.215.

- [44] « Materials for Automobile Bodies - Geoffrey Davies - Google Livres ». <https://books.google.ca/books?hl=fr&lr=&id=lVTYEHgfrWsC&oi=fnd&pg=PP2&dq=Materials+for+Automobile+Bodies+-+Geoffrey+Davies+-+Google+Livres.%E2%80%9D&ots=GxX63dxun4&sig=edsvh0Un6zqbcePPJ cwdCI2UJQU#v=onepage&q=20%25&f=false> (consulté le 7 janvier 2023).
- [45] M. Tisza et I. Czinege, « Comparative study of the application of steels and aluminium in lightweight production of automotive parts », *International Journal of Lightweight Materials and Manufacture*, vol. 1, n° 4, p. 229-238, déc. 2018, doi: 10.1016/J.IJLMM.2018.09.001.
- [46] F. Delzendehrooy *et al.*, « A comprehensive review on structural joining techniques in the marine industry », *Compos Struct*, vol. 289, p. 115490, juin 2022, doi: 10.1016/J.COMPSTRUCT.2022.115490.
- [47] P. T. Pedersen, « Marine Structures: Future Trends and the Role of Universities », *Engineering*, vol. 1, n° 1, p. 131-138, mars 2015, doi: 10.15302/J-ENG-2015004.
- [48] « Marine Structures Engineering: Specialized Applications: Specialized ... - Gregory Tsinker - Google Livres ». [https://books.google.ca/books?hl=fr&lr=&id=ulsFCAAAQBAJ&oi=fnd&pg=PR14&ots=j67Hxq205H&sig=RqxVUxKGI\\_h9Q7gI4Gj4nHLFj88&redir\\_esc=y#v=onepage&q&f=false](https://books.google.ca/books?hl=fr&lr=&id=ulsFCAAAQBAJ&oi=fnd&pg=PR14&ots=j67Hxq205H&sig=RqxVUxKGI_h9Q7gI4Gj4nHLFj88&redir_esc=y#v=onepage&q&f=false) (consulté le 7 janvier 2023).
- [49] « What methods are used to join materials? - Medical Design and Outsourcing ». <https://www.medicaldesignandoutsourcing.com/methods-used-join-materials/> (consulté le 7 janvier 2023).
- [50] Y. Feng, H. Qiu, Y. Gao, H. Zheng, et J. Tan, « Creative design for sandwich structures: A review », *Int J Adv Robot Syst*, vol. 17, n° 3, mai 2020, doi: 10.1177/1729881420921327/ASSET/IMAGES/LARGE/10.1177\_1729881420921327-FIG2.JPG.

- [51] R. D. Adams, « Adhesive bonding : science, technology and applications », Consulté le: 7 janvier 2023. [En ligne]. Disponible à: [https://books.google.com/books/about/Adhesive\\_Bonding.html?hl=fr&id=AQhEAAAQBAJ](https://books.google.com/books/about/Adhesive_Bonding.html?hl=fr&id=AQhEAAAQBAJ)
- [52] M. Shishesaz et M. Hosseini, « Effects of joint geometry and material on stress distribution, strength and failure of bonded composite joints: an overview », <https://doi.org/10.1080/00218464.2018.1554483>, vol. 96, n° 12, p. 1053-1121, sept. 2018, doi: 10.1080/00218464.2018.1554483.
- [53] R. Ceylan, E. Ozun, O. Çoban, M. Ö. Bora, et T. Kutluk, « The effect of hygrothermal aging on the adhesion performance of nanomaterial reinforced aluminium adhesive joints », *Int J Adhes Adhes*, vol. 121, p. 103304, janv. 2023, doi: 10.1016/J.IJADHADH.2022.103304.
- [54] L. F. M. da Silva, A. Öchsner, et R. D. Adams, « Introduction to Adhesive Bonding Technology », *Handbook of Adhesion Technology*, p. 1-7, 2011, doi: 10.1007/978-3-642-01169-6\_1.
- [55] « Handbook of Adhesion Technology », *Handbook of Adhesion Technology*, 2011, doi: 10.1007/978-3-642-01169-6.
- [56] E. Knox, « Marine applications for structural adhesives », 1996, Consulté le: 7 janvier 2023. [En ligne]. Disponible à: [https://search.proquest.com/openview/c41dd2990788f08365509f8bbe2d1b5/1?pq-origsite=gscholar&cbl=51922&diss=y&casa\\_token=Hh3CIaruSmkAAAAA:aMnfzA44cbhntNo-bUpf9CPrkJMumyALO\\_kzg2KG6\\_9MVPKhVRzzs1IDoxDRLe4OX89xT3QQiQ](https://search.proquest.com/openview/c41dd2990788f08365509f8bbe2d1b5/1?pq-origsite=gscholar&cbl=51922&diss=y&casa_token=Hh3CIaruSmkAAAAA:aMnfzA44cbhntNo-bUpf9CPrkJMumyALO_kzg2KG6_9MVPKhVRzzs1IDoxDRLe4OX89xT3QQiQ)
- [57] A. Akhavan-Safar, F. Ramezani, F. Delzendehrooy, M. R. Ayatollahi, et L. F. M. da Silva, « A review on bi-adhesive joints: Benefits and challenges », *Int J Adhes Adhes*, vol. 114, p. 103098, avr. 2022, doi: 10.1016/J.IJADHADH.2022.103098.

- [58] H. Osnes et D. McGeorge, « Analysis of overlaminated double-lap joints », *Compos B Eng*, vol. 36, n° 6-7, p. 544-558, janv. 2005, doi: 10.1016/J.COMPOSITESB.2005.01.002.
- [59] T. Qin, L. Zhao, et H. Huang, « Damage Investigation and Design of Woven Composite Bonded Joint », *Key Eng Mater*, vol. 417-418, p. 861-864, 2010, doi: 10.4028/WWW.SCIENTIFIC.NET/KEM.417-418.861.
- [60] « Difference Between Joining and Fastening ». <http://www.differencebox.com/engineering/difference-between-joining-and-fastening/> (consulté le 7 janvier 2023).
- [61] B. Schork *et al.*, « The effect of the local and global weld geometry as well as material defects on crack initiation and fatigue strength », *Eng Fract Mech*, vol. 198, p. 103-122, juill. 2018, doi: 10.1016/J.ENGFRACTMECH.2017.07.001.
- [62] D. F. O. Braga, L. M. C. de Sousa, V. Infante, L. F. M. da Silva, et P. M. G. P. Moreira, « Aluminium Friction-stir Weld-bonded Joints », <https://doi.org/10.1080/00218464.2015.1085860>, vol. 92, n° 7-9, p. 665-678, sept. 2016, doi: 10.1080/00218464.2015.1085860.
- [63] M. K. B. Givi et P. Asadi, *Advances in Friction-Stir Welding and Processing*. Woodhead Publishing, 2014. doi: 10.1533/9780857094551.1.
- [64] R. Kumar, R. Singh, I. P. S. Ahuja, R. Penna, et L. Feo, « Weldability of thermoplastic materials for friction stir welding- A state of art review and future applications », *Compos B Eng*, vol. 137, p. 1-15, mars 2018, doi: 10.1016/J.COMPOSITESB.2017.10.039.
- [65] S. Patil, M. Nagamadhu, et T. Malyadri, « A critical review on microstructure and hardness of aluminum alloy 6061 joints obtained by friction stir welding-past, present, and its prospects », *Mater Today Proc*, déc. 2022, doi: 10.1016/J.MATPR.2022.11.362.

- [66] X. M. Cheng, K. Yang, J. Wang, W. T. Xiao, et S. S. Huang, « Ultrasonic system and ultrasonic metal welding performance: A status review », *J Manuf Process*, vol. 84, p. 1196-1216, déc. 2022, doi: 10.1016/J.JMAPRO.2022.10.067.
- [67] D. Zhao, W. Wang, D. Ren, et K. Zhao, « Research on ultrasonic welding of copper wire harness and aluminum alloy: based on experimental method and GA-ANN model », *Journal of Materials Research and Technology*, vol. 22, p. 3180-3191, janv. 2023, doi: 10.1016/J.JMRT.2022.12.155.
- [68] B. Sanga, R. Wattal, et D. S. Nagesh, « Mechanism of joint formation and characteristics of interface in ultrasonic welding: Literature review », *Periodicals of Engineering and Natural Sciences (PEN)*, vol. 6, n° 1, p. 107-119, mai 2018, doi: 10.21533/PEN.V6I1.158.
- [69] B. Langenecker, « Effects of Ultrasound on Deformation Characteristics of Metals », *IEEE Trans Sonics Ultrason*, vol. 13, n° 1, p. 1-8, 1966, doi: 10.1109/T-SU.1966.29367.
- [70] J. Liu, B. Cao, et J. Yang, « Texture and intermetallic compounds of the Cu/Al dissimilar joints by high power ultrasonic welding », *J Manuf Process*, vol. 76, p. 34-45, avr. 2022, doi: 10.1016/J.JMAPRO.2022.02.001.
- [71] A. Fröhlich, P. Rochala, D. Matthe, et V. Kräusel, « A Sustainable Hybrid Inductive Joining Technology for Aluminum and Composites », *Procedia Manuf*, vol. 35, p. 143-148, janv. 2019, doi: 10.1016/J.PROMFG.2019.05.017.
- [72] A. Al-Obaidi, J. Kimme, et V. Kräusel, « Hybrid Joining by Induction Heating of Basalt Fiber Reinforced Thermoplastic Laminates », *Journal of Composites Science 2021, Vol. 5, Page 10*, vol. 5, n° 1, p. 10, janv. 2021, doi: 10.3390/JCS5010010.
- [73] B. Jiang, Q. Chen, et J. Yang, « Advances in joining technology of carbon fiber-reinforced thermoplastic composite materials and aluminum alloys », *International*

*Journal of Advanced Manufacturing Technology*, vol. 110, n° 9-10, p. 2631-2649, oct. 2020, doi: 10.1007/S00170-020-06021-2/FIGURES/21.

- [74] C. A. Walsh, « LASER WELDING-Literature Review », 2002.
- [75] K. Sleiman, M. Legutko, K. Rettschlag, P. Jäschke, L. Overmeyer, et S. Kaierle, « CO<sub>2</sub> laser based welding of borosilicate glass by Laser Glass Deposition », *Procedia CIRP*, vol. 111, p. 466-469, janv. 2022, doi: 10.1016/J.PROCIR.2022.08.068.
- [76] D. D. Vâlsan, V. Bolocan, M. Burca, et C. M. Craiciunescu, « Experiments on Nd:YAG pulsed laser welding of thin sheets », *Mater Today Proc*, déc. 2022, doi: 10.1016/J.MATPR.2022.11.435.
- [77] B. Acherjee, « Hybrid laser arc welding: State-of-art review », *Opt Laser Technol*, vol. 99, p. 60-71, févr. 2018, doi: 10.1016/J.OPTLASTEC.2017.09.038.
- [78] C. Bagger et F. O. Olsen, « Review of laser hybrid welding », *J Laser Appl*, vol. 17, n° 1, p. 2, févr. 2005, doi: 10.2351/1.1848532.
- [79] M. Mazar Atabaki, M. Nikodinovski, P. Chenier, J. Ma, W. Liu, et R. Kovacevic, « Experimental and numerical investigations of hybrid laser arc welding of aluminum alloys in the thick T-joint configuration », *Opt Laser Technol*, vol. 59, p. 68-92, juill. 2014, doi: 10.1016/J.OPTLASTEC.2013.12.008.
- [80] Z. Shenghai, S. Yifu, et Q. Huijuan, « The technology and welding joint properties of hybrid laser-tig welding on thick plate », *Opt Laser Technol*, vol. 48, p. 381-388, juin 2013, doi: 10.1016/J.OPTLASTEC.2012.11.014.
- [81] A. Ascari, A. Fortunato, L. Orazi, et G. Campana, « The influence of process parameters on porosity formation in hybrid LASER-GMA welding of AA6082 aluminum alloy », *Opt Laser Technol*, vol. 44, n° 5, p. 1485-1490, juill. 2012, doi: 10.1016/J.OPTLASTEC.2011.12.014.

- [82] T. Ishide, S. Tsubota, et M. Watanabe, « Latest MIG, TIG arc-YAG laser hybrid welding systems for various welding products », <https://doi.org/10.1117/12.497771>, vol. 4831, p. 347-352, mars 2003, doi: 10.1117/12.497771.
- [83] E. le Guen, R. Fabbro, M. Carin, F. Coste, et P. le Masson, « Analysis of hybrid Nd:Yag laser-MAG arc welding processes », *Opt Laser Technol*, vol. 43, n° 7, p. 1155-1166, oct. 2011, doi: 10.1016/J.OPTLASTEC.2011.03.002.
- [84] E. le Guen, R. Fabbro, M. Carin, F. Coste, et P. le Masson, « Analysis of hybrid Nd:Yag laser-MAG arc welding processes », *Opt Laser Technol*, vol. 43, n° 7, p. 1155-1166, oct. 2011, doi: 10.1016/J.OPTLASTEC.2011.03.002.
- [85] T. Ishide, S. Tsubota, et M. Watanabe, « Latest MIG, TIG arc-YAG laser hybrid welding systems for various welding products », <https://doi.org/10.1117/12.497771>, vol. 4831, p. 347-352, mars 2003, doi: 10.1117/12.497771.
- [86] A. Ascari, A. Fortunato, L. Orazi, et G. Campana, « The influence of process parameters on porosity formation in hybrid LASER-GMA welding of AA6082 aluminum alloy », *Opt Laser Technol*, vol. 44, n° 5, p. 1485-1490, juill. 2012, doi: 10.1016/J.OPTLASTEC.2011.12.014.
- [87] Z. Shenghai, S. Yifu, et Q. Huijuan, « The technology and welding joint properties of hybrid laser-tig welding on thick plate », *Opt Laser Technol*, vol. 48, p. 381-388, juin 2013, doi: 10.1016/J.OPTLASTEC.2012.11.014.
- [88] M. Mazar Atabaki, M. Nikodinovski, P. Chenier, J. Ma, W. Liu, et R. Kovacevic, « Experimental and numerical investigations of hybrid laser arc welding of aluminum alloys in the thick T-joint configuration », *Opt Laser Technol*, vol. 59, p. 68-92, juill. 2014, doi: 10.1016/J.OPTLASTEC.2013.12.008.
- [89] L. Xu, X. Tang, S. Han, R. Zhang, C. Shao, et H. Cui, « Study on root hump formation mechanism in full penetration laser welding with backing gas for aluminum alloy », *J*

*Mater Process Technol*, vol. 307, p. 117674, sept. 2022, doi: 10.1016/J.JMATPROTEC.2022.117674.

- [90] L. Zhang, J. Zhang, G. Zhang, W. Bo, et S. Gong, « An investigation on the effects of side assisting gas flow and metallic vapour jet on the stability of keyhole and molten pool during laser full-penetration welding », *J Phys D Appl Phys*, vol. 44, n° 13, p. 135201, mars 2011, doi: 10.1088/0022-3727/44/13/135201.
- [91] M. Xiao, C. Gao, C. Tan, Y. Zhao, H. Liu, et J. Yang, « Experimental and numerical assessment of interfacial microstructure evolution in dissimilar Al/steel joint by diode laser welding-brazing », *Optik (Stuttg)*, vol. 245, p. 167706, nov. 2021, doi: 10.1016/J.IJLEO.2021.167706.
- [92] J. Ahn, E. He, L. Chen, J. Dear, et C. Davies, « The effect of Ar and He shielding gas on fibre laser weld shape and microstructure in AA 2024-T3 », *J Manuf Process*, vol. 29, p. 62-73, oct. 2017, doi: 10.1016/J.JMAPRO.2017.07.011.
- [93] S. Yang, L. Yang, D. Wang, F. Zhang, C. Liu, et G. Huang, « Effect of welding stability on process porosity in laser arc hybrid welding of dissimilar steel », *Optik (Stuttg)*, vol. 271, p. 170165, déc. 2022, doi: 10.1016/J.IJLEO.2022.170165.
- [94] J. Zhao, J. Wang, X. Kang, X. Wang, et X. Zhan, « Effect of beam oscillation and oscillating frequency induced heat accumulation on microstructure and mechanical property in laser welding of Invar alloy », *Opt Laser Technol*, vol. 158, p. 108831, févr. 2023, doi: 10.1016/J.OPTLASTEC.2022.108831.
- [95] X. Yang, H. Chen, M. V. Li, H. Bu, Z. Zhu, et C. Cai, « Porosity suppressing and grain refining of narrow-gap rotating laser-MIG hybrid welding of 5A06 aluminum alloy », *J Manuf Process*, vol. 68, p. 1100-1113, août 2021, doi: 10.1016/J.JMAPRO.2021.06.036.

- [96] C. Chen, H. Zhou, C. Wang, L. Liu, Y. Zhang, et K. Zhang, « Laser welding of ultra-high strength steel with different oscillating modes », *J Manuf Process*, vol. 68, p. 761-769, août 2021, doi: 10.1016/J.JMAPRO.2021.06.004.
- [97] A. Das, I. Masters, et D. Williams, « Understanding novel gap-bridged remote laser welded (RLW) joints for automotive high-rate and temperature applications », *Int J Mech Sci*, vol. 190, p. 106043, janv. 2021, doi: 10.1016/J.IJMECSCI.2020.106043.
- [98] C. Zhang, Y. Yu, C. Chen, X. Zeng, et M. Gao, « Suppressing porosity of a laser keyhole welded Al-6Mg alloy via beam oscillation », *J Mater Process Technol*, vol. 278, p. 116382, avr. 2020, doi: 10.1016/J.JMATPROTEC.2019.116382.
- [99] C. Chen, H. Zhou, C. Wang, L. Liu, Y. Zhang, et K. Zhang, « Laser welding of ultra-high strength steel with different oscillating modes », *J Manuf Process*, vol. 68, p. 761-769, août 2021, doi: 10.1016/J.JMAPRO.2021.06.004.
- [100] J. Zhao, J. Wang, X. Kang, X. Wang, et X. Zhan, « Effect of beam oscillation and oscillating frequency induced heat accumulation on microstructure and mechanical property in laser welding of Invar alloy », *Opt Laser Technol*, vol. 158, p. 108831, févr. 2023, doi: 10.1016/J.OPTLASTEC.2022.108831.
- [101] Y. Zhang, X. Li, Y. Wang, L. Kang, T. Wang, et F. Qiu, « Effect of laser fusion repair on the microstructure and properties of stainless steel laser welds », *Journal of Materials Research and Technology*, vol. 22, p. 2781-2791, janv. 2023, doi: 10.1016/J.JMRT.2022.12.099.
- [102] W. Cai, J. Z. Wang, P. Jiang, L. C. Cao, G. Y. Mi, et Q. Zhou, « Application of sensing techniques and artificial intelligence-based methods to laser welding real-time monitoring: A critical review of recent literature », *J Manuf Syst*, vol. 57, p. 1-18, oct. 2020, doi: 10.1016/J.JMSY.2020.07.021.
- [103] L. Zhang, A. C. Basantes-Defaz, D. Ozevin, et E. Indacochea, « Real-time monitoring of welding process using air-coupled ultrasonics and acoustic emission »,

*International Journal of Advanced Manufacturing Technology*, vol. 101, n° 5-8, p. 1623-1634, avr. 2019, doi: 10.1007/S00170-018-3042-2/METRICS.

- [104] H. Zhao et H. Qi, « Vision-based keyhole detection in laser full penetration welding process », *J Laser Appl*, vol. 28, n° 2, p. 022412, mars 2016, doi: 10.2351/1.4944003.
- [105] A. F. H. Kaplan et J. Powell, « Spatter in laser welding », *J Laser Appl*, vol. 23, n° 3, p. 032005, juin 2011, doi: 10.2351/1.3597830.
- [106] T. Sibillano, A. Ancona, D. Rizzi, V. Lupo, L. Tricarico, et P. M. Lugarà, « Plasma Plume Oscillations Monitoring during Laser Welding of Stainless Steel by Discrete Wavelet Transform Application », *Sensors 2010, Vol. 10, Pages 3549-3561*, vol. 10, n° 4, p. 3549-3561, avr. 2010, doi: 10.3390/S100403549.
- [107] B. Ribic, T. A. Palmer, et T. DebRoy, « Problems and issues in laser-arc hybrid welding », <http://dx.doi.org/10.1179/174328009X411163>, vol. 54, n° 4, p. 223-244, 2013, doi: 10.1179/174328009X411163.
- [108] J. Stavridis, A. Papacharalampopoulos, et P. Stavropoulos, « Quality assessment in laser welding: a critical review », *International Journal of Advanced Manufacturing Technology*, vol. 94, n° 5-8, p. 1825-1847, févr. 2018, doi: 10.1007/S00170-017-0461-4/METRICS.
- [109] S. Katayama, Y. Kawahito, et M. Mizutani, « Elucidation of laser welding phenomena and factors affecting weld penetration and welding defects », *Phys Procedia*, vol. 5, n° PART 2, p. 9-17, janv. 2010, doi: 10.1016/J.PHPRO.2010.08.024.
- [110] W. Cai, J. Z. Wang, P. Jiang, L. C. Cao, G. Y. Mi, et Q. Zhou, « Application of sensing techniques and artificial intelligence-based methods to laser welding real-time monitoring: A critical review of recent literature », *J Manuf Syst*, vol. 57, p. 1-18, oct. 2020, doi: 10.1016/J.JMSY.2020.07.021.

- [111] S. Kaierle, M. Ungers, C. Franz, S. Mann, et P. Abels, « Understanding the Laser Process », *Laser Technik Journal*, vol. 7, n° 2, p. 49-52, avr. 2010, doi: 10.1002/LATJ.201090027.
- [112] S. Katayama, « Defect formation mechanisms and preventive procedures in laser welding », *Handbook of Laser Welding Technologies*, p. 332-373, janv. 2013, doi: 10.1533/9780857098771.2.332.
- [113] D. You, X. Gao, et S. Katayama, « WPD-PCA-based laser welding process monitoring and defects diagnosis by using FNN and SVM », *IEEE Transactions on Industrial Electronics*, vol. 62, n° 1, p. 628-636, janv. 2015, doi: 10.1109/TIE.2014.2319216.
- [114] Y. Kawahito, T. Ohnishi, et S. Katayama, « In-process monitoring and feedback control for stable production of full-penetration weld in continuous wave fibre laser welding », *J Phys D Appl Phys*, vol. 42, n° 8, p. 085501, mars 2009, doi: 10.1088/0022-3727/42/8/085501.
- [115] R.-S. Huang, L.-M. Liu, et G. Song, « Infrared temperature measurement and interference analysis of magnesium alloys in hybrid laser-TIG welding process », *Materials Science and Engineering A*, vol. 447, p. 239-243, 2007, doi: 10.1016/j.msea.2006.10.069.
- [116] J. Dowden, P. Kapadia, A. Clucas, R. Ducharme, et W. M. Steen, « On the relation between fluid dynamic pressure and the formation of pores in laser keyhole welding », *J Laser Appl*, vol. 8, n° 4, p. 183, août 2012, doi: 10.2351/1.4745420.
- [117] S. A. Uspenskiy, P. Y. Shcheglov, V. N. Petrovskiy, A. v. Gumenyuk, et M. Rethmeier, « Spectral diagnostics of a vapor-plasma plume produced during welding with a high-power ytterbium fiber laser », *Optics and Spectroscopy (English translation of Optika i Spektroskopiya)*, vol. 115, n° 1, p. 140-146, juill. 2013, doi: 10.1134/S0030400X13070205/METRICS.

- [118] V. Wippo *et al.*, « Evaluation of a pyrometric-based temperature measuring process for the laser transmission welding », *Phys Procedia*, vol. 39, p. 128-136, 2012, doi: 10.1016/j.phpro.2012.10.022.
- [119] P. Bertrand, I. Smurov, et D. Grevey, « Application of near infrared pyrometry for continuous Nd:YAG laser welding of stainless steel », *Appl Surf Sci*, vol. 168, n° 1-4, p. 182-185, déc. 2000, doi: 10.1016/S0169-4332(00)00586-9.
- [120] H. Köhler, C. Thomy, et F. Vollertsen, « Contact-less temperature measurement and control with applications to laser cladding », *Welding in the World*, vol. 60, n° 1, p. 1-9, janv. 2016, doi: 10.1007/S40194-015-0275-7/METRICS.
- [121] F. Dorsch, H. Braun, S. Keßler, D. Pfitzner, et V. Rominger, « NIR-camera-based online diagnostics of laser beam welding processes », <https://doi.org/10.1117/12.908646>, vol. 8239, p. 229-239, févr. 2012, doi: 10.1117/12.908646.
- [122] T. Sibillano, A. Ancona, V. Berardi, et P. M. Lugarà, « A Real-Time Spectroscopic Sensor for Monitoring Laser Welding Processes », *Sensors 2009, Vol. 9, Pages 3376-3385*, vol. 9, n° 5, p. 3376-3385, mai 2009, doi: 10.3390/S90503376.
- [123] T. Sibillano *et al.*, « Spectroscopic monitoring of penetration depth in CO<sub>2</sub> Nd:YAG and fiber laser welding processes », *J Mater Process Technol*, vol. 212, n° 4, p. 910-916, avr. 2012, doi: 10.1016/J.JMATPROTEC.2011.11.016.
- [124] F. M. Haran, D. P. Hand, C. Peters, et J. D. C. Jones, « Real-time focus control in laser welding », *Meas Sci Technol*, vol. 7, n° 8, p. 1095, août 1996, doi: 10.1088/0957-0233/7/8/001.
- [125] I. Eriksson, J. Powell, et A. F. H. Kaplan, « Signal overlap in the monitoring of laser welding », *Meas Sci Technol*, vol. 21, n° 10, p. 105705, sept. 2010, doi: 10.1088/0957-0233/21/10/105705.

- [126] S. Kaierle, « Process Monitoring and Control of Laser Beam Welding », *Laser Technik Journal*, vol. 5, n° 3, p. 41-43, mai 2008, doi: 10.1002/LATJ.200890024.
- [127] F. Kong, J. Ma, B. Carlson, et R. Kovacevic, « Real-time monitoring of laser welding of galvanized high strength steel in lap joint configuration », 2012, doi: 10.1016/j.optlastec.2012.03.003.
- [128] T. Ilar, I. Eriksson, J. Powell, et A. Kaplan, « Root humping in laser welding-an investigation based on high speed imaging », *Phys Procedia*, vol. 39, p. 27-32, 2012, doi: 10.1016/j.phpro.2012.10.010.
- [129] Z. M. Liu, C. S. Wu, et M. A. Chen, « Visualizing the influence of the process parameters on the keyhole dimensions in plasma arc welding », *Meas Sci Technol*, vol. 23, n° 10, p. 105603, sept. 2012, doi: 10.1088/0957-0233/23/10/105603.
- [130] X. F. Liu, C. B. Jia, C. S. Wu, G. K. Zhang, et J. Q. Gao, « Measurement of the keyhole entrance and topside weld pool geometries in keyhole plasma arc welding with dual CCD cameras », 2017, doi: 10.1016/j.jmatprotec.2017.05.012.
- [131] H. Roozbahani, P. Marttinen, et A. Salminen, « Real-Time Monitoring of Laser Scribing Process of CIGS Solar Panels Utilizing High-Speed Camera », *IEEE Photonics Technology Letters*, vol. 30, n° 20, p. 1741-1744, oct. 2018, doi: 10.1109/LPT.2018.2867274.
- [132] Y. Zhang, C. Zhang, L. Tan, et S. Li, « Coaxial monitoring of the fibre laser lap welding of Zn-coated steel sheets using an auxiliary illuminant », *Opt Laser Technol*, vol. 50, p. 167-175, sept. 2013, doi: 10.1016/J.OPTLASTEC.2013.03.001.
- [133] Z. Ye, G. Fang, S. Chen, et J. J. Zou, « Passive vision based seam tracking system for pulse-MAG welding », *International Journal of Advanced Manufacturing Technology*, vol. 67, n° 9-12, p. 1987-1996, août 2013, doi: 10.1007/S00170-012-4625-Y/METRICS.

- [134] S. Kaierle et • • Stefan Kaierle, « Process Monitoring and Control of Laser Beam Welding », *Laser Technik Journal*, vol. 5, n° 3, p. 41-43, mai 2008, doi: 10.1002/LATJ.200890024.
- [135] S. Kaierle et • • Stefan Kaierle, « Process Monitoring and Control of Laser Beam Welding », *Laser Technik Journal*, vol. 5, n° 3, p. 41-43, mai 2008, doi: 10.1002/LATJ.200890024.
- [136] S. Kaierle, « Process Monitoring and Control of Laser Beam Welding », *Laser Technik Journal*, vol. 5, n° 3, p. 41-43, mai 2008, doi: 10.1002/LATJ.200890024.
- [137] Z. Chen, X. Gao, S. Katayama, Z. Xiao, et X. Chen, « Elucidation of high-power disk laser welding phenomena by simultaneously observing both top and bottom of weldment », *International Journal of Advanced Manufacturing Technology*, vol. 88, n° 1-4, p. 1141-1150, janv. 2017, doi: 10.1007/S00170-016-8837-4/METRICS.
- [138] F. Tenner, B. Berg, et C. Brock, « Experimental approach for quantification of fluid dynamics in laser metal welding », *J. Laser Appl*, vol. 27, p. 29003, 2015, doi: 10.2351/1.4906302.
- [139] R. Subramanian *et al.*, « Feasibility of using acoustic method in monitoring the penetration status during the Pulse Mode Laser Welding process », *IOP Conf Ser Mater Sci Eng*, vol. 238, n° 1, p. 012006, sept. 2017, doi: 10.1088/1757-899X/238/1/012006.
- [140] R. Subramanian *et al.*, « Feasibility of using acoustic method in monitoring the penetration status during the Pulse Mode Laser Welding process », *IOP Conf Ser Mater Sci Eng*, vol. 238, n° 1, p. 012006, sept. 2017, doi: 10.1088/1757-899X/238/1/012006.
- [141] S. S. Ao, Z. Luo, C. F. Zhao, M. N. Feng, et W. D. Liu, « Acoustic signal generated by vapour flow in laser welding », *Lasers in Engineering*, vol. 34, n° 1-3, p. 145-165, 2016.

- [142] N. Lv, J. Zhong, H. Chen, T. Lin, et S. Chen, « Real-time control of welding penetration during robotic GTAW dynamical process by audio sensing of arc length », *International Journal of Advanced Manufacturing Technology*, vol. 74, n° 1-4, p. 235-249, mai 2014, doi: 10.1007/S00170-014-5875-7/METRICS.
- [143] H. Mizota, Y. Nagashima, et T. Obama, « Fundamental study of molten pool depth measurement method using an ultrasonic phased array system », *Jpn J Appl Phys*, vol. 54, n° 7, p. 07HC03, juill. 2015, doi: 10.7567/JJAP.54.07HC03/XML.
- [144] A. Passini, A. Capella de Oliveira, R. Riva, D. Nagle Travessa, et K. Regina Cardoso, « Ultrasonic Inspection of AA6013 Laser Welded Joints », 2011, doi: 10.1590/S1516-14392011005000057.
- [145] Z. Al-Sarraf et M. Lucas, « A study of weld quality in ultrasonic spot welding of similar and dissimilar metals », *J Phys Conf Ser*, vol. 382, n° 1, p. 012013, août 2012, doi: 10.1088/1742-6596/382/1/012013.
- [146] X. P. Gu, G. C. Xu, J. Liu, et X. Y. Gu, « Ultrasonic testing and evaluation of laser welds in stainless steel », *Lasers in Engineering*, vol. 26, n° 1-2, p. 103-113, 2013.
- [147] P. Kustoń, M. Korzeniowski, M. Lewandowski, B. Witek, et J. Rozbicki, « A high frequency ultrasonic imaging of welded joints », *IEEE International Ultrasonics Symposium, IUS*, vol. 2016-November, nov. 2016, doi: 10.1109/ULTSYM.2016.7728848.
- [148] H. Zhao et H. Qi, « Vision-based keyhole detection in laser full penetration welding process », *J Laser Appl*, vol. 28, n° 2, p. 022412, mars 2016, doi: 10.2351/1.4944003.
- [149] S. Kaierle, « Process Monitoring and Control of Laser Beam Welding », *Laser Technik Journal*, vol. 5, n° 3, p. 41-43, mai 2008, doi: 10.1002/LATJ.200890024.
- [150] « Scopus - Document details - On-line optical monitoring of Nd:YAG laser lap welding of Zn-coated steel sheets | Signed in ».

<https://www.scopus.com/record/display.uri?eid=2-s2.0-79551678922&origin=inward&txGid=b490d8cc371141437fe73b2d3b8c1be1>  
(consulté le 27 février 2023).

- [151] M. Boley, R. Weber, et T. Graf, « Online Detection of Pore Formation during Laser Deep-Penetration Welding », 2015.
- [152] N. Zhang et Y. J. Xu, « Aggregation- and leaching-resistant, reusable, and multifunctional Pd@CeO<sub>2</sub> as a robust nanocatalyst achieved by a hollow core-shell strategy », *Chemistry of Materials*, vol. 25, n° 9, p. 1979-1988, mai 2013, doi: 10.1021/CM400750C/SUPPL\_FILE/CM400750C\_SI\_001.PDF.
- [153] W. Huang et R. Kovacevic, « Feasibility study of using acoustic signals for online monitoring of the depth of weld in the laser welding of high-strength steels », <http://dx.doi.org/10.1243/09544054JEM1320>, vol. 223, n° 4, p. 343-361, févr. 2009, doi: 10.1243/09544054JEM1320.
- [154] J. Yan, M. Gao, et X. Zeng, « Study on microstructure and mechanical properties of 304 stainless steel joints by TIG, laser and laser-TIG hybrid welding », *Opt Lasers Eng*, vol. 48, p. 512-517, 2009, doi: 10.1016/j.optlaseng.2009.08.009.
- [155] M. West, A. T. Ellis, P. J. Potts, C. Streli, C. Vanhoof, et P. Wobraushek, « 2015 Atomic Spectrometry Update – a review of advances in X-ray fluorescence spectrometry and their applications », *J Anal At Spectrom*, vol. 30, n° 9, p. 1839-1889, août 2015, doi: 10.1039/C5JA90033F.
- [156] F. Kong et R. Kovacevic, « 3D finite element modeling of the thermally induced residual stress in the hybrid laser/arc welding of lap joint », *J Mater Process Technol*, vol. 210, n° 6-7, p. 941-950, avr. 2010, doi: 10.1016/J.JMATPROTEC.2010.02.006.
- [157] C. C. Dobson et L. M. Smith, « Absolute displacement measurements using modulation of the spectrum of white light in a Michelson interferometer », *Applied*

*Optics*, Vol. 28, Issue 16, pp. 3339-3342, vol. 28, n° 16, p. 3339-3342, août 1989, doi: 10.1364/AO.28.003339.

- [158] J. M. Fraser, « Laser process monitoring and automatic control at kHz rates through inline coherent imaging », *AIP Conf Proc*, vol. 1464, n° 1, p. 492, juill. 2012, doi: 10.1063/1.4739903.
- [159] P. Ackermann et R. Schmitt, « Tomographical process monitoring of laser transmission welding with OCT », <https://doi.org/10.1117/12.2269108>, vol. 10329, p. 101-108, juin 2017, doi: 10.1117/12.2269108.
- [160] N. D. Dupriez et A. Denkl, « Advances of OCT Technology for Laser Beam Processing », *Laser Technik Journal*, vol. 14, n° 4, p. 34-38, sept. 2017, doi: 10.1002/LATJ.201700021.
- [161] L. G. Wright *et al.*, « Automatic laser welding and milling with in situ inline coherent imaging », *Optics Letters*, Vol. 39, Issue 21, pp. 6217-6220, vol. 39, n° 21, p. 6217-6220, nov. 2014, doi: 10.1364/OL.39.006217.
- [162] Z. Liu, Z. Wang, et J. Zhu, « Observational studies on amyloplasts with single-starch granule in rice endosperm », *Revista Brasileira de Botanica*, vol. 39, n° 3, p. 821-832, sept. 2016, doi: 10.1007/S40415-016-0291-X/METRICS.
- [163] G. Turichin, E. Zemlyakov, K. Babkin, et A. Kuznetsov, « Monitoring of Laser and Hybrid Welding of Steels and Al-alloys », *Phys Procedia*, vol. 56, p. 1232-1241, 2014, doi: 10.1016/j.phpro.2014.08.039.
- [164] W. Liu, S. Liu, J. Ma, et R. Kovacevic, « Real-time monitoring of the laser hot-wire welding process », 2013, doi: 10.1016/j.optlastec.2013.09.026.
- [165] C. Brock, R. Hohenstein, et M. Schmidt, « Mechanisms of vapour plume formation in laser deep penetration welding », *Opt Lasers Eng*, vol. 58, p. 93-101, juill. 2014, doi: 10.1016/J.OPTLASENG.2014.02.001.

- [166] D. You, X. Gao, et S. Katayama, « Data-driven based analyzing and modeling of MIMO laser welding process by integration of six advanced sensors », *International Journal of Advanced Manufacturing Technology*, vol. 82, n° 5-8, p. 1127-1139, févr. 2016, doi: 10.1007/S00170-015-7455-X/METRICS.
- [167] H. K. Lee, S. H. Park, et C. Y. Kang, « Effect of plasma current on surface defects of plasma-MIG welding in cryogenic aluminum alloys », *J Mater Process Technol*, vol. 223, p. 203-215, sept. 2015, doi: 10.1016/J.JMATPROTEC.2015.04.008.
- [168] A. Oezmert, A. Drenker, et V. Nazery, « Detectability of penetration based on weld pool geometry and process emission spectrum in laser welding of copper », *Phys Procedia*, vol. 41, p. 509-514, 2013, doi: 10.1016/J.PHPRO.2013.03.108.
- [169] X. W. Wang et R. R. Li, « Intelligent modelling of back-side weld bead geometry using weld pool surface characteristic parameters », *J Intell Manuf*, vol. 25, n° 6, p. 1301-1313, nov. 2014, doi: 10.1007/S10845-013-0731-4/METRICS.
- [170] Z. Zhang, G. Wen, et S. Chen, « Multisensory data fusion technique and its application to welding process monitoring », *Proceedings of IEEE Workshop on Advanced Robotics and its Social Impacts, ARSO*, vol. 2016-November, p. 294-298, nov. 2016, doi: 10.1109/ARSO.2016.7736298.
- [171] Z. Gao *et al.*, « Multi-objective optimization of weld geometry in hybrid fiber laser-arc butt welding using Kriging model and NSGA-II », *Appl Phys A Mater Sci Process*, vol. 122, n° 6, p. 1-12, juin 2016, doi: 10.1007/S00339-016-0144-2/METRICS.
- [172] E. M. Anawa et A. G. Olabi, « Using Taguchi method to optimize welding pool of dissimilar laser-welded components », *Opt Laser Technol*, vol. 40, n° 2, p. 379-388, mars 2008, doi: 10.1016/J.OPTLASTEC.2007.07.001.
- [173] B. Acherjee, A. S. Kuar, S. Mitra, et D. Misra, « Application of grey-based Taguchi method for simultaneous optimization of multiple quality characteristics in laser transmission welding process of thermoplastics », *International Journal of Advanced*

*Manufacturing Technology*, vol. 56, n° 9-12, p. 995-1006, oct. 2011, doi: 10.1007/S00170-011-3224-7/METRICS.

- [174] S. Pal, S. K. Pal, et A. K. Samantaray, « Artificial neural network modeling of weld joint strength prediction of a pulsed metal inert gas welding process using arc signals », 2007, doi: 10.1016/j.jmatprotec.2007.09.039.
- [175] H. L. Lin et C. P. Chou, « Modeling and optimization of Nd:YAG laser micro-weld process using Taguchi Method and a neural network », *International Journal of Advanced Manufacturing Technology*, vol. 37, n° 5-6, p. 513-522, mai 2008, doi: 10.1007/S00170-007-0982-3/METRICS.
- [176] D. S. Badkar, K. S. Pandey, et G. Buvanashkaran, « Parameter optimization of laser transformation hardening by using Taguchi method and utility concept », *International Journal of Advanced Manufacturing Technology*, vol. 52, n° 9-12, p. 1067-1077, févr. 2011, doi: 10.1007/S00170-010-2787-Z/METRICS.
- [177] Y. Rong *et al.*, « Parameters optimization of laser brazing in crimping butt using Taguchi and BPNN-GA », 2014, doi: 10.1016/j.optlaseng.2014.10.009.
- [178] L. Cao *et al.*, « Optimization of processing parameters of AISI 316L laser welding influenced by external magnetic field combining RBFNN and GA », 2017, doi: 10.1016/j.rinp.2017.03.029.
- [179] S. Liu, G. Mi, F. Yan, C. Wang, et P. Jiang, « Correlation of high power laser welding parameters with real weld geometry and microstructure », 2017, doi: 10.1016/j.optlastec.2017.03.004.
- [180] N. Chandrasekhar, M. Vasudevan, A. K. Bhaduri, et T. Jayakumar, « Intelligent modeling for estimating weld bead width and depth of penetration from infra-red thermal images of the weld pool », *J Intell Manuf*, vol. 26, n° 1, p. 59-71, févr. 2015, doi: 10.1007/S10845-013-0762-X/METRICS.

- [181] S. Lee, S. Ahn, et C. Park, « Analysis of acoustic emission signals during laser spot welding of SS304 stainless steel », *J Mater Eng Perform*, vol. 23, n° 3, p. 700-707, mars 2014, doi: 10.1007/S11665-013-0791-9/METRICS.
- [182] J. Günther, P. M. Pilarski, G. Helfrich, H. Shen, et K. Diepold, « Intelligent laser welding through representation, prediction, and control learning: An architecture with deep neural networks and reinforcement learning », 2015, doi: 10.1016/j.mechatronics.2015.09.004.
- [183] X. Wan, Y. Wang, D. Zhao, Y. Huang, et Z. Yin, « Weld quality monitoring research in small scale resistance spot welding by dynamic resistance and neural network », 2016, doi: 10.1016/j.measurement.2016.12.010.
- [184] Z. Luo, J. S. Dai, C. Wang, F. Wang, Y. Tian, et M. Zhao, « Predictive seam tracking with iteratively learned feedforward compensation for high-precision robotic laser welding », *J Manuf Syst*, vol. 31, p. 2-7, 2012, doi: 10.1016/j.jmsy.2011.03.005.
- [185] B. Regaard, S. Kaierle, et R. Poprawe, « Seam-tracking for high precision laser welding applications—Methods, restrictions and enhanced concepts », *J Laser Appl*, vol. 21, n° 4, p. 183, mars 2010, doi: 10.2351/1.3267476.
- [186] A. Fernández Villán *et al.*, « Low-cost system for weld tracking based on artificial vision », *IEEE Trans Ind Appl*, vol. 47, n° 3, p. 1159-1167, mai 2011, doi: 10.1109/TIA.2011.2124432.
- [187] L. Nele, E. Sarno, et A. Keshari, « An image acquisition system for real-time seam tracking », *International Journal of Advanced Manufacturing Technology*, vol. 69, n° 9-12, p. 2099-2110, déc. 2013, doi: 10.1007/S00170-013-5167-7/METRICS.
- [188] F. Shi, T. Lin, et S. Chen, « Efficient weld seam detection for robotic welding based on local image processing », *Industrial Robot: An International Journal*, vol. 36, n° 3, p. 277-283, mai 2009, doi: 10.1108/01439910910950559.

- [189] D. Lévesque, L. Dubourg, et A. Blouin, « Laser ultrasonics for defect detection and residual stress measurement of friction stir welds », <https://doi.org/10.1080/10589759.2011.573551>, vol. 26, n° 3-4, p. 319-333, sept. 2011, doi: 10.1080/10589759.2011.573551.
- [190] H. H. Chu et Z. Y. Wang, « A vision-based system for post-welding quality measurement and defect detection », *International Journal of Advanced Manufacturing Technology*, vol. 86, n° 9-12, p. 3007-3014, oct. 2016, doi: 10.1007/S00170-015-8334-1/METRICS.
- [191] J. Mirapeix, R. Ruiz-Lombera, J. J. Valdiande, L. Rodriguez-Cobo, F. Anabitarte, et A. Cobo, « Defect detection with CCD-spectrometer and photodiode-based arc-welding monitoring systems », *J Mater Process Technol*, vol. 211, p. 2132-2139, 2011, doi: 10.1016/j.jmatprot.2011.07.011.
- [192] A. Passini, A. Capella de Oliveira, R. Riva, D. Nagle Travessa, et K. Regina Cardoso, « Ultrasonic Inspection of AA6013 Laser Welded Joints », 2011, doi: 10.1590/S1516-14392011005000057.
- [193] S. Saludes Rodil, R. Arnanz Gómez, J. M. Bernárdez, F. Rodríguez, L. J. Miguel, et J. R. Perán, « Laser welding defects detection in automotive industry based on radiation and spectroscopical measurements », *International Journal of Advanced Manufacturing Technology*, vol. 49, n° 1-4, p. 133-145, juill. 2010, doi: 10.1007/S00170-009-2395-Y/METRICS.
- [194] D. You, X. Gao, et S. Katayama, « Multisensor fusion system for monitoring high-power disk laser welding using support vector machine », *IEEE Trans Industr Inform*, vol. 10, n° 2, p. 1285-1295, 2014, doi: 10.1109/TII.2014.2309482.
- [195] S. Moos et E. Vezzetti, « Resistance spot welding process simulation for variational analysis on compliant assemblies », *J Manuf Syst*, vol. 37, n° 1, p. 44-71, oct. 2015, doi: 10.1016/J.JMSY.2015.09.006.

- [196] T. F. Flint, J. A. Francis, M. C. Smith, et J. Balakrishnan, « Extension of the double-ellipsoidal heat source model to narrow-groove and keyhole weld configurations », *J Mater Process Technol*, vol. 246, p. 123-135, 2017, doi: 10.1016/j.jmatprotec.2017.02.002.
- [197] K. Abderrazak, S. Bannour, H. Mhiri, G. Lepalec, et M. Autric, « Numerical and experimental study of molten pool formation during continuous laser welding of AZ91 magnesium alloy », *Comput Mater Sci*, vol. 44, n° 3, p. 858-866, 2009, doi: 10.1016/J.COMMATSCI.2008.06.002.
- [198] S. Wu, H. Gao, W. Zhang, et Y. Zhang, « Real-time estimation of weld penetration using weld pool surface based calibration », *IECON Proceedings (Industrial Electronics Conference)*, p. 294-299, déc. 2016, doi: 10.1109/IECON.2016.7793485.
- [199] Z. H. Rao, S. M. Liao, et H. L. Tsai, « Modelling of hybrid laser-GMA welding: review and challenges », <https://doi.org/10.1179/1362171811Y.0000000022>, vol. 16, n° 4, p. 300-305, mai 2013, doi: 10.1179/1362171811Y.0000000022.
- [200] Y. Liu et Y. Zhang, « Iterative local ANFIS-based human welder intelligence modeling and control in pipe GTAW process: A data-driven approach », *IEEE/ASME Transactions on Mechatronics*, vol. 20, n° 3, p. 1079-1088, juin 2015, doi: 10.1109/TMECH.2014.2363050.
- [201] F. Abt *et al.*, « Camera based closed loop control for partial penetration welding of overlap joints », *Phys Procedia*, vol. 12, n° PART 1, p. 730-738, 2011, doi: 10.1016/J.PHPRO.2011.03.091.
- [202] S. Kaierle, M. Ungers, C. Franz, S. Mann, et P. Abels, « Understanding the Laser Process », *Laser Technik Journal*, vol. 7, n° 2, p. 49-52, avr. 2010, doi: 10.1002/LATJ.201090027.

- [203] T. Stehr, J. Hermsdorf, T. Henning, et R. Kling, « Closed loop control for laser micro spot welding using fast pyrometer systems », *Phys Procedia*, vol. 5, n° PART 2, p. 465-471, 2010, doi: 10.1016/J.PHPRO.2010.08.074.
- [204] Y. K. Liu et Y. M. Zhang, « Toward Welding Robot With Human Knowledge: A Remotely-Controlled Approach », *IEEE Transactions on Automation Science and Engineering*, vol. 12, n° 2, p. 769-774, avr. 2015, doi: 10.1109/TASE.2014.2359006.
- [205] Y. Liu, W. Zhang, et Y. Zhang, « Dynamic neuro-fuzzy-based human intelligence modeling and control in GTAW », *IEEE Transactions on Automation Science and Engineering*, vol. 12, n° 1, p. 324-335, janv. 2015, doi: 10.1109/TASE.2013.2279157.
- [206] Y. M. Z. BY X. R. LI, « Penetration Depth Monitoring and Control in Submerged Arc Welding ».
- [207] L. Mrňa, M. Šarbort, S. Řeřucha, et P. Jedlička, « Feedback Control of Laser Welding Based on Frequency Analysis of Light Emissions and Adaptive Beam Shaping », *Phys Procedia*, vol. 39, p. 784-791, 2012, doi: 10.1016/J.PHPRO.2012.10.101.
- [208] J. T. Hofman, B. Pathiraj, J. Van Dijk, D. F. De Lange, et J. Meijer, « A camera based feedback control strategy for the laser cladding process », *J Mater Process Technol*, vol. 212, n° 11, p. 2455-2462, nov. 2012, doi: 10.1016/J.JMATPROTEC.2012.06.027.
- [209] F. Farrokhi, B. Endelt, et M. Kristiansen, « A numerical model for full and partial penetration hybrid laser welding of thick-section steels », *Opt Laser Technol*, vol. 111, p. 671-686, avr. 2019, doi: 10.1016/J.OPTLASTEC.2018.08.059.
- [210] M. Idriss, F. Mirakhorli, A. Desrochers, et A. Maslouhi, « Overlap laser welding of 5052-H36 aluminum alloy: experimental investigation of process parameters and mechanical designs », *International Journal of Advanced Manufacturing Technology*, vol. 119, n° 11-12, p. 7653-7667, avr. 2022, doi: 10.1007/S00170-022-08783-3/FIGURES/15.

- [211] N. Murali, Y. Chi, et X. Li, « Natural aging of dissimilar high-strength AA2024/AA7075 joints arc welded with nano-treated filler », *Mater Lett*, vol. 322, p. 132479, sept. 2022, doi: 10.1016/J.MATLET.2022.132479.
- [212] K. Gao, G. Liu, H. Gu, K. Li, et L. Zhu, « Experimental Investigation and Optimization on the Process Parameters during Induction Pressure Welding for Steel and Aluminum Alloy Using Response Surface Method », *J Mater Eng Perform*, vol. 31, n° 8, p. 6572-6583, août 2022, doi: 10.1007/S11665-022-06734-3/METRICS.
- [213] Z. Li, G. Yu, X. He, S. Li, C. Tian, et B. Dong, « Analysis of surface tension driven flow and solidification behavior in laser linear welding of stainless steel », *Opt Laser Technol*, vol. 123, p. 105914, mars 2020, doi: 10.1016/J.OPTLASTEC.2019.105914.
- [214] Z. Gan, Y. Lian, S. E. Lin, K. K. Jones, W. K. Liu, et G. J. Wagner, « Benchmark Study of Thermal Behavior, Surface Topography, and Dendritic Microstructure in Selective Laser Melting of Inconel 625 », *Integr Mater Manuf Innov*, vol. 8, n° 2, p. 178-193, juin 2019, doi: 10.1007/S40192-019-00130-X/METRICS.
- [215] Z. Li, G. Yu, X. He, S. Li, H. Li, et Q. Li, « Study of thermal behavior and solidification characteristics during laser welding of dissimilar metals », *Results Phys*, vol. 12, p. 1062-1072, mars 2019, doi: 10.1016/J.RINP.2018.12.017.
- [216] A. Rajesh Kannan, N. Siva Shanmugam, Y. Palguna, B. Girinath, W. Lee, et J. Yoon, « Effect of double-side welding on the microstructural characteristics and mechanical performance of dissimilar AA6061-AA5052 aluminium alloys », *Mater Lett*, vol. 331, p. 133444, janv. 2023, doi: 10.1016/J.MATLET.2022.133444.
- [217] T. Iwase, H. Sakamoto, K. Shibata, B. Hohenberger, et F. Dausinger, « Dual-focus technique for high-power Nd:YAG laser welding of aluminum alloys », <https://doi.org/10.11117/12.377042>, vol. 3888, p. 348-358, févr. 2000, doi: 10.11117/12.377042.

- [218] T. Dursun et C. Soutis, « Recent developments in advanced aircraft aluminium alloys », *Materials & Design* (1980-2015), vol. 56, p. 862-871, avr. 2014, doi: 10.1016/J.MATDES.2013.12.002.
- [219] H. Ramiarison, N. Barka, F. Mirakhori, F. Nadeau, et C. Pilcher, « Parameter optimization for laser welding of dissimilar aluminum alloy: 5052-H32 and 6061-T6 considering wobbling technique », *International Journal of Advanced Manufacturing Technology*, vol. 118, n° 11-12, p. 4195-4211, févr. 2022, doi: 10.1007/S00170-021-08122-Y/TABLES/14.
- [220] S. Katayama, « Defect formation mechanisms and preventive procedures in laser welding », *Handbook of Laser Welding Technologies*, p. 332-373, janv. 2013, doi: 10.1533/9780857098771.2.332.
- [221] Y. M. Baqer, S. Ramesh, F. Yusof, et S. M. Manladan, « Challenges and advances in laser welding of dissimilar light alloys: Al/Mg, Al/Ti, and Mg/Ti alloys », *International Journal of Advanced Manufacturing Technology*, vol. 95, n° 9-12, p. 4353-4369, avr. 2018, doi: 10.1007/S00170-017-1565-6.
- [222] M. Vyskoč, M. Sahul, et M. Sahul, « Effect of Shielding Gas on the Properties of AW 5083 Aluminum Alloy Laser Weld Joints », *J Mater Eng Perform*, vol. 27, n° 6, p. 2993-3006, juin 2018, doi: 10.1007/S11665-018-3383-X/FIGURES/11.
- [223] R. H. M. de Siqueira, A. C. de Oliveira, R. Riva, A. J. Abdalla, C. A. R. P. Baptista, et M. S. F. de Lima, « Mechanical and microstructural characterization of laser-welded joints of 6013-T4 aluminum alloy », *Journal of the Brazilian Society of Mechanical Sciences and Engineering*, vol. 37, n° 1, p. 133-140, avr. 2014, doi: 10.1007/S40430-014-0175-6/FIGURES/13.
- [224] F. Vakili-Farahani, J. Lungershausen, et K. Wasmer, « Process Parameter Optimization for Wobbling Laser Spot Welding of Ti6Al4V Alloy », *Phys Procedia*, vol. 83, p. 483-493, janv. 2016, doi: 10.1016/J.PHPRO.2016.08.050.

- [225] J. Ahn, L. Chen, E. He, J. P. Dear, et C. M. Davies, « Optimisation of process parameters and weld shape of high power Yb-fibre laser welded 2024-T3 aluminium alloy », *J Manuf Process*, vol. 34, p. 70-85, août 2018, doi: 10.1016/J.JMAPRO.2018.05.028.
- [226] T. W. Kim et Y. W. Park, « Parameter optimization using a regression model and fitness function in laser welding of aluminum alloys for car bodies », *International Journal of Precision Engineering and Manufacturing*, vol. 12, n° 2, p. 313-320, avr. 2011, doi: 10.1007/S12541-011-0041-8/METRICS.
- [227] T. E. Abioye, N. Mustar, H. Zuhailawati, et I. Suhaina, « Prediction of the tensile strength of aluminium alloy 5052-H32 fibre laser weldments using regression analysis », *International Journal of Advanced Manufacturing Technology*, vol. 102, n° 5-8, p. 1951-1962, juin 2019, doi: 10.1007/S00170-019-03310-3/METRICS.
- [228] J. Fathi, P. Ebrahimzadeh, R. Farasati, et R. Teimouri, « Friction stir welding of aluminum 6061-T6 in presence of watercooling: Analyzing mechanical properties and residual stress distribution », *International Journal of Lightweight Materials and Manufacture*, vol. 2, n° 2, p. 107-115, juin 2019, doi: 10.1016/J.IJLMM.2019.04.007.
- [229] A. Bhowmik et A. Kumar Khandelwal, « Mechanical behaviour of annealed Al 5052 at different temperatures », *Mater Today Proc*, vol. 46, p. 6091-6096, janv. 2021, doi: 10.1016/J.MATPR.2020.03.331.
- [230] V. RajKumar, M. VenkateshKannan, P. Sadeesh, N. Arivazhagan, et K. Devendranath Ramkumar, « Studies on Effect of Tool Design and Welding Parameters on the Friction Stir Welding of Dissimilar Aluminium Alloys AA 5052 – AA 6061 », *Procedia Eng*, vol. 75, p. 93-97, janv. 2014, doi: 10.1016/J.PROENG.2013.11.019.
- [231] R. Xiao, « Laser beam welding of aluminum alloys », <https://doi.org/10.11117/12.771519>, vol. 6825, p. 40-49, févr. 2008, doi: 10.11117/12.771519.

- [232] M. Vyskoč, M. Sahul, et M. Sahul, « Effect of Shielding Gas on the Properties of AW 5083 Aluminum Alloy Laser Weld Joints », *J Mater Eng Perform*, vol. 27, n° 6, p. 2993-3006, juin 2018, doi: 10.1007/S11665-018-3383-X/METRICS.
- [233] J. M. Sánchez Amaya, M. R. Amaya-Vázquez, et F. J. Botana, « Laser welding of light metal alloys: aluminium and titanium alloys », *Handbook of Laser Welding Technologies*, p. 215-254, janv. 2013, doi: 10.1533/9780857098771.2.215.
- [234] B. N. Coelho, M. S. F. de Lima, S. M. de Carvalho, et A. R. da Costa, « A Comparative Study of the Heat Input During Laser Welding of Aeronautical Aluminum Alloy AA6013-T4 », *Journal of Aerospace Technology and Management*, vol. 10, p. e2918, juin 2018, doi: 10.5028/JATM.V10.925.
- [235] Z. Wang, J. P. Oliveira, Z. Zeng, X. Bu, B. Peng, et X. Shao, « Laser beam oscillating welding of 5A06 aluminum alloys: Microstructure, porosity and mechanical properties », *Opt Laser Technol*, vol. 111, p. 58-65, avr. 2019, doi: 10.1016/J.OPTLASTEC.2018.09.036.
- [236] A. Haboudou, P. Peyre, A. B. Vannes, et G. Peix, « Reduction of porosity content generated during Nd:YAG laser welding of A356 and AA5083 aluminium alloys », *Materials Science and Engineering: A*, vol. 363, n° 1-2, p. 40-52, déc. 2003, doi: 10.1016/S0921-5093(03)00637-3.
- [237] S. Janasekaran, M. F. Jamaludin, M. R. Muhamad, F. Yusof, et M. H. Abdul Shukor, « Autogenous double-sided T-joint welding on aluminum alloys using low power fiber laser », *International Journal of Advanced Manufacturing Technology*, vol. 90, n° 9-12, p. 3497-3505, juin 2017, doi: 10.1007/S00170-016-9677-Y/METRICS.
- [238] H. Ramiarison, N. Barka, et S. Amira, « Optimization of parameters in laser welding of aluminum alloy 5052-H32 using beam oscillation technique for mechanical performance improvement », *International Journal of Lightweight Materials and Manufacture*, vol. 5, n° 4, p. 470-483, déc. 2022, doi: 10.1016/J.IJLMM.2022.05.006.

- [239] A. Majeed, A. Ahmed, A. Salam, et M. Z. Sheikh, « Surface quality improvement by parameters analysis, optimization and heat treatment of AlSi10Mg parts manufactured by SLM additive manufacturing », 2019, doi: 10.1016/j.ijlmm.2019.08.001.
- [240] S. Li, G. Chen, et C. Zhou, « Effects of welding parameters on weld geometry during high-power laser welding of thick plate », *International Journal of Advanced Manufacturing Technology*, vol. 79, n° 1-4, p. 177-182, juill. 2015, doi: 10.1007/S00170-015-6813-Z/METRICS.
- [241] C. C. Chang, C. P. Chou, S. N. Hsu, G. Y. Hsiung, et J. R. Chen, « Effect of Laser Welding on Properties of Dissimilar Joint of Al-Mg-Si and Al-Mn Aluminum Alloys », *J Mater Sci Technol*, vol. 26, n° 3, p. 276-282, 2010, doi: 10.1016/S1005-0302(10)60046-1.
- [242] C. Yuce, M. Tutar, et F. Karpat, « Effect of Process Parameters on the Microstructure and Mechanical Performance of Fiber Laser Welded AA5182 Aluminum Alloys Stability of Structures View project Prototype lightweight passenger seat for commercial vehicles View project », 2017, doi: 10.5545/sv-jme.2017.4442.
- [243] G. Barbieri, F. Cognini, M. Moncada, A. Rinaldi, et G. Lapi, « Welding of Automotive Aluminum Alloys by Laser Wobbling Processing », *Materials Science Forum*, vol. 879, p. 1057-1062, 2017, doi: 10.4028/WWW.SCIENTIFIC.NET/MSF.879.1057.
- [244] Q. Chu, R. Bai, H. Jian, Z. Lei, N. Hu, et C. Yan, « Microstructure, texture and mechanical properties of 6061 aluminum laser beam welded joints », 2018, doi: 10.1016/j.matchar.2018.01.030.
- [245] M. Sommer, « Utilization of laser beam oscillation: To enhance the process efficiency for deep-penetration welding in aluminum », *LIA Today*, vol. 25, n° 6, p. 10-11, nov. 2017, doi: 10.2351/1.4983252/97080.

- [246] F. Mirakhori, F. Nadeau, et G. C. Guillemette, « Single pass laser cold-wire welding of thick section AA6061-T6 aluminum alloy », *J Laser Appl*, vol. 30, n° 3, p. 032421, août 2018, doi: 10.2351/1.5040645/700085.
- [247] T. W. Kim et Y. W. Park, « Parameter optimization using a regression model and fitness function in laser welding of aluminum alloys for car bodies », *International Journal of Precision Engineering and Manufacturing*, vol. 12, n° 2, p. 313-320, avr. 2011, doi: 10.1007/S12541-011-0041-8/METRICS.
- [248] T. Lei, Y. Rong, J. Xu, et Y. Huang, « Experiment study and regression analysis of molten pool in laser welding », 2018, doi: 10.1016/j.optlastec.2018.07.053.
- [249] T. E. Abioye, N. Mustar, H. Zuhailawati, et I. Suhaina, « Prediction of the tensile strength of aluminium alloy 5052-H32 fibre laser weldments using regression analysis », *International Journal of Advanced Manufacturing Technology*, vol. 102, n° 5-8, p. 1951-1962, juin 2019, doi: 10.1007/S00170-019-03310-3/METRICS.
- [250] K. Y. Benyounis et A. G. Olabi, « Optimization of different welding processes using statistical and numerical approaches – A reference guide », *Advances in Engineering Software*, vol. 39, n° 6, p. 483-496, juin 2008, doi: 10.1016/J.ADVENGSOFT.2007.03.012.
- [251] G. Çam et M. Koçak, « Progress in joining of advanced materials », <http://dx.doi.org/10.1179/imr.1998.43.1.1>, vol. 43, n° 1, p. 1-44, 2013, doi: 10.1179/IMR.1998.43.1.1.
- [252] J. Jiao, Y. Ye, S. Jia, Z. Xu, W. Ouyang, et W. Zhang, « CFRTP -Al alloy laser assisted joining with a high speed rotational welding technology », *Opt Laser Technol*, vol. 127, p. 106187, juill. 2020, doi: 10.1016/J.OPTLASTEC.2020.106187.
- [253] S. F. Chua, H. C. Chen, et G. Bi, « Influence of pulse energy density in micro laser weld of crack sensitive Al alloy sheets », *J Manuf Process*, vol. 38, p. 1-8, févr. 2019, doi: 10.1016/J.JMAPRO.2018.12.035.

- [254] « Total Materia - La Base de Données sur les Matériels la Plus Complète au Monde ». <https://www.totalmateria.com/page.aspx?ID=Home&LN=FR> (consulté le 29 avril 2023).
- [255] J. Enz, S. Riekehr, V. Ventzke, N. Huber, et N. Kashaev, « Fibre laser welding of high-alloyed Al–Zn–Mg–Cu alloys », *J Mater Process Technol*, vol. 237, p. 155-162, nov. 2016, doi: 10.1016/J.JMATPROTEC.2016.06.002.
- [256] J. C. Ion, « Laser beam welding of wrought aluminium alloys », <http://dx.doi.org/10.1179/136217100101538308>, vol. 5, n° 5, p. 265-276, 2013, doi: 10.1179/136217100101538308.
- [257] A. W. Alshaer, L. Li, et A. Mistry, « The effects of short pulse laser surface cleaning on porosity formation and reduction in laser welding of aluminium alloy for automotive component manufacture », *Opt Laser Technol*, vol. 64, p. 162-171, déc. 2014, doi: 10.1016/J.OPTLASTEC.2014.05.010.
- [258] H. Zhao, D. R. White, et T. Debroy, « Current issues and problems in laser welding of automotive aluminium alloys », <https://doi.org/10.1179/095066099101528298>, vol. 44, n° 6, p. 238-266, 2013, doi: 10.1179/095066099101528298.
- [259] J. Hirsch et T. Al-Samman, « Superior light metals by texture engineering: Optimized aluminum and magnesium alloys for automotive applications », *Acta Mater*, vol. 61, n° 3, p. 818-843, févr. 2013, doi: 10.1016/J.ACTAMAT.2012.10.044.
- [260] T. Dursun et C. Soutis, « Recent developments in advanced aircraft aluminium alloys », *Materials & Design (1980-2015)*, vol. 56, p. 862-871, avr. 2014, doi: 10.1016/J.MATDES.2013.12.002.
- [261] L. Zheng, D. Petry, H. Rapp, et T. Wierzbicki, « Characterization of material and fracture of AA6061 butt weld », *Thin-Walled Structures*, vol. 47, n° 4, p. 431-441, avr. 2009, doi: 10.1016/J.TWS.2008.08.008.

- [262] « 6061-T6 Aluminum Properties ». <https://www.hydro.com/en-us/profiles/6061-t6-aluminum-properties/> (consulté le 29 avril 2023).
- [263] K. Vasu, H. Chelladurai, A. Ramaswamy, S. Malarvizhi, et V. Balasubramanian, « Effect of fusion welding processes on tensile properties of armor grade, high thickness, non-heat treatable aluminium alloy joints », 2018, doi: 10.1016/j.dt.2018.11.004.
- [264] V. Balasubramanian, V. Ravisankar, et G. Madhusudhan Reddy, « Effect of pulsed current welding on mechanical properties of high strength aluminum alloy », *International Journal of Advanced Manufacturing Technology*, vol. 36, n° 3-4, p. 254-262, mars 2008, doi: 10.1007/S00170-006-0848-0/METRICS.
- [265] « Alüminyum Alaşımlarında Kullanılan Kaynak Yöntemleri ». <https://malzemebilimi.net/aluminyum-alasimlarinda-kullanilan-kaynak-yontemleri.html> (consulté le 29 avril 2023).
- [266] F. Nie *et al.*, « Microstructure and Mechanical Properties of Pulse MIG Welded 6061/A356 Aluminum Alloy Dissimilar Butt Joints », *J Mater Sci Technol*, vol. 34, n° 3, p. 551-560, mars 2018, doi: 10.1016/J.JMST.2016.11.004.
- [267] R. R. Ambriz, G. Barrera, R. García, et V. H. López, « The microstructure and mechanical strength of Al-6061-T6 GMA welds obtained with the modified indirect electric arc joint », *Mater Des*, vol. 31, n° 6, p. 2978-2986, juin 2010, doi: 10.1016/J.MATDES.2009.12.017.
- [268] H. Wang, « Applications of laser welding in the railway industry », *Handbook of Laser Welding Technologies*, p. 575-595, janv. 2013, doi: 10.1533/9780857098771.4.575.
- [269] L. Pellone, G. Inamke, K. M. Hong, et Y. C. Shin, « Effects of interface gap and shielding gas on the quality of alloy AA6061 fiber laser lap weldings », *J Mater*

*Process Technol.*, vol. 268, p. 201-212, juin 2019, doi: 10.1016/J.JMATPROTEC.2019.01.025.

- [270] T. Iwase, H. Sakamoto, K. Shibata, B. Hohenberger, et F. Dausinger, « Dual-focus technique for high-power Nd:YAG laser welding of aluminum alloys », <https://doi.org/10.1111/12.377042>, vol. 3888, p. 348-358, févr. 2000, doi: 10.1111/12.377042.
- [271] T. Dursun et C. Soutis, « Recent developments in advanced aircraft aluminium alloys », *Materials & Design (1980-2015)*, vol. 56, p. 862-871, avr. 2014, doi: 10.1016/J.MATDES.2013.12.002.
- [272] H. Ramiarison, N. Barka, F. Mirakhorli, F. Nadeau, et C. Pilcher, « Parameter optimization for laser welding of dissimilar aluminum alloy: 5052-H32 and 6061-T6 considering wobbling technique », *International Journal of Advanced Manufacturing Technology*, vol. 118, n° 11-12, p. 4195-4211, févr. 2022, doi: 10.1007/S00170-021-08122-Y/METRICS.
- [273] S. Katayama, « Defect formation mechanisms and preventive procedures in laser welding », *Handbook of Laser Welding Technologies*, p. 332-373, janv. 2013, doi: 10.1533/9780857098771.2.332.
- [274] Y. M. Baqer, S. Ramesh, F. Yusof, et S. M. Manladan, « Challenges and advances in laser welding of dissimilar light alloys: Al/Mg, Al/Ti, and Mg/Ti alloys », *International Journal of Advanced Manufacturing Technology*, vol. 95, n° 9-12, p. 4353-4369, avr. 2018, doi: 10.1007/S00170-017-1565-6/METRICS.
- [275] M. Vyskoč, M. Sahul, et M. Sahul, « Effect of Shielding Gas on the Properties of AW 5083 Aluminum Alloy Laser Weld Joints », *J Mater Eng Perform*, vol. 27, n° 6, p. 2993-3006, juin 2018, doi: 10.1007/S11665-018-3383-X/METRICS.
- [276] R. H. M. de Siqueira, A. C. de Oliveira, R. Riva, A. J. Abdalla, C. A. R. P. Baptista, et M. S. F. de Lima, « Mechanical and microstructural characterization of laser-welded

joints of 6013-T4 aluminum alloy », *Journal of the Brazilian Society of Mechanical Sciences and Engineering*, vol. 37, n° 1, p. 133-140, avr. 2014, doi: 10.1007/S40430-014-0175-6/METRICS.

- [277] F. Vakili-Farahani, J. Lungerhausen, et K. Wasmer, « Process Parameter Optimization for Wobbling Laser Spot Welding of Ti6Al4V Alloy », *Phys Procedia*, vol. 83, p. 483-493, janv. 2016, doi: 10.1016/J.PHPRO.2016.08.050.
- [278] J. Ahn, L. Chen, E. He, J. P. Dear, et C. M. Davies, « Optimisation of process parameters and weld shape of high power Yb-fibre laser welded 2024-T3 aluminium alloy », *J Manuf Process*, vol. 34, p. 70-85, août 2018, doi: 10.1016/J.JMAPRO.2018.05.028.
- [279] T. W. Kim et Y. W. Park, « Parameter optimization using a regression model and fitness function in laser welding of aluminum alloys for car bodies », *International Journal of Precision Engineering and Manufacturing*, vol. 12, n° 2, p. 313-320, avr. 2011, doi: 10.1007/S12541-011-0041-8/METRICS.
- [280] T. E. Abioye, N. Mustar, H. Zuhailawati, et I. Suhaina, « Prediction of the tensile strength of aluminium alloy 5052-H32 fibre laser weldments using regression analysis », *International Journal of Advanced Manufacturing Technology*, vol. 102, n° 5-8, p. 1951-1962, juin 2019, doi: 10.1007/S00170-019-03310-3/METRICS.
- [281] M. Ilangoan, S. Rajendra Boopathy, et V. Balasubramanian, « Effect of tool pin profile on microstructure and tensile properties of friction stir welded dissimilar AA 6061-AA 5086 aluminium alloy joints », *Defence Technology*, vol. 11, n° 2, p. 174-184, juin 2015, doi: 10.1016/J.DT.2015.01.004.
- [282] T. Sun, P. Franciosa, et D. Ceglarek, « Effect of focal position offset on joint integrity of AA1050 battery busbar assembly during remote laser welding », *Journal of Materials Research and Technology*, vol. 14, p. 2715-2726, sept. 2021, doi: 10.1016/J.JMRT.2021.08.002.



